8-20-2004

Peripheral Nerve Repair Using Biomaterial Nerve Guides Containing Guidance Channels

Oren D. Rosenthal
University of South Florida

Peripheral Nerve Repair Using Biomaterial Nerve Guides Containing Guidance Channels

by

Oren D. Rosenthal

A dissertation submitted in partial fulfillment
of the requirements for the degree of
Doctor of Philosophy
Department of Anatomy
College of Medicine
University of South Florida

Major Professor: Francis J. Liuzzi, Ph.D.
Paula Bickford, Ph.D.
Kendall F. Morris, Ph.D.
Michael Nolan, Ph.D.
Samuel Saporta, Ph.D.

Date of Approval:
August 20, 2004

Keywords: Collagen, Injury, Entubulation, Autograft, Regeneration

Dedication

I owe the greatest gratitude to my wife Jeri. Not only was she steadfast in her personal support and belief in me, she took care of the most essential duties in our household, the care of our children, while I pursued the Ph.D. Without her, I would not have been able to complete this goal. She did all this, and excelled in her full time job as a physical therapist. My daughter Emily and son Jeffrey, with their wonderful smiles, lifted my spirits and made me realize that all the hard work would be worth it.

Acknowledgments

I would like to thank my committee members, Paula Bickford, Ph.D., Kendall F. Morris, Ph.D., Michael Nolan, Ph.D., Samuel Saporta, Ph.D. for their interest in the dissertation project. I would especially like to thank my major professor, Francis J. Liuzzi, Ph.D., for accepting me into his laboratory, providing me with guidance, and giving me the confidence to complete this research. He has been a mentor and a friend. I would like to recognize and thank all members of the Department of Anatomy faculty who have contributed to my education at the College of Medicine. I would also like to thank Daniel Greenwald, M.D. for taking the time to serve as the chairperson of the dissertation defense.

Table of Contents

List of Tables

List of Figures

Peripheral Nerve Repair Using Biomaterial Nerve Guides Containing Guidance Channels

Oren D. Rosenthal

ABSTRACT

Traumatic injuries to peripheral nerves often leave gaps that cannot be repaired by direct suture methods. In such instances, repair with a tubular nerve guide, allows connection of the nerve ends, provides directional guidance, and concentrates endogenous trophic factors for regenerating axons. We hypothesized that collagen nerve guides containing longitudinally oriented channels would further improve the outcome of nerve repair by increasing the surface area available for cell migration. We restored the continuity of a 10mm peripheral nerve gap (rat sciatic nerve) by suturing the nerve stumps into a type I collagen nerve guide (1.5 mm ID), which contained longitudinal channels. Two different channel designs were tested. They were compared to empty nerve guides and autografts. One channel design contained five longitudinally-oriented collagen microtubes (0.4 mm ID) and the other contained 32 longitudinally-oriented collagen filaments (90 μm diameter). Nerve regeneration was examined at 6 weeks and 12 weeks post repair by a determination of the number and diameter of myelinated axons in the middle sections of the nerve guides. Sciatic

function Indices were calculated from walking tracks and static stance images, and electrophysiological assessments were performed.

Compound muscle action potentials of the gastrocnemius and intrinsic muscles of the foot were recorded from animals in each group at 12 weeks, indicating that axons regenerated through the nerve repair site, into the distal nerve stump, and successfully reinnervated peripheral targets. At 6 weeks, there was no significant difference between the mean number of myelinated axons with the mid sections of the 3 types of nerve guides ($P = 0.488$). At 12 weeks, the nerve guide that contained 5 microtubes within its lumen had significantly more axons than the nerve guide that contained 32 filaments in its lumen ($P = 0.008$). The mean myelinated axon number in the microtube group is larger than the empty nerve guide group but this difference was not statistically significance ($P < 0.05$). Autografts at both 6 and 12 weeks had significantly more myelinated axons in the mid section of the repair site than either of the nerve guide repairs at the respective time points ($P < 0.05$).

Preface

The research reported herein is a component of one phase of a multiphase, multicenter study. The overall goal of this multicenter study is to design, manufacture, and test biomaterial nerve guides, which can eventually be used in human patients to repair traumatic peripheral nerve gap injuries. Shu-Tung Li, Ph.D. is the principle investigator for research funded under the National Institute of Health (NIH) RO1 grant. Dr. Li is the founder and Chief Executive Officer of the biotechnology firm Collagen Matrix Inc., which is located in Franklin Lakes, New Jersey. The research collaborators are Francis J. Liuzzi, Ph.D. from the University of South Florida, College of Medicine, Anatomy Department, and Roger D. Madison, Ph.D. from the Nerve Regeneration Laboratory at Duke University, Medical Center and Veterans Affairs Medical Center, Durham, North Carolina.

The project scope is briefly summarized below. Collagen Matrix Inc. designed and fabricated several different prototypes of bovine type I collagen nerve guides. To thoroughly evaluate the effectiveness of these biomaterial nerve guides, they were tested in cell culture first, and then used to repair a sciatic nerve injury in the rat. The nerve guides will eventually be used to repair a median nerve injury in the forearm of the primate. The laboratory of Dr. Liuzzi

at the University of South Florida is responsible for *in vitro* (cell culture) and *in vivo* (rat) experiments using the nerve guides fabricated by Collagen Matrix Inc. Following the *in vivo* screening in the rat a final nerve guide prototype will be chosen for evaluation in primates at the Duke University Laboratory.

The *in vivo* study at USF is composed of three phases. Each phase follows the same experimental design. The difference between the three phases is in the design parameters of the nerve guides. The goal of these experiments is to determine which nerve guide most favorably affects nerve regeneration when implanted to bridge a ten-millimeter nerve gap in the transected rat sciatic nerve.

The first phase compared collagen tubes of two different permeabilities. The second phase evaluated collagen nerve guides that contain longitudinal channels within the nerve guide lumen. Two different designs with channels were evaluated. The third phase of the rat study evaluates collagen nerve guides that incorporate laminin, basic fibroblast growth factor (bFGF), insulin-like growth factor II (IGFII), either alone or in combination. This final rat study will also include nerve guides that combine these molecules with the optimal guidance channel design chosen from the second phase of the rat study. One of these designs will be the final prototype used for evaluation in the primate.

The dissertation research carried out by Oren D. Rosenthal, M.P.T., graduate student, in the laboratory of Francis Liuzzi, Ph.D., pertains to the *in vivo* evaluation of nerve guides with longitudinal guidance channels (phase II). We

hypothesized that increasing the surface area of a resorbable biomaterial nerve guide; by incorporating longitudinal guiding channels within its lumen, will improve axonal regeneration and functional recovery as compared to an empty tube. Although integrally involved in the entire *in vivo* study (phase I, II, & III) at the University of South Florida, the author has focused the dissertation research on the effect of repairing a peripheral nerve gap injury with a biomaterial nerve guide containing intra-luminal guidance channels. Nerve guide permeability, growth factors, and cellular adhesion molecules, as they relate to peripheral nerve regeneration, are discussed in the background and discussion sections to provide the reader with a brief history of peripheral nerve repair and its possible future directions.

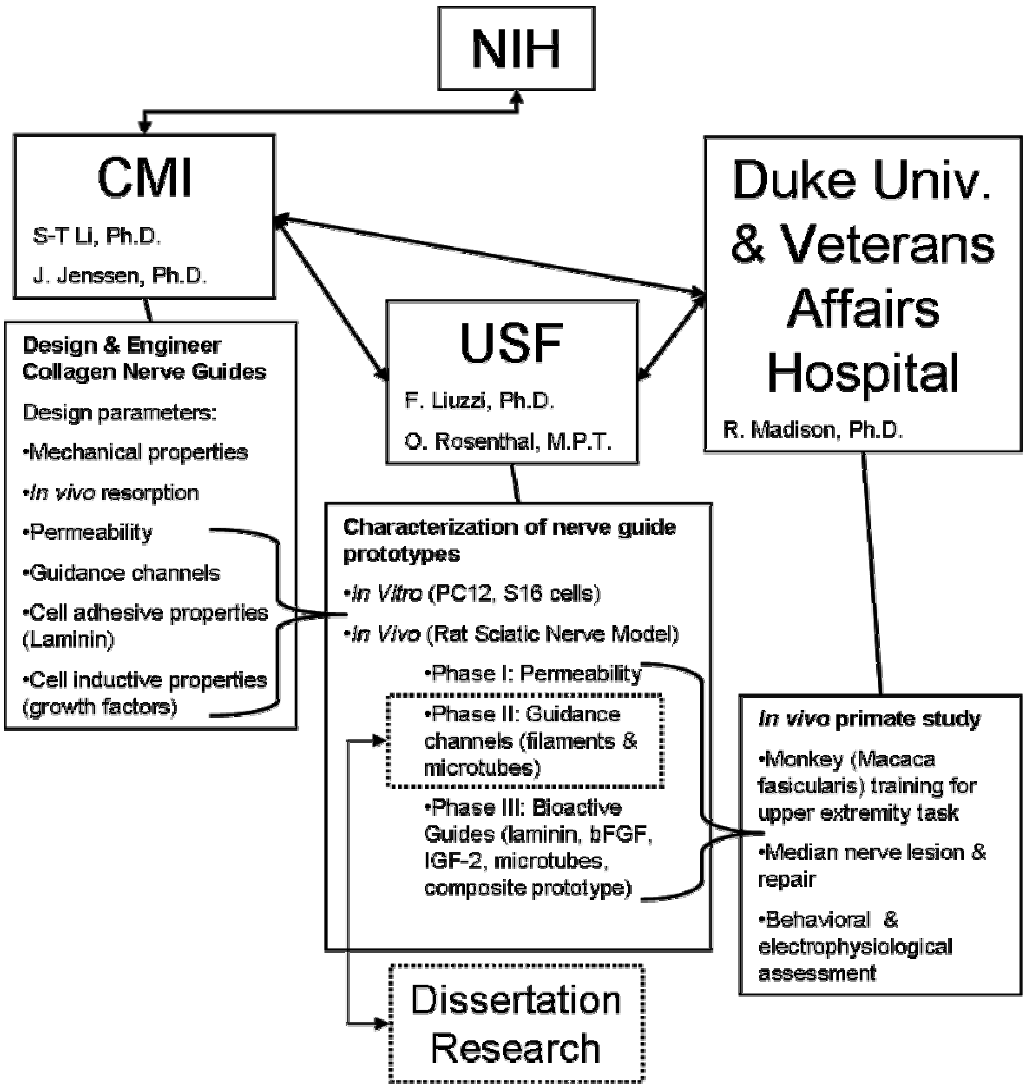

Figure 1 Diagram of Multicenter Project

The dissertation research (enclosed in dotted box) is comprised of *in vivo* evaluation of type 1 collagen nerve guides containing longitudinal guidance channels for the repair of a 10 mm gap in the rat sciatic nerve.

Chapter 1: Research Objectives

Aims of Research

When an individual suffers a peripheral nerve transection injury, the nerve must be surgically repaired to insure optimal functional recovery (Archibald, Krarup et al. 1991; Evans 2000). When extensive tissue damage prevents direct union of the cut nerve ends, an autograft is often harvested from the leg to bridge the gap (Evans 2000). Most often, the sural nerve, a large sensory nerve, serves as the graft (Evans 2001). Although this practice compromises sensation in the region of the donor site for the benefit of reestablishing motor and sensory function in a denervated region, it is justified when the goal is reinnervation of a region critical for normal daily function, such as the hand. According to the 9th revision of the International Classification of Diseases (ICD-9), patients received over 50,000 peripheral nerve surgeries in 1995.

Biomaterial guide tubes can be used to bridge nerve gaps, but nerve regeneration through a biomaterial tube, to-date, has not surpassed that through an autograft (Keeley, Atagi et al. 1993; Chamberlain, Yannas et al. 1998; Evans, Brandt et al. 1999; Evans 2001). Because of this, most clinicians choose autografts to repair peripheral nerve injuries in their patients. Although autografts currently provide the greatest functional restoration to a denervated region, the risk of sensory deficits, infection, and the formation of a painful neuroma at the

autograft donor site are always present (Keeley, Atagi et al. 1993; Evans 2001). Bridging a nerve gap with a biomaterial guide tube eliminates all of these side effects. Consequently, there is a need to improve the efficacy of biomaterial grafts so they become a viable alternative to the autograft (Evans 2000).

Although many investigators have added exogenous neurotrophins and improved nerve regeneration through guide tubes in animal models, few have explored the effect of different guide tube architectures (Fine, Decosterd et al. 2002; Xu, Yee et al. 2003). In addition, many of the neurotrophin delivery methods are impractical and have not been tested in humans (Evans 2000; Lundborg 2000; Lundborg 2002). We believe that the lack of focus on guide tube architecture represented a significant gap in the literature that we addressed in this study. Only recently have researchers noticed the effect that increased surface area of guide tubes has on axon regeneration (Arai, Lundborg et al. 2000; Hadlock, Sundback et al. 2001). We now possess the technology to incorporate these concepts into the design and fabrication of a biomaterial nerve guide.

Main Objective

We examined axonal regeneration and functional nerve recovery following repair of a 10 mm peripheral nerve gap with bovine type I collagen nerve guides that contain longitudinally oriented collagen guidance channels within their lumen. We collected data (outlined in the specific aims) at 6 and 12 weeks post

nerve transection/repair to analyze and compare nerve regeneration in nerve guides with guidance channels, nerve guides without guidance channels, and autografts. We hypothesized that increasing the surface area of a resorbable biomaterial nerve guide, by incorporating longitudinal guiding channels within its lumen, will improve axonal regeneration and functional recovery as compared to an empty tube.

Specific Aims

The overall goal of the this study was to compare the efficacy of nerve guides with guidance channels of two different designs in the repair of a 10 mm gap in the rat sciatic nerve. One contained longitudinally oriented microtubes within its lumen; the other contained longitudinally oriented filaments. They were compared to both nerve guides without longitudinal channels and to the "gold standard", autograft repair.

Aim 1:

To quantify and compare by morphometric analyses, axonal regeneration through the different nerve repairs by measuring mean myelinated axonal diameter and by counting the number of myelinated axons in the middle segment of the nerve guide tube or autograft.

Aim 2:

To examine by electrophysiological analyses, the effect of each type of nerve repair on facilitating axon elongation into the distal nerve stumps and reestablishing synaptic connections with denervated muscle. We analyzed the evoked compound muscle action potential (CMAP) in the gastrocnemius (a muscle that is distal to the repair site and is normally innervated by the tibial branch of the sciatic nerve).

Aim 3:

To examine by behavior analysis, the effect of each type of nerve repair on the gross motor function of the reinnervated limb by using walking track and static stance footprint analyses. This included calculating a sciatic function index (SFI) and a static sciatic index (SSI) to compare functional recovery of the sciatic nerve following repair with different nerve guides.

Chapter 2: Background & Significance

Introduction

When a peripheral nerve is severed during trauma, the victim suffers loss of motor and sensory function distal to the injury (Sunderland 1991). Although axons will elongate from the proximal nerve stump following nerve transection injury, the likelihood that a majority of the axons will successfully find and enter the distal nerve stump, and subsequently reinnervate appropriate target tissues is small (Sunderland 1991). Therefore, surgical intervention is necessary to reunite the cut ends of the nerve (Evans 2000; Evans 2001). When this is not possible because the trauma has created a gap, a nerve autograft is harvested to bridge the nerve gap (Evans 2001). Frequently the sural nerve, a pure sensory nerve from the lower extremity, is chosen for the repair (Evans 2000; Evans 2001). An acceptable trade off exists, where the patient is willing to sacrifice sensation in a region of the lower leg and foot for a chance of functional recovery in a more important region such as the hand. A major disadvantage of the autograft repair method is the limited amount of tissue available to use for grafting. Another problem is that of size mismatch, where the donor autograft is significantly smaller in diameter than the nerve that requires repair.

Peripheral Nerve Injury

Following a peripheral nerve crush or transection injury, axons and myelin distal to the injury fragment and degenerate (see figure 2), (Waller 1850; Lubinska 1977; Stoll, Griffin et al. 1989). Waller (1850) first described degenerative changes in transected distal nerve segments of frog glossopharyngeal and hypoglossal nerves (Waller 1850). These changes are now commonly referred to as Wallerian degeneration. It is now known that calcium-dependent proteases, at least in part, are responsible for degeneration of the axonal cytoskeleton (George, Glass et al. 1995). Schwann cells in the proximal and distal nerve stumps of a transected nerve proliferate (Ramon Y Cajal 1928). Schwann cells and macrophages phagocytose myelin and degenerated axon fragments of the distal nerve segment (Ramon Y Cajal 1928; Stoll, Griffin et al. 1989). The same phenomenon also occurs for a short distance in the proximal nerve stump. This is an essential step as there are myelin proteins that are inhibitory to axonal regeneration both in the peripheral nervous system (PNS), and in the central nervous system (CNS) (Grados-Munro and Fournier 2003; Schwab 2004)

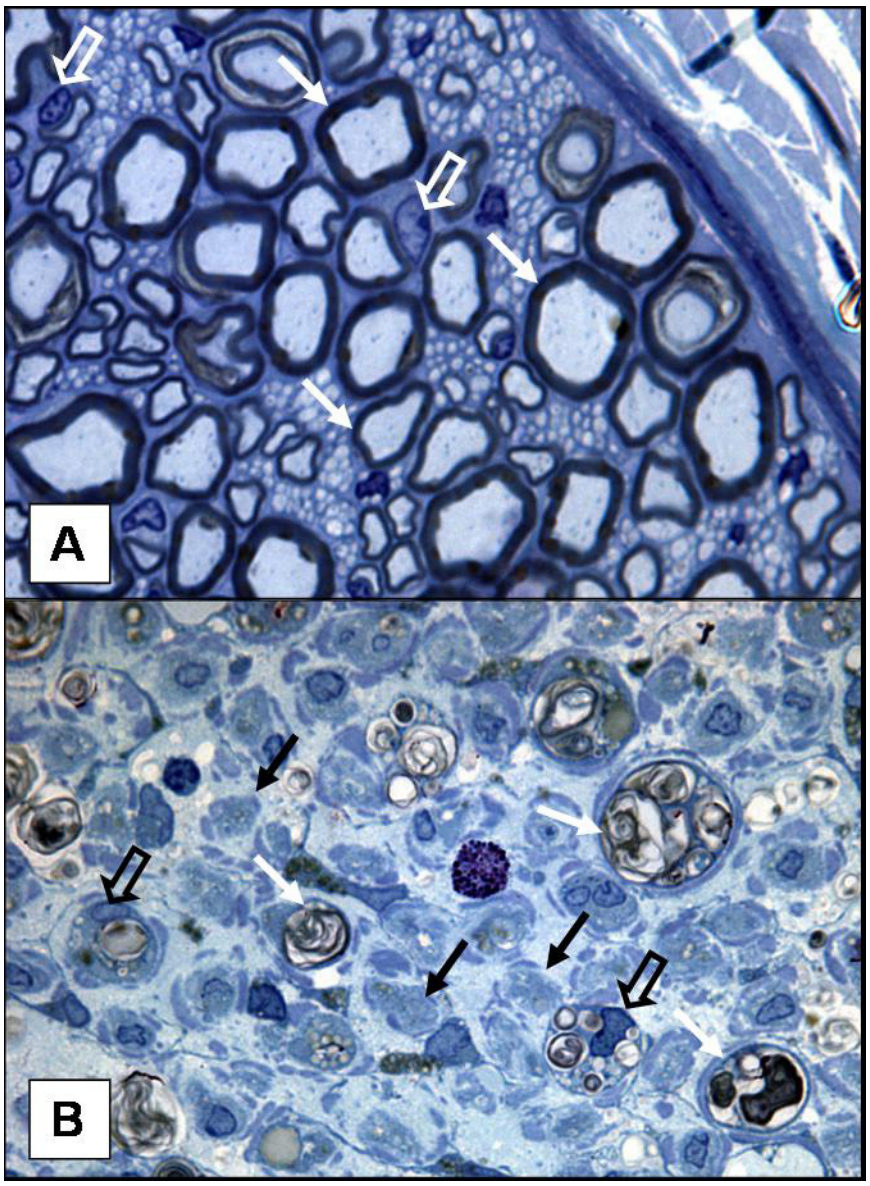

Figure 2 Normal Nerve & Wallerian Degeneration

Photomicrographs (100x oil objective lens) of toluidine blue stained 2 µm plastic sections. Normal sciatic nerve (A) shows large myelinated axons (solid white arrows), and nuclei of Schwann cells (open white arrow). Many small unmyelinated axons are visible between the myelinated axons. Image (B) is from a nerve segment distal to an autograft repair at 3 weeks showing Wallerian degeneration (solid white arrows), nuclei of macrophages/Schwann cells (open black arrow) phagocytosing whirls of myelin debris, mast cell in center of image, empty/collapsed basal lamina endoneurial tubes already cleared of myelin (solid black arrows). These are spaces formerly occupied by myelinated axons. There is no evidence of regeneration in this section of nerve, no myelinated or unmyelinated axons have entered this region of the sciatic nerve at this time.

One difference between the PNS and CNS, regarding axonal regeneration, is that myelin is efficiently removed from the lesion in the PNS by the many macrophages that enter the injury site from the blood (Stoll, Griffin et al. 1989; Stoll, Trapp et al. 1989). In the CNS, the influx of blood-derived phagocytotic cells that can clear myelin from degenerating axons is far less and myelin remains in the CNS for months after injury. In the PNS, mast cells in the region surrounding the injury degranulate. They release histamine, which dramatically increases vascular permeability and facilitates entry of monocyte-derived macrophages to the injury site (Esposito, De Santis et al. 2002). Additionally, mast cell numbers dramatically increase in the injury site and contribute to nerve regeneration by releasing nerve growth factor (NGF), and vascular endothelial growth factor (VEGF) (Zochodne and Cheng 2000; Norrby 2002; Rosenstein and Krum 2004). Mast cells and Schwann cells both release tumor necrosis factor alpha (TNF-α), which causes monocytes to increase expression of adhesion molecules, allowing them to form attachments to vessel endothelium and to extravasate to the injury site.

After debris has been cleared from a peripheral nerve lesion, capillaries and endoneurial tubes lined with Schwann cells remain in the distal nerve stump (Ramon Y Cajal 1928). Schwann cells from both the distal and proximal stumps proliferate and migrate across the lesion. These cells facilitate axon elongation across the lesion by secreting neurotrophic factors, which are chemoattractants for axonal growth cones, and by depositing extracellular matrix molecules, which

offer contact guidance for growth cone filopodia (Rogers, Letourneau et al. 1983; Fornaro, Tos et al. 2001; Goldberg 2003). Eventually, Schwann cells invest regenerating axons and elaborate new myelin (Ramon Y Cajal 1928).

Functional reinnervation of target tissues is more complete following nerve crush injuries than after transection injuries (Hare, Evans et al. 1992). In crush injury the connective tissues of the nerve may remain intact and provide channels that guide axon elongation to peripheral targets (Ide, Tohyama et al. 1983; Ramon Y Cajal 1928). Although no nerve graft or guide-tube can direct axons precisely to their former endoneurial tubes, the addition of longitudinal channels in a biomaterial nerve guide dramatically increases the surface area for axon growth cone adhesion during elongation (Ngo, Waggoner et al. 2003). These channels may also provide improved directional guidance when compared to an empty nerve guide. We used type I collagen guide tubes that have type I collagen longitudinal channels in the current study.

Peripheral Nerve Repair

Direct suture of severed nerve offers the best functional outcome as long as the final repair is tension free at the suture line (Terzis, Faibisoff et al. 1975; Evans 2000; Evans 2001). Immobilizing joints adjacent to the repair, in either excessive flexion or extension, to minimize tension to a repaired nerve, is counterproductive since nerve tension will be greater once movement is reinitiated. During the period of immobility there would likely be fibrotic

adherence of the repair site to the underlying structures and thus normal nerve gliding with joint movement would be restricted to a greater degree than would occur if movement was allowed (Sunderland 1991). Prolonged joint immobilization surrounding denervated limb regions may also lead to articular, periarticular fibrosis, and adhesion formation, which limits functional recovery even if regenerating axons reach their distal targets (Sunderland 1991). In addition to the increased risk of tension, a possible complication of the direct suture method is the failure of axons to penetrate the scar that forms at the suture line (Sunderland 1991). Using a nerve graft or guide tube to bridge a large gap can prevent excessive tension on the repair and improve the functional outcome (Terzis, Faibisoff et al. 1975).

Using autologous tissues to repair large nerve gaps (vein, muscle, tendon, artery, or nerve) affords the benefit of immunological acceptance, but unfortunately, requires the sacrifice of healthy donor tissues (Brandt, Dahlin et al. 1999; Battiston, Tos et al. 2000; Geuna, Tos et al. 2000; Fornaro, Tos et al. 2001; Rodrigues Ade and Silva 2001). Cadaveric nerve allografts eliminate the side effects associated with surgical harvesting of nerve autografts, but outcomes are not as good (Trumble and Shon 2000; Evans 2001). Allografts may also require immunosuppression, which cannot be justified for non-life threatening peripheral nerve repair (Trumble and Shon 2000; Evans 2001). This has lead to the design and fabrication of synthetic and biomaterial nerve guides for the repair of transection injuries with large gaps (Madison, da Silva et al. 1987; Keeley,

Nguyen et al. 1991; Chamberlain, Yannas et al. 1998; Hadlock, Sundback et al. 2001; Young, Wiberg et al. 2002; Ahmed, Underwood et al. 2003; Ngo, Waggoner et al. 2003).

Surgical nerve repair using guide tubes to join proximal and distal ends of a transected nerve provides directional guidance for Schwann cells and axon growth cones. In addition, it may concentrate essential trophic factors for elongating axons. This technique is frequently referred to as “entubulation repair” (Madison, da Silva et al. 1987; Madison, Da Silva et al. 1988; Keeley, Atagi et al. 1993). Additional variables that may effect regeneration through guide tubes are permeability, bioresorption, immunoreactivity, kink-resistance, presence of growth factors, vascularization, cell adhesive properties, and presence of Schwann cells (Evans, Brandt et al. 1999; Fornaro, Tos et al. 2001). With this in mind, a myriad of nerve grafting and guide tube technologies have been explored (Godard, Coulon et al. 1984; Glasby, Gschmeissner et al. 1986; Archibald, Krarup et al. 1991; Keeley, Nguyen et al. 1991; Evans, Brandt et al. 1999; Hadlock, Sundback et al. 2001; Hashimoto, Suzuki et al. 2002; Young, Wiberg et al. 2002; Ahmed, Underwood et al. 2003; Ngo, Waggoner et al. 2003).

What follows is a brief review of the relevant research of entubulation nerve repair.

Entubulation Nerve Repair

Bridging a 4 mm nerve gap with a collagen nerve guide restores nerve function as effectively as an autograft. This was demonstrated by electrophysiology of target muscle and sensory nerves in rats and *Macaca fascicularis* monkeys (Archibald, Krarup et al. 1991). Nerve gaps of 10 mm or larger, however, provide a greater challenge to regenerating axons in a guide tube and this challenge is a driving force for the multitude of designs and tissues employed as nerve guides.

Ceballos (1999) demonstrated that a collagen tube filled with collagen fibrils suspended in a gel and aligned longitudinally by a magnetic field, improved peripheral nerve regeneration across a six mm gap in the mouse (Ceballos, Navarro et al. 1999). However, when the collagen was cross-linked with ribose to improve stability, nerve regeneration was inhibited. Consequently, the degree of cross-linking and the specific cross-linking agent are important variables that affect nerve regeneration through fabricated guide tubes (Itoh, Takakuda et al. 2002).

In another study, parallel longitudinally oriented fibrils of collagen matrix inside a silicone tube facilitated axon regeneration better than a random orientation of collagen matrix, as evidenced by an earlier and more complete target reinnervation (Verdu, Labrador et al. 2002). Aria (2000) was able to successfully bridge a 15 mm gap in the rat sciatic nerve by including 7 resorbable synthetic filaments inside a silicone tube (Arai, Lundborg et al. 2000). He

repeated this with 5 different filament materials and all supported regeneration better than empty tubes. This result is significant because it is widely reported that repair of rat sciatic nerve gaps greater than 10 mm with empty tubes, fail.

Nerve guide tubes packed with poly(L-lactide) microfilaments facilitated regeneration in the rat sciatic nerve at 10 weeks following entubulation repair better than empty tubes (Ngo, Waggoner et al. 2003). However, these guide tubes were silicone and therefore not resorbable, unlike the collagen tubes in the current study (Chamberlain, Yannas et al. 1998). This is an important distinction.

When silicone tubes are used for nerve guides, they eventually cause constriction of the tissue cable, which can lead to ischemia and failure of functional reinnervation of target tissues (Chamberlain, Yannas et al. 1998). Nerve repair with silicone tubes requires a second surgery to remove the tubes after axons have bridged the nerve gap. In a long term study of entubulation repair of the rat sciatic nerve, collagen tubes filled with a collagen-glycosaminoglycan (collagen-GAG) matrix, which was designed to degrade in six weeks, had more myelinated axons growing through them than empty tubes did at both the 30 and 60-week time points (Chamberlain, Yannas et al. 1998). Silicone tubes filled with GAG-collagen matrix tubes also proved beneficial for axon regeneration when compared to empty tubes (Chamberlain, Yannas et al. 1998). Although a collagen tube filled with collagen-GAG matrix provides a porous and resorbable substrate for axon regeneration (Chamberlain, Yannas et

al. 1998), this intraluminal material is unlikely to decrease the risk of nerve guide collapse.

Biomaterials For Nerve Repair

High tensile strength is a characteristic of type I collagen that makes it an ideal biomaterial for the fabrication of nerve guide tubes (Daamen, van Moerkerk et al. 2003). Collagen, found in the extracellular matrix of many tissues, is composed of a parallel arrangement of collagen fibers (Boot-Handford and Tuckwell 2003). These fibers are composed of fibrils, which in turn are composed of a triple helix of polypeptides (tropocollagen) (Boot-Handford and Tuckwell 2003). Tropocollagen molecules are covalently cross-linked to one another in the extracellular environment, giving collagen fibrils their high tensile strength (Daamen, van Moerkerk et al. 2003).

When purified collagen fibers are formed into tubes in the laboratory, they are chemically cross-linked to increase stability and tensile strength (Berglund, Mohseni et al. 2003; Charulatha and Rajaram 2003). The improved strength of the collagen tubes allows suture fixation during nerve repair. Varying the degree of cross-linking not only affects the mechanical properties of the formed tube, but also alters *in vivo* degradation (Charulatha and Rajaram 2003). Tubes with a higher degree of cross-linking resist degradation (Charulatha and Rajaram 2003). The degree of chemical cross-linking and the wall thickness of the guide tube are

parameters that were tightly controlled during the fabrication of collagen tubes for this study.

A major advantage of collagen over synthetic materials for fabrication of nerve guides is biocompatibility. Collagen is an integral structural protein of the extracellular matrix, and is found in all tissues (Boot-Handford and Tuckwell 2003). When bovine type I collagen vascular stents were implanted in rabbits it proved biocompatible (Cloft, Kallmes et al. 2000). In another study, bovine collagen sponges that were implanted subcutaneously in rats for three months did not elicit antibody production to foreign material (Anselme, Bacques et al. 1990).

In addition to the support provided by animal studies, type I bovine collagen has been safely used in humans to improve healing of leg ulcers and pressure sores (Beghe, Menicagli et al. 1992). Since type I collagen protein is highly conserved among vertebrate species, immune rejection of purified bovine collagen tissue grafts implanted in humans is unlikely (Boot-Handford and Tuckwell 2003). Moreover, macrophages possess the necessary mechanisms to phagocytose and enzymatically digest collagen. Consequently, resorption and remodeling of implanted collagen nerve guides can take place with minimal inflammation.

By contrast, synthetic nerve guides made from poly L-lactide, and those made from Poly-hydroxybutyric acid (PHB), demonstrate delayed resorption and significant inflammation, as evidenced by the presence of giant cells surrounding

residual material at 24 weeks post implantation (Borkenhagen, Stoll et al. 1998; Ngo, Waggoner et al. 2003). When silicone tubes are used as nerve guides they eventually constrict the regenerating axons and myofibroblasts take residence in a continuous layer around the tubes (Chamberlain, Yannas et al. 1998). Clearly, collagen is a superior material for implantation in human patients. It is readily available from bovine tendon and is an excellent biomaterial for fabrication of nerve guide tubes with guidance channels (Archibald, Krarup et al. 1991).

Sciatic Nerve Gross Anatomy

For the rat sciatic nerve to serve as a model for peripheral nerve injury and repair, a thorough understanding of its anatomy is essential. Greene gives a comprehensive anatomical report of the rat hind limb anatomy in his 1968 text Anatomy of the Rat. The cell bodies of motor neurons with axons that travel through the sciatic nerve and innervate skeletal muscle of the lower limb reside in the ventral horn of the spinal cord. The cell bodies of sensory neurons with axons that travel through the sciatic nerve reside in the dorsal root ganglia, which lie just outside of the spinal cord. They send central axons into the dorsal horn of the spinal cord and peripheral axons into spinal nerves. Segmental spinal nerves from the caudal spinal cord divide into dorsal and ventral primary rami, which form the lumbosacral plexus. In addition to the motor and sensory nerve fibers, autonomic axons that innervate blood vessels and skin travel in the sciatic nerve.

In an anatomical study of twenty four adult Sprague-Dawley rats, the L4 & L5 spinal nerves joined to form the sciatic nerve in all animals studied (Asato, Butler et al. 2000). The L6 spinal nerve joined the sciatic nerve in 54% of the rats, while in the rest of the animals the L6 spinal nerve ran along with the sciatic nerve but never merged with it. The L3 spinal nerve joined the sciatic nerve in 25% of the rats studied. It is presumed that the largest contribution to the sciatic nerve in the Lewis rat (strain used in the present study) is via the L4 & L5 spinal nerves (figure 3).

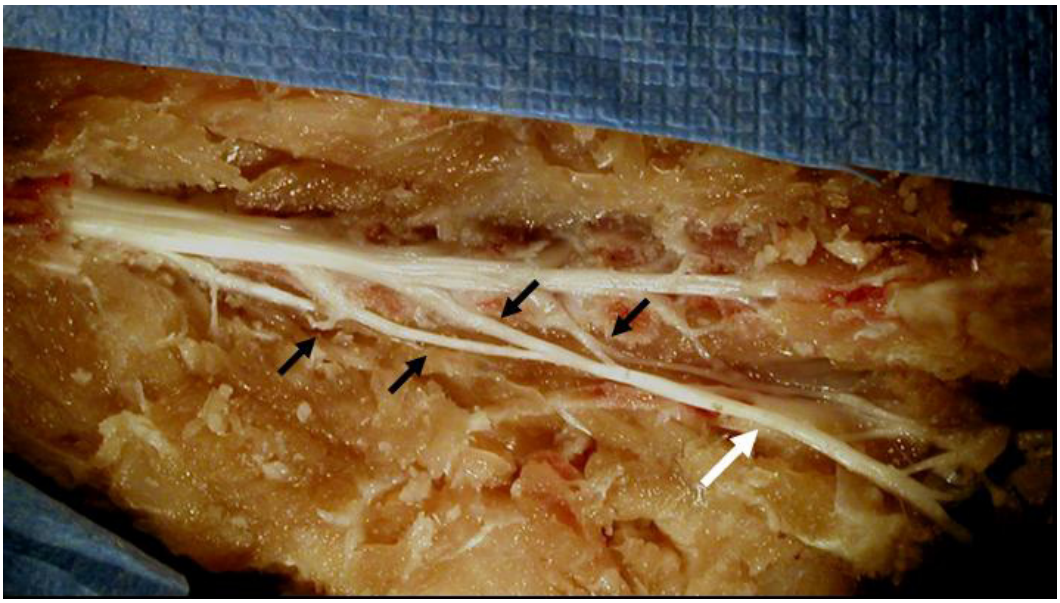

Figure 3 Sciatic and Spinal Nerve Dissection

Dissection of a Lewis rat following formalin fixation. The left laminae of the lumbar vertebra removed to expose the L3-L6 dorsal root ganglia and spinal nerves. A small slip of nervous tissue (black arrow farthest to the left) connects the L3 spinal nerve to the L4 spinal nerve. Solid black arrows from left to right point to the L3, L4, L5, and L6 spinal nerves respectively that all appear to contribute to the sciatic nerve (white arrow) in this specimen.

The most proximal location of the sciatic nerve is in the pelvis. It travels through the sciatic notch and enters the gluteal region. The sciatic nerve has two main divisions that are held together by connective tissue ensheathment. These divisions, the tibial and peroneal nerves, can be divided by dissection but normally appear as one nerve in the proximal to mid thigh. The tibial and peroneal nerves are the terminal branches of the sciatic nerve and are named the same: common peroneal nerve and the tibial nerve (Greene 1968). There are many muscular and sensory branches given off by the sciatic nerve along its course. These branches will not be reviewed here.

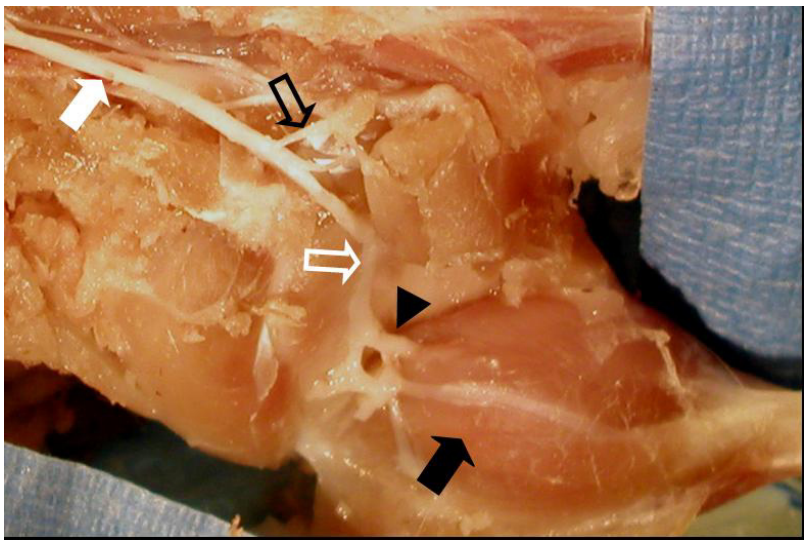

Figure 4 Sciatic Nerve Dissection

The sciatic nerve (solid white arrow) after it emerges from the sciatic notch continues through gluteal region where it gives off a muscular branch (open black arrow) to the biceps femoris from its tibial division. The sciatic nerve continues distally though the thigh (open white arrow). The tibial nerve (solid arrowhead) travels between the lateral (black arrow) and medial gastrocnemius muscle heads.

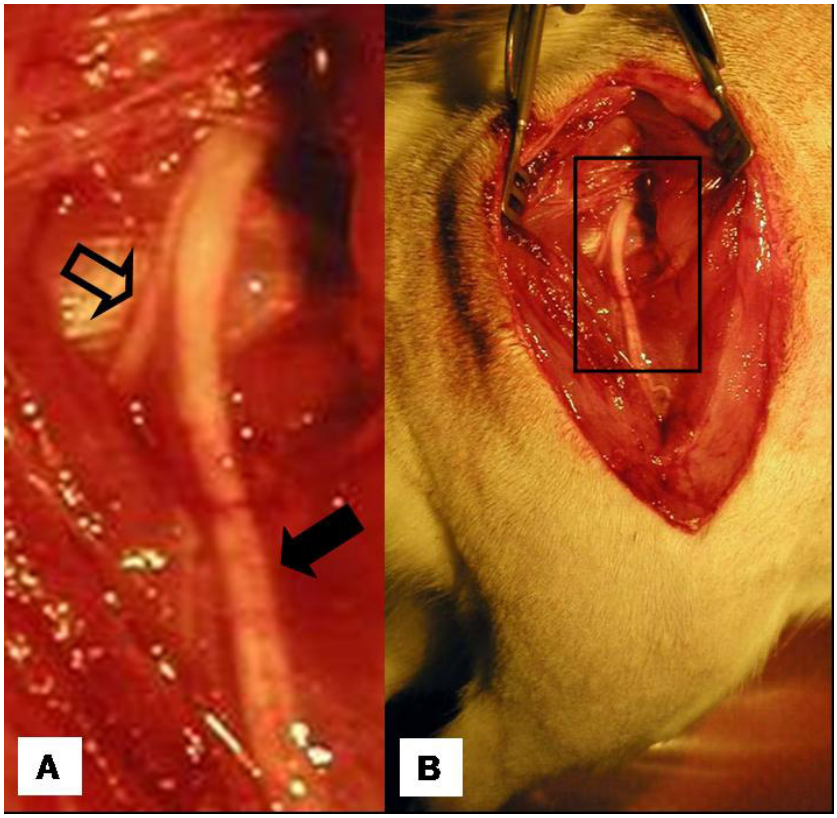

Figure 5 Normal Gross Anatomy Rat Sciatic Nerve

(A) High magnification view of the sciatic nerve from the boxed region of image (B), which was captured during the terminal surgical exposure of the normal sciatic nerve. The sciatic nerve emerges in the top half of the image in the gluteal region and gives rise to a large muscular branch (open arrow) that innervates the biceps femoris. The sciatic nerve (solid arrow) continues down the thigh where the tibial and common peroneal divisions of the sciatic nerve can be seen in the thigh through the translucent connective tissue that ensheathes both nerves.

The common peroneal and tibial nerves diverge at the popliteal fossa. The tibial nerve remains deep and medial, while the common peroneal takes a more lateral course in the lower leg. The tibial nerve travels between the two heads of the gastrocnemius muscle where it gives off three muscular branches. The first of these innervates the lateral head of the gastrocnemius, the soleus, and the plantaris muscles. The second branch of the tibial nerve, in this region, innervates the medial gastrocnemius. The last of the three muscular branches

runs to the deep posterior compartment and innervates all of the deep muscles of the posterior lower leg: the flexor hallucis longus, the tibialis posterior, and the flexor digitorum longus muscles. The tibial nerve continues distally until it divides into the medial and lateral plantar nerves, which innervate the intrinsic muscles of the foot and sensory receptors in the digits.

The common peroneal nerve divides into deep and superficial branches. The superficial peroneal nerve innervates the peroneal muscles, which are lateral to the fibula. The deep peroneal nerve innervates the tibialis anterior muscle and the digital extensors. Its terminal branches supply the dorsum of the foot and end in the second interdigital space (Greene 1968).

All of the above muscles are denervated when the sciatic nerve is transected in the thigh. They do not recover function unless axons from the proximal sciatic nerve stump regenerate and reach the formerly denervated neuromuscular junctions.

Microanatomy of Peripheral Nerve

Individual axons of peripheral nerves are surrounded by a connective tissue termed the endoneurium, which contains small diameter collagen fibers (Ross, Romrell et al. 1995). The perineurium surrounds bundles of axons, and delineates fascicles (Ross, Romrell et al. 1995). Peripheral nerves contain one or more fascicles, which are contained within a connective tissue termed the epineurium (Ross, Romrell et al. 1995). Of the three connective tissues, the

epineurium contains the largest diameter collagen fibers. Mast cells are found in the spaces bound by the epineurium and perineurium, and can be easily identified by their large cytoplasmic metachromatic granules.

Schwann cells, from neural crest, are predominant cell type in the endoneurial compartment, and are responsible for ensheathing axons of the PNS. Although a single Schwann cell can envelope many small diameter unmyelinated axons, a single Schwann cell can only wrap a myelin sheath around a single large diameter axon. When Schwann cells wrap their plasma membranes successively around large axons, most of the Schwann cell cytoplasm is squeezed from the concentric layers, leaving a sphingomyelin rich sheath termed the myelin sheath or the “sheath of Schwann”. The larger diameter axons receive more myelin wrappings, leaving them with a thicker myelin sheath. A myelin sheath from a single Schwann cell may occupy approximately 1 mm of the axons length. The axonal area between two successive myelin sheaths is called a node of Ranvier (Ross, Romrell et al. 1995).

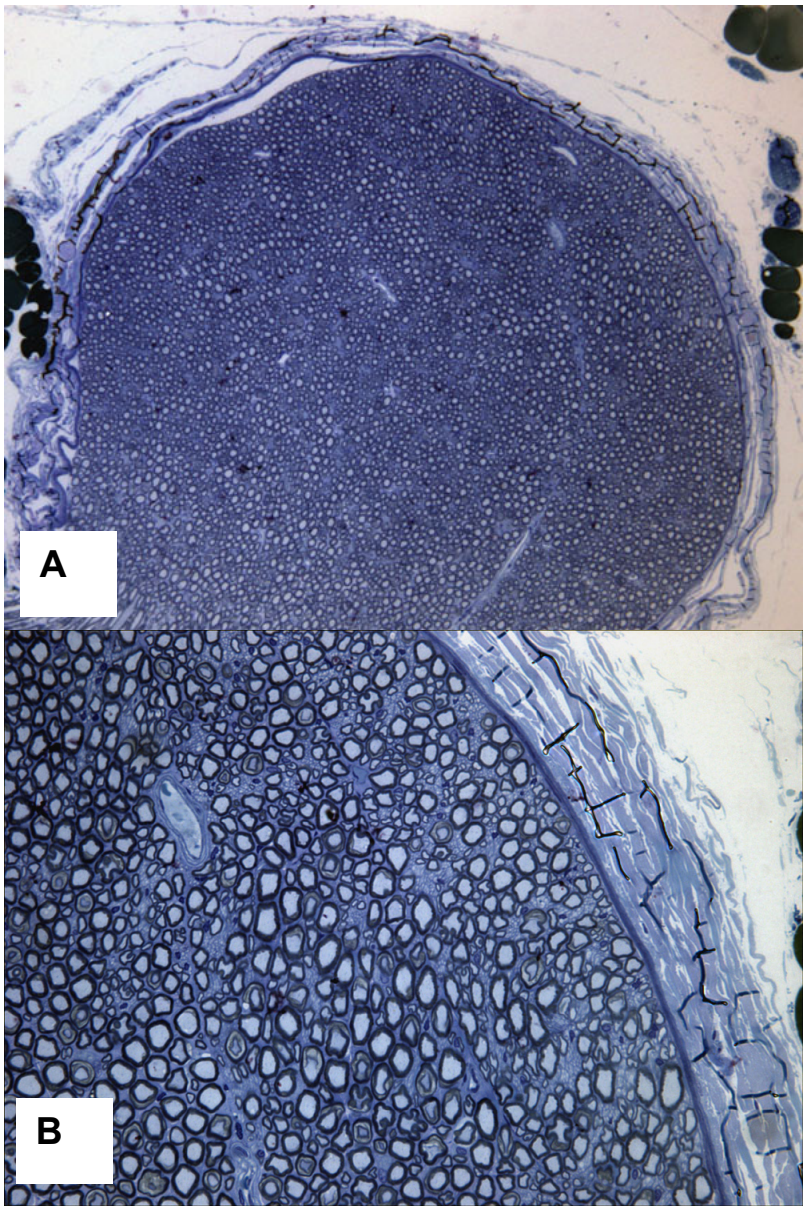

Figure 6 Normal Rat Sciatic Nerve Microanatomy

(A) Image (10x objective lens) of 2 micrometer cross section of normal rat sciatic nerve stained with toluidine blue. Nearly the entire cross sectional area of the sciatic nerve is shown. The dense collagen epineurium encircles the nerve and a circular cross section is noted. A large venule can easily be distinguished in (B) at (40x objective).

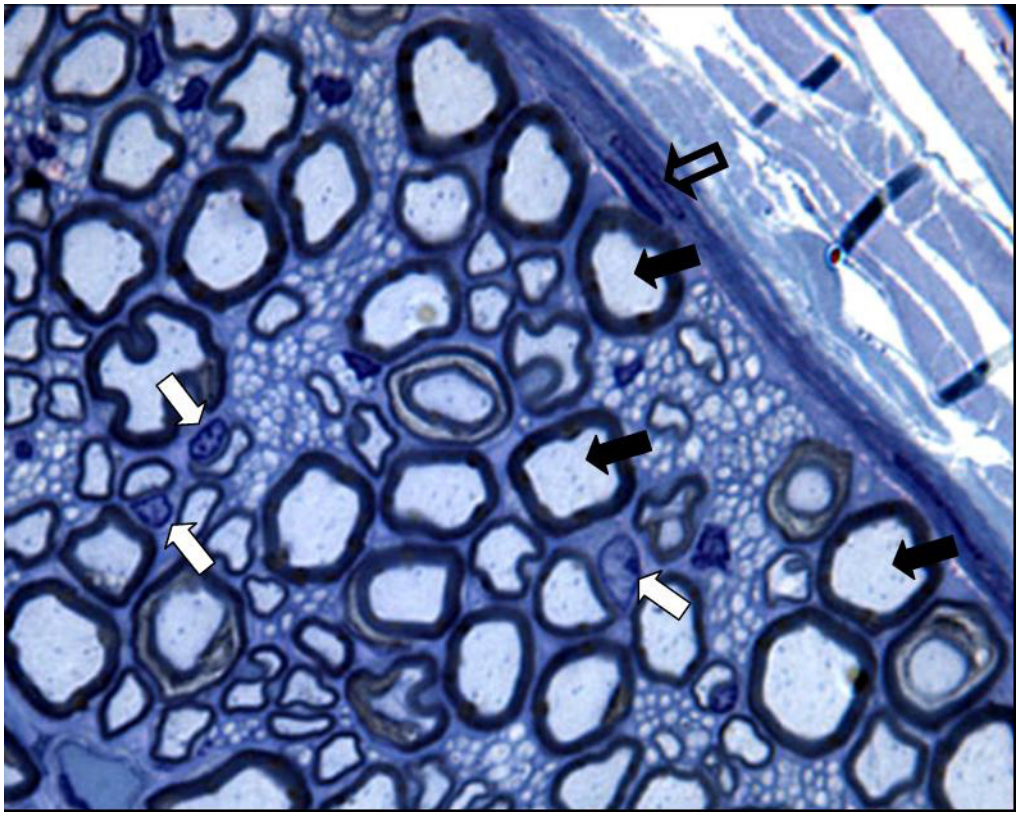

Figure 7 Normal Sciatic Nerve High Power Micrograph

Many small unmyelinated axons are visible between the larger myelinated axons (solid black arrows). The thick dark blue border that encircles these large axons is the myelin sheath. It appears as one thick layer, multiple layers of the myelin sheath can be resolved with the electron microscope. In the center of these large axons, very small dark staining bodies are discernable. From studies using electron microscopy, these are known to be mitochondria. Schwann cell nuclei (white arrows) can be identified in close proximity to the axonal myelin sheath. Some axons appear to have a double ring of myelin, this is a region of Schwann cell cytoplasm either perinodal or at a Schmidt-Lanterman cleft. In the upper right corner of the image, collagen bundles of the epineurium are visible along with a perineurial cell nucleus (open black arrow).

Nerve Conduction In Myelinated Axons

Voltage-gated sodium channels are highly concentrated at the nodes of Ranvier. When they reach threshold potential, these channels open and sodium rapidly flows into the axon down an electrochemical gradient. This depolarization creates the voltage differential that forces the current to flow, and propagates the

nerve action potential along the axon (Oh 1993). Voltage gated potassium channels allow potassium to flow out of the axon down a electrochemical gradient hyperpolarizing the axonal membrane. The sodium potassium pump and potassium leak channels are responsible for establishing the resting membrane potential of -75mV. Myelin insulates axons between nodes, and permits current to flow easily from node to node with out signal loss. This saltatory nerve conduction greatly increases conduction velocity (Daube 1996). Another factor influencing conduction velocity is axon diameter; larger axons have less axoplasmic electrical resistance so they are faster conducting (Daube 1996). The largest axons with the thickest myelin sheath are therefore the fastest conducting axons. Thus, the number of myelinated axons and the size distribution of myelinated axons in the distal stump of a regenerating nerve provide 2 indices by which to evaluate nerve regeneration (Bain, Mackinnon et al. 1988; Keeley, Atagi et al. 1993; Chamberlain, Yannas et al. 1998; Evans, Brandt et al. 1999; Hashimoto, Suzuki et al. 2002). The number of myelinated axons in the nerve guide tube was assessed in this study.

Summary

In the future, nerve repair should combine the concepts that have successfully improved nerve regeneration, such as those containing longitudinally oriented fibers, constructed of a biomaterial that is both resorbable over time and kink-resistant for the first several weeks post-implantation. Type I

collagen tubes packed with longitudinally oriented collagen microfilaments or packed with longitudinally oriented collagen microtubes, were tested in this study. We hypothesized this architecture would optimize the surface area available for cell migration and axon elongation, and that it would prevent collapse of the guide tube during the early phase of regeneration. Both of these factors should improve axon elongation and navigation into the distal nerve stump when incorporated in nerve guides used to repair gap injuries.

Numerous investigators have demonstrated that adding exogenous neurotrophins improves nerve regeneration through guide tubes (Utley, Lewin et al. 1996; Santos, Rodrigo et al. 1998; Yin, Kemp et al. 2001; Fansa, Schneider et al. 2002; Fine, Decosterd et al. 2002). There are, however, questions as to which single neurotrophin or combinations of neurotrophins provide optimal nerve regeneration. Additionally, the optimal delivery method of exogenous neurotrophins has not been determined (Evans 2000; Lundborg 2000; Lundborg 2002).

Another technology recently employed to improve axon regeneration across long nerve gaps is the use of cellular grafts (Fansa, Schneider et al. 2001; Hadlock, Sundback et al. 2001; Mosahebi, Fuller et al. 2002). Although Schwann cell-laden grafts may aid regeneration by providing trophic support and extracellular matrix molecules, there is currently no practical way to deliver this technology in a clinical setting (Mosahebi, Fuller et al. 2002). What is needed is

a ready “off the shelf” nerve guide that provides the clinician and patient a viable alternative to the autograft.

Our goal in this study was to optimize nerve guide architecture for entubulation repair before we proceeded with the inclusion of trophic factors or adhesion molecules in our design. We believe that once nerve guide architecture is optimized it will provide a better platform from which to study the benefits of exogenous growth factors on nerve regeneration.

We used histological, electrophysiological, and functional assessments to provide evidence of nerve regeneration in this study. It is imperative to understand how regenerating axons interact with collagen guidance channels and to determine if more axons grow through nerve guides with guidance channels than grow through empty nerve guides. We designed histological assessments to answer these questions. Many investigators studying nerve regeneration through nerve guides have successfully used axon counting and axon diameter measurements to assess nerve regeneration (Bain, Mackinnon et al. 1988; Keeley, Atagi et al. 1993; Chamberlain, Yannas et al. 1998; Evans, Brandt et al. 1999; Hashimoto, Suzuki et al. 2002).

If axons grow through the nerve guide, but do not enter the distal nerve stump and eventually reinnervate muscle, it cannot be considered a successful nerve repair. Therefore, electrophysiological assessments, including measurement of latency and amplitude of evoked compound muscle action potentials (CMAPs), and calculations of conduction velocity, are frequently used

to assess nerve regeneration following nerve repair. Such methods can confirm muscle reinnervation (Bain, Mackinnon et al. 1988; Archibald, Krarup et al. 1991; Keeley, Atagi et al. 1993; Chamberlain, Yannas et al. 1998; Valero-Cabre, Tsironis et al. 2001). Additional electrophysiological methods provide an estimate of the number of motor units in a muscle following nerve injury (1996; Krarup, Archibald et al. 2002). We employed these methods in the present study.

It must be noted that regenerating axons sprout multiple growth cones and frequently form simultaneous synaptic connections with agonist and antagonist muscles (Valero-Cabre, Tsironis et al. 2001). Functional reorganization of newly re-afferented cortical and cerebellar regions challenge motor control (Lundborg 2000). The need to assess motor function as a measure of nerve regeneration cannot be overstated, as it is the ultimate goal of nerve repair to restore function. This study incorporated two sciatic function indices that have been used by many investigators who have studied muscle function recovery following nerve transection and entubulation repair (de Medinaceli, Freed et al. 1982; Bain, Mackinnon et al. 1988; Bain, Mackinnon et al. 1989; Hare, Evans et al. 1992; Keeley, Atagi et al. 1993; Evans, Brandt et al. 1999; Evans, Brandt et al. 2000).

Chapter 3: Materials And Methods

Animals

Ninety 250g male Lewis rats were used in this study. The Lewis rat was chosen because this strain displays autophagia of the denervated limb less frequently than other rat species (Hare, Evans et al. 1992; Chamberlain, Yannas et al. 1998). The number of animals chosen is based on the minimum number necessary to apply statistical analysis that will discriminate between groups. The animals were housed in the fully accredited animal facility in the University of South Florida Division Comparative Medicine. There are four fulltime licensed veterinarians in the Division of Comparative Medicine to offer any veterinary care if the need had arisen. Animals were housed in pairs, and provided with food and water *ad libitum.* They were on a 12-hour light/dark cycle. Rats were randomly assigned to each group. Twenty rats were designated to receive autograft nerve repair (AG), twenty rats were designated to receive empty collagen nerve guides (CT), twenty rats were designated to rats received nerve guides with filaments inside (MF), and twenty rats were designated to receive nerve guides that contained microtubes inside (MT). For each type of nerve repair (AG, CT, MF, MT) there were two time points: 6 weeks and 12 weeks.

The rats in each repair group were divided equally to each time point so there were initially 10 rats per group at each time point. During the course of the study five additional rats were added, 2 rats were added to the 12 week MT group and 3 rats were added to the MF group. The CT group also contained a 24-week time point with 5 animals. Table 1 summarizes the number of rats in each nerve repair group and each time point.

Table 1 Nerve Repair Groups and Time Points

Nerve Repair Type	Survival Time	Number of Rats per group
Autograft (AG)	6 weeks	10
Empty Collagen Tube (CT)	6 weeks	10
Collagen tube with filaments (MF)	6 weeks	10
Collagen tube with microtubes (MT)	6 weeks	10
Autograft (AG)	12 weeks	10
Empty Collagen Tube (CT)	12 weeks	10
Collagen tube with microtubes (MT)	12 weeks	12
Collagen tube with filament (MF)	12 weeks	13
Empty Collagen Tube (CT)	24 weeks	5
Total Number of Animals		90

Nerve Guide Fabrication and Design

All type I collagen used in this study was derived from bovine tendon collagen. Collagen Matrix Inc. was responsible for the purification of bovine type I collagen and fabrication of the nerve guides according to the following methods and design specifications. A fixed dry weight (5.0 % of the collagen dry weight) of heparin (Diosynth, Chicago, IL) was added to a collagen and lactic acid dispersion. The collagen and heparin dispersion was homogenized and the solution was brought to the isoelectric point of collagen (pH 5.0). This coacervated (quantitatively co-precipitated) the collagen-heparin dispersion. All

components of the nerve guides were fabricated with this type I collagen and heparin composite material. The heparin molecule was incorporated into the collagen in order to bind and provide a slow release for both exogenous bFGF and laminin for the Phase III rat sciatic nerve study. Heparin was used in this study to avoid it being a confounding variable when attempting to systematically determine the effect of bFGF and laminin in phase III. All components of the nerve guides in this study (phase II) were fabricated with the collagen-heparin composite. Hereafter, the collagen-heparin composite is simply referred to as collagen.

The coacervated fibers were spun onto a rotating mandrel and then freeze-dried. The outer collagen tube which contains the guidance channels within it, has a diameter of 1.5 mm and 0.1 mm wall thickness. Bovine type I collagen filaments of 50-100 μm diameters were produced by adjusting the extrusion nozzle. Microtubes with an inner diameter of 0.2-0.6 mm were produced in the same fashion as the outer collagen tubes. All outer collagen tubes and microtubes were mechanically crimped, leaving longitudinal folds to improve resistance to kinking. The tubes were cross-linked with formaldehyde gas to improve tensile strength and to control the rate of *in vivo* degradation. They were targeted to degrade within 3 months. The collagen filaments and guide tubes are cross linked in the same manner as the outer tubes. Prior studies on crosslinking of purified bovine collagen and *in vivo* resorption have been carried out by Dr. Li (Cloft, Kallmes et al. 2000). The length of the

microtubes and filaments are 10 mm. When assembled and packed longitudinally into the outer 14mm length tube there will be 2mm region on each end of the guide tube that does not contain guidance channels. This empty region allows for insertion of the sciatic nerve stumps during the nerve repair procedure. Nerve guides that contain microtubes as guidance channels, contained 5 microtubes in the lumen of the larger guide tube. Nerve guides with filaments, contained 32 collagen filaments in the lumen of the outer guide tube. In the tubes that contain filaments, the guidance channels are formed by the spaces that exist between the solid collagen filaments. Figure 8 provides a three dimensional visualization (not drawn to scale) of the three nerve guides that were used in this study. Figure 9 provides a cross-sectional schematic diagram of the three nerve guides.

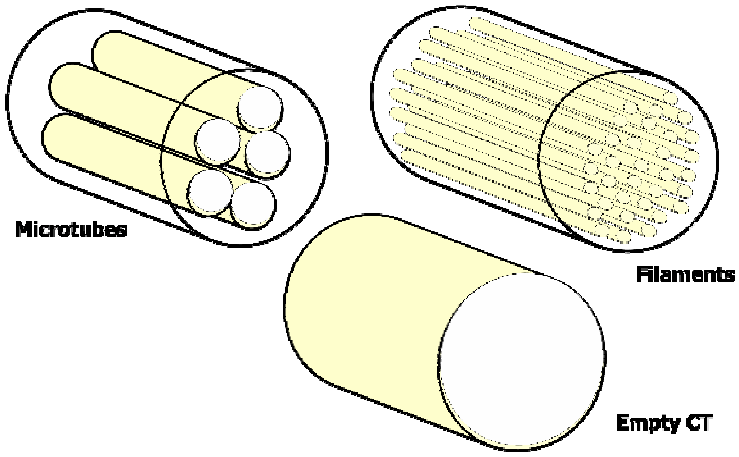

Figure 8 Three Dimensional Schematic of Collagen Nerve Guides

Schematic diagram (not drawn to scale) of the three designs of collagen nerve guides used in this study. (Top left) depicts the nerve guide with 5 hollow collagen microtubes with in the lumen of an outer collagen nerve guide. (Top right) depicts the nerve guide with 32 solid collagen filaments with in the outer collagen nerve guide. In this design, the microguidance channels are provided by the space between the solid filaments. (Bottom center) is the empty collagen nerve guide.

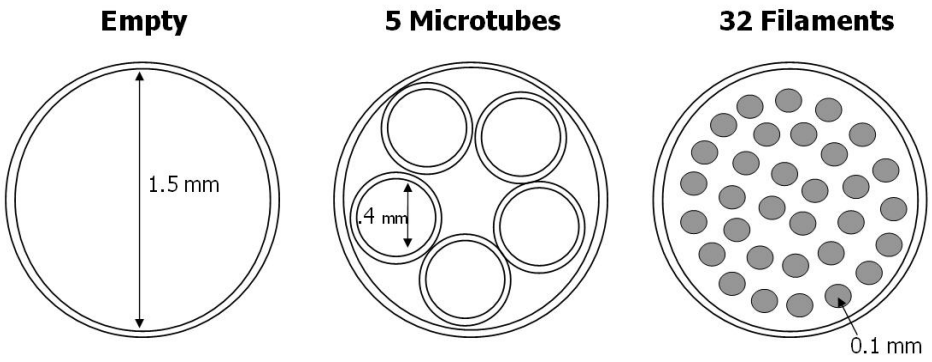

Figure 9 Cross Section Schematic Diagram of Nerve Guides

Schematic diagrams (not drawn to scale) of the cross-section of the three collagen nerve guides used in this study. All dimensions given are from dry nerve guides. The outer tube wall thickness is 0.02mm and the inner diameter is1.5mm for all three nerve guides. The nerve guide in the middle contains 5 collagen microtubes with a wall thickness of 0.02mm and an inner diameter of 0.4mm. The nerve guide on the right contains 32 solid collagen filaments, each with a diameter of 90 μm. The theoretical maximum surface area as calculated from dry dimensions: Collagen tube (CT) = 17.1mm², Collagen tube with microtubes (MT) = 179.2 mm², collagen tube with filaments (MF) = 147.6 mm².

Residual formaldehyde was less than .04% of the nerve guide by weight following the crosslinking step (communication Jenssen, 2004). Nerve guides were packaged and sterilized by gamma irradiation. Although in many animal studies, the aldehyde cross linking step is accepted as a sterilization procedure, the food and drug administration (FDA) mandates that implants for human use are more stringently sterilized. Since the ultimate goal of this study is to provide a product that can be used in humans, it is designed and tested as such. This step has more significance for the phase III rat study, which incorporates growth factors and laminin into the nerve guides. Irradiation affects the activity of these molecules, so their concentrations must be set initially to allow for this loss of activity. They undergo testing in cell culture prior to implantation in the rat.

Nerve Repair

The rats were anesthetized with an intraperitoneal injection of a mixture of ketamine HCl (90 mg/kg) and xylazine HCl (10 mg/kg), the hindquarters shaved on the right side, scrubbed with Betadine, and draped with a sterile towel while in the left side lying position. The right sciatic nerve was exposed through a longitudinal muscle splitting incision in the mid-thigh and dissected free from the underlying muscle bed (figure 10). The nerve was further anesthetized with several drops of 2% lidocaine (Butler). The sciatic nerve was then transected with sharp scissors at the mid-thigh level and a 2 mm segment resected. The proximal nerve stump was inserted 2mm into the lumen of one end of a 14 mm long collagen guide tube and fixed in place with a single sling stitch (7.0 Vicryl). Next, the distal nerve stump was inserted into the other end of the nerve guide and sutured in the same fashion. Removal of a 2 mm segment of the rat sciatic nerve provides an acceptable balance between the nerve slack lost due to retraction of the proximal and distal sciatic nerve stumps, which occurs immediately upon transection, and the length gained by the addition of the nerve guide, which contains the 10 mm gap lesion within its lumen. In this model, this procedure eliminates excessive tension on the newly repaired nerve. Figure 11 provides an schematic illustration of the surgery. Polyglycolic acid (Vicryl) suture was chosen for the repair since it is resorbable and causes minimal inflammation. A small gauge needle and suture were chosen to minimize trauma to the sciatic

nerve stumps. The muscle borders were approximated and then sutured with 3.0 Vicryl. Next, the skin incision was closed with stainless steal staples (Autoclip).

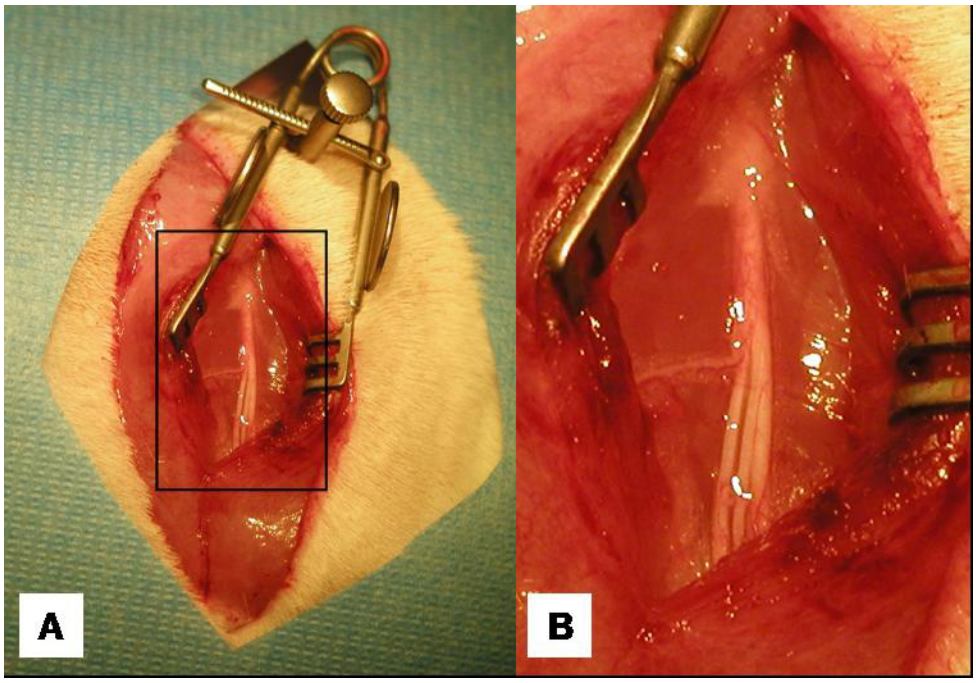

Figure 10 Surgical Exposure of the Rat Sciatic Nerve

(A) Rat sciatic nerve viewed through the muscle splitting incision at the mid thigh of the hind limb. (B) Magnified view from enclosed region in (A).

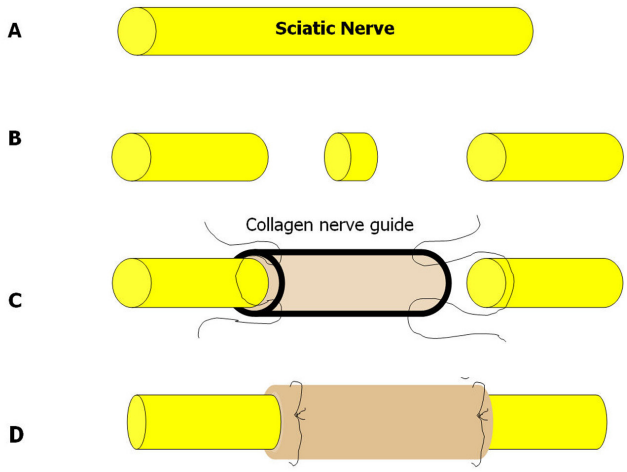

Figure 11 Schematic Diagram of Nerve Transection & Entubulation Repair

(A) Sciatic nerve, (B) Nerve transection, and resection, (C) & (D) entubulation repair. The nerve was transected at mid thigh and 2 mm segment resected. The collagen nerve guide was placed into the surgical field and aligned with the proximal sciatic nerve. A single suture was place through the nerve guide, then through the proximal sciatic nerve, and again through the nerve guide. The suture was pulled taught to pull the nerve into the guide tube. The suture was tied to secure the repair while maintaining the patency of the nerve guide. This process is repeated on the distal nerve stump to complete the repair.

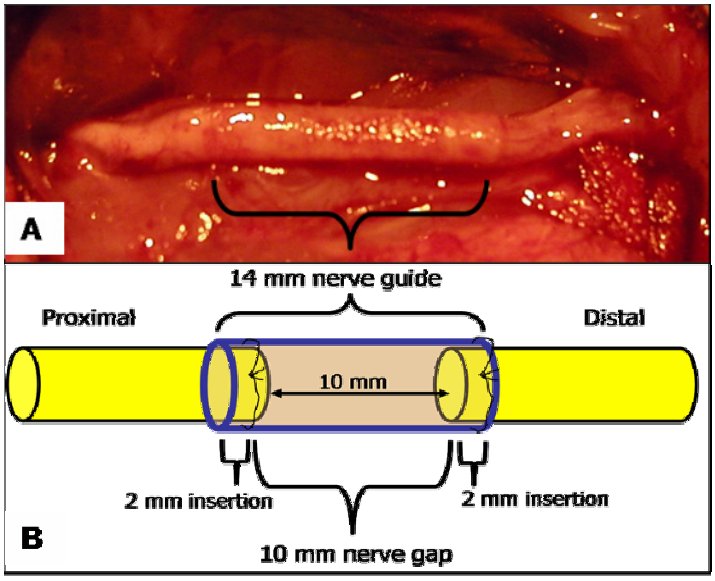

Figure 12 Schematic Diagram of Entubulation Nerve Repair

Image (A) is of an entubulation nerve repair of the rat sciatic nerve *in vivo*. Image (B) illustrates the nerve guide as if it were transparent, allowing visualization of the final 10 mm nerve gap at the conclusion of the repair.

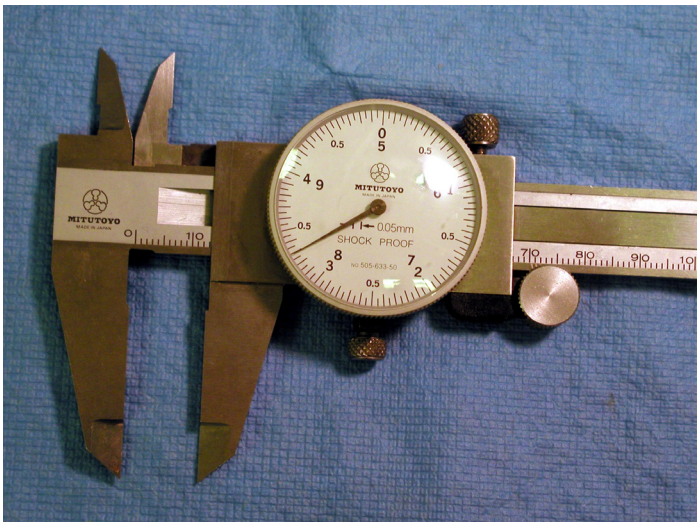

Figure 13 Calipers for Measuring Sciatic Nerve

Vernier calipers used for all measurements during the initial surgical procedure and the terminal electrophysiological procedure.

After completion of the surgery, the animal was observed and its body temperature maintained with a thermostatic heating pad until it awoke and moved about the cage. To minimize post operative pain, rats received buprenorphine (Buprenex, 0.1-0.5 mg/kg) via intramuscular injection twice daily for three days following surgery. They received biweekly sessions of passive range of motion to the right hip, knee, and ankle to minimize joint contracture in the right hindlimb throughout the six or twelve week time points. The rats were housed two per cage, kept on a 12-hour light/dark cycle, provided with standard rat chow and water *ad libitum* following the surgery. We removed the skin staples seven days after the nerve repair surgery.

Functional Assessment

Walking Tracks

A sciatic function index (SFI) was calculated from walking track measurements (de Medinaceli, Freed et al. 1982). The rats' hind paws were dipped into black non-toxic water-soluble ink (Evans, Brandt et al. 1999). The rats walked across a clean sheet of white paper that had been place in the walking chamber (10 cm wide x 85 cm long), leaving footprints from the hind limbs. After several practice sessions, the rats became accustomed to the walking track and walked directly to the other end of the chamber into a dark box. The paper sheet with ink footprints was left to dry before measurements were taken. Print length (PL) was measured from the heel print to the farthest mark left by the toes. Toes spread (TS) was measured from the widest prints made from the first and fifth toes. Intermediate toe spread (ITS) was measured from the middle of the second to forth toe. The largest value, during each walk, for each parameter was recorded. Walking tracks were taken prior to surgery and at weeks 1, 3, 6, 9, and 12 following surgery.

The use of walking tracks to assess sciatic nerve function after injury is a widely used method and was first implemented by De Mendinaceli in 1982 (de Medinaceli, Freed et al. 1982). De Mendinaceli's formula for SFI includes a measurement of step length from one foot to the opposite foot. Bain (1989) modified De Mendinaceli'sl SFI formula to exclude the distance to opposite foot measurement, as it is believed to be an inconsistent indicator of changed sciatic

nerve function following injury (Bain, Mackinnon et al. 1989). This modified formula was used for this study.

Formula: SFI = -38.3 ((EPL-NPL)/NPL) + 109.5((EPS-NTS)/NTS) + 13.3 ((EIP-NIT)/NIT) – 8.8

This formula contains several correction factors that cause the toe spread measurements to most heavily reflect in the final SFI. The formula creates an index and during normal sciatic function, the calculated value is approximately zero. Following sciatic nerve transection there is complete conduction block to the previously innervated muscles. The print length measurement increases because the rat is unable to actively plantar flex the ankle and support weight on its toes (de Medinaceli, Freed et al. 1982). The toe spread measurements decrease because the rat is unable to abduct the toes. The intrinsic muscles of the foot that abduct the toes have their innervations originating in the sciatic nerve (Greene 1968; Woodburne and Burkel 1988). The calculated value of the SFI under these conditions is approximately –100. As reinnervation of target muscle takes place the SFI value increases from –100 back toward zero, thus providing a functional index of sciatic nerve regeneration (Evans, Brandt et al. 1999).

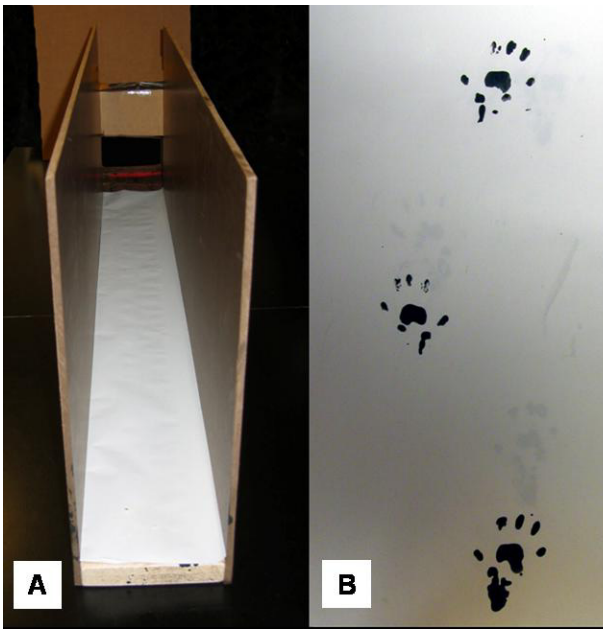

Figure 14 Walking Tracks For Sciatic Function Index

(A) Walking track lined with white paper used to record the rats' hind limb footprints, which enables calculation of the sciatic function index (SFI). (B) Prints taken from a rat prior to sciatic nerve injury.

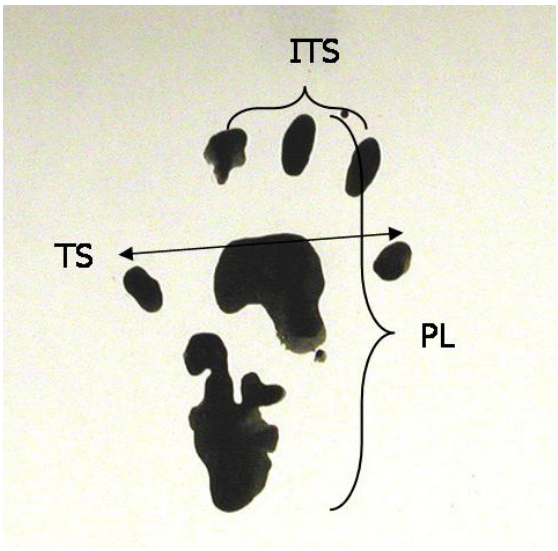

Figure 15 Enlargement Of Normal Rat Hind Paw Print

Enlargement of a normal rat hind paw demonstrating the three measurements obtained for calculation of the SFI. Intermediate toe spread (ITS) is the distance between the 2nd and 4th toes. Toes spread (TS) is the distance between the 1st and 5th toes. Print length (PL) is the distance from the furthest mark left by the heel to the tip of the 3d toe. These values were recorded for the experimental hind paw prints, the contralateral paw, and were entered into a formula to calculate the SFI.

Static Stance

A second index, percent of pre-injury toe spread, was calculated from static stance photographs. The rats were placed in a clear Plexiglas box (20x20x20 cm) supported on a frame above a 45 degree angled mirror. This apparatus allowed a photograph to be taken of the plantar aspect of the feet. A ruler with a millimeter scale was included in the image to allow calibration of the software (ImageJ, NIH) measuring tool. The digital photographs allowed a more accurate measurement of toe spread than could be obtained by measuring the ink walking tracks. Static stance phototgraphs and measurements were taken prior to surgery, one week following surgery, and at the final six or twelve week time point. A static stance sciatic index was calculated by dividing the toe spread at the terminal time point into the pre injury toe spread to obtain percent of normal toe spread. Bervar (2000) used a video camera to obtain similar images and found that using this simple formula did not decrease accuracy significantly for determining sciatic nerve function (Bervar 2000).

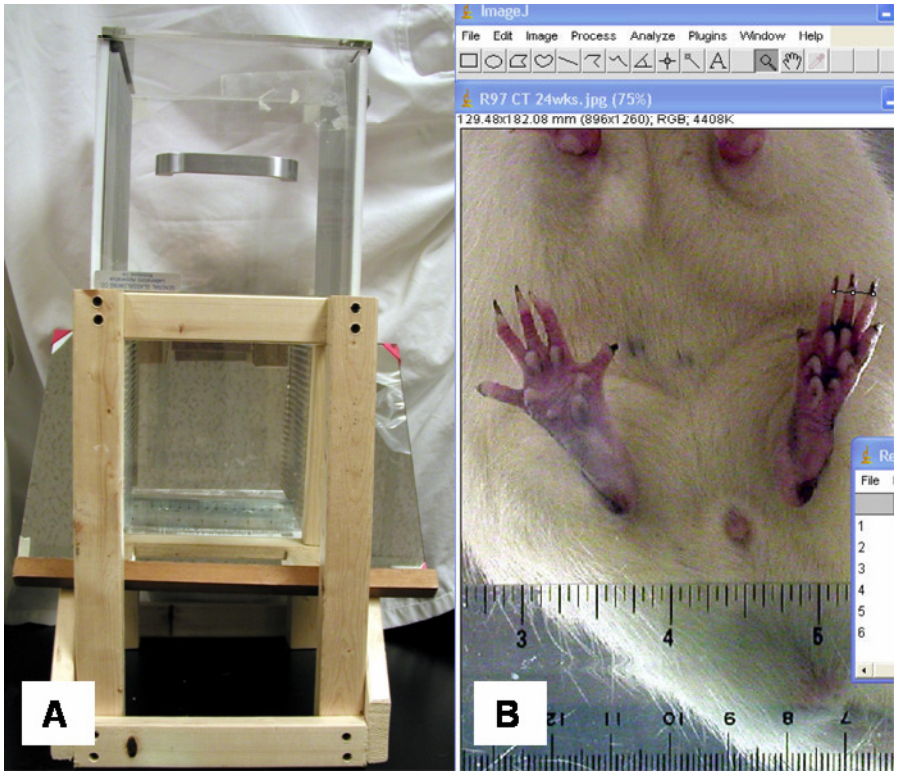

Figure 16 Image Static Stance Photography Box

(A) Frame, clear box, and mirror set to a 45-degree incline, was used to capture images of the plantar surface of the rats' hind paws. (B) Image obtained after a rat was placed in the box and a camera was placed on a tripod and aimed at the mirror. A ruler with a millimeter scale is included in the image. When the digital image was imported into the computer and subsequently loaded into the image analysis software (NIH, ImageJ) the ruler was used to set the scale, enabling accurate measurements of both intermediate toe spread and 1st to 5th toe spread.

Electrophysiology

Great efforts were made at the onset of this study to delineate an electrophysiological protocol that would provide objective quantitative data, which would allow testing for statistically significant differences in functional recovery between groups. It was realized at several points during the study that our electrophysiology protocols were not going to give us the quantitative data on which we had originally planned. After consultation with by Drs. Liuzzi, Madison,

and Li, decisions were made to modify the electrophysiology methods several times during the course of this study. We started the study recording evoked compound nerve action potentials directly from the sciatic nerve distal to the repair. We then changed the protocol to record compound muscle action potentials from muscles innervated by the sciatic nerve. There were several derivations of muscle recording techniques.

With each change in protocol, we believe the accuracy and relevance of the data improved. However, this came at the cost of inadequate and non-uniform sampling of the different repair groups and time points needed for statistical analysis. We accepted this trade off, during the guidance channel (phase II) rat study, because we wanted the most refined methods prior to entering the growth factor and adhesive molecule phase (phase III) of the study at USF. The results of these different methods and the discussion of their limitations are elaborated upon in the respective sections of the dissertation.

General Electrophysiology Principles

When either the nerve or muscle depolarize in the region perpendicular to the active extracellular recording electrodes the electrical potential becomes more negative relative to the reference electrode (Oh 1993). This is represented by a negative deflection on the computer monitor at the positive electrode. However, the cathode is used as the active recording electrode, so the initial deflection on the computer monitor appears in the positive direction (Misulis

1997). By convention, it is referred to as the negative deflection of the compound muscle action potential (Misulis 1997).

Latency, measured in ms, from the stimulus to the initial negative deflection from baseline of the supramaximal CMAP is the time it takes for the fastest conducting axons to conduct the action potentials from the stimulating electrodes, down the sciatic nerve, and to depolarize muscle tissue under the recording electrodes (Oh 1993). Estimates of nerve conduction velocity (NCV) can be calculated by dividing the distance in millimeters from the stimulating electrode on the sciatic nerve to the active recording electrode in the gastrocnemius by the latency of the CMAP. Latency is defined either as the time interval between the stimulus and the peak of the first negative deflection of the CMAP, or as the time interval between the stimulus and the first deviation from baseline of the CMAP. Finally, the amplitude, measured in mV, of the supramaximal CMAP was noted.

Although latency or latency divided by distance, provide an estimate of conduction velocity, a more accurate method for evaluating nerve conduction velocity was employed near the end of this study. By first stimulating the sciatic nerve proximal to the repair site (S1), and recording supramaximal CMAPs from the gastrocnemius muscle, and then stimulating the sciatic nerve distal to the repair site (S2), while recording from the same gastrocnemius recording electrode, two latency values are derived. In normal nerve, the latency is shorter from the S2 site than S1 because the nerve conducts over a shorter distance to

the recording electrode in the gastrocnemius muscle. The distance from each stimulation site to the active recording electrode in the gastrocnemius muscle is measured with calipers and recorded. Finally, NCV across the nerve repair site is calculated by taking the difference in the two distance measurements and dividing it by the difference in the latency values.

To verify that the recorded signals are indeed derived from the nerve of interest, some investigators cut the nerve at the end of the experiment (Krarup, Archibald et al. 2002). If a stimulus no longer produces a CMAP following nerve transection, there is confirmation that the previously recorded signal originated from the nerve of interest. While this provides a control, it prevents fixation by perfusion and the possibility to test for correlations between the electrophysiological results and the histological results in the same animal. In this study we perfused the rats to optimize tissue fixation for morphological study. This is an important design element of this study.

One important consideration in this study was the possibility that while inserting needle electrodes into the gastrocnemius in animals with muscle atrophy, the needle would pass into deeper posterior tibial muscles. Therefore, every attempt was made to prevent this from occurring. It is important to realize, however, that all deep muscles below the knee have their innervation originating in the sciatic nerve (Greene 1968; Woodburne and Burkel 1988). This means that all CMAPs recorded from this region, following repair of the sciatic nerve, should represent successful reinnervation via the nerve graft.

Animal Preparation for Electrophysiology

At 6 or 12 weeks post nerve guide implantation, rats were anesthetized with an intraperitoneal injection of a mixture of Ketamine (90 mg/kg) and Xylazine (8 mg/kg). Anesthesia was maintained with supplemental injections. The animal was prepared for surgery as previously described and body temperature was maintained at 37°C on a thermostatic pad. The right sciatic nerve was reexposed through a longitudinal muscle splitting incision in the mid-thigh. The nerve repair site was typically surrounded by fibrous adhesions, but immediately proximal to this region normal nerve was identified. Recording electrodes were connected to a bio amplifier (AD/Instruments) which was wired to a signal integration unit (AD/Instruments PowerLab 4/SP). This equipment displays the recorded signal on a computer monitor. The electrophysiological methods evolved during the course of this study and each method is described below in the order they were implemented.

Method 1: Compound Nerve Action Potentials

The first electrophysiology method used in this study was the recording of the sciatic compound nerve action potential (CNAP). The nerve was exposed as described above, and carefully mobilized from the underlying tissue interface before it was suspended on two pairs of hook electrodes (Figure 17). The stimulating electrode pair was place proximal to the nerve repair site with the

distal hook set as the cathode. The pair of recording electrodes was placed immediately distal to the repair site. With this set up, only nerve conduction across the repair site was recorded. A piece of Parafilm was cut and placed between the nerve and the underlying muscle to facilitate isolation of the stimulus and recording electrodes, and to prevent conduction though ionic fluids present in the surgical area. We slowly increased the stimulus intensity from zero and noted both the stimulus level in milliamperes (mA) at which a visible muscle twitch below the knee could first be observed and the lowest stimulation level at which a CNAP was recorded. This was performed on the contralateral normal sciatic nerve in the same manner.

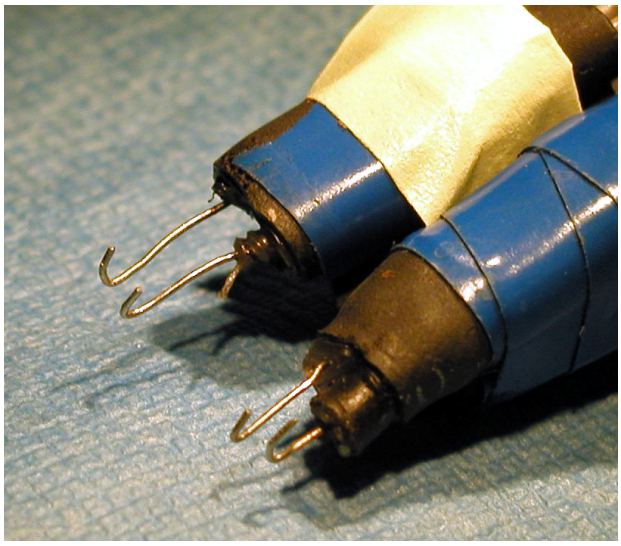

Figure 17 **Hook Electrodes for Elevating the Sciatic Nerve**

Method 2: Compound Muscle Action Potentials

All of the remaining derivations in the electrophysiology methods used in this study involved recording CMAPs from the gastrocnemius muscle. Initially, we maintained the same stimulation electrode setup as was used for the recording of nerve action potentials. We elevated the sciatic nerve, proximal to the repair site, with a pair of platinum hook electrodes. A monopolar stainless steel uncoated needle electrode was inserted percutaneously in the midpoint of the right lateral gastrocnemius muscle, 30 mm proximal to the calcaneus. This electrode was the cathode and served as the active recording electrode. A second monopolar needle electrode was inserted 5 mm distal to the cathode and was positioned subcutaneously over the gastrocnemius. A second pair of needle recording electrodes was inserted into the interosseous muscle of the third metatarsal space of the right foot. A common ground for each pair of recording electrodes was inserted in the anterior thigh of the same limb. Each pair of recording electrodes was connected to a separate bio amplifier (AD/Instruments) which was attached to a signal integration unit (AD/Instruments PowerLab 4/SP). The signal was displayed on a computer monitor and recorded (figure 18).

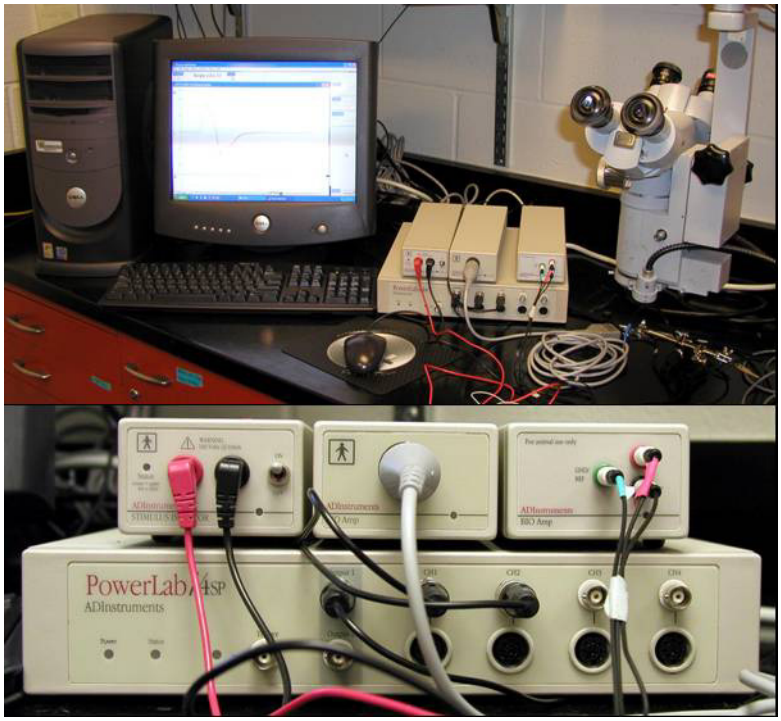

Figure 18 Electrophysiology Equipment with Surgical Microscope

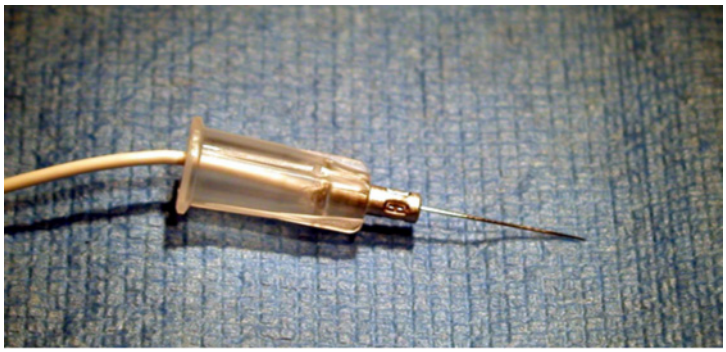

Figure 19 Needle Electrode

10 mm 30 gauge stainless steel monopolar needle electrode used for recording compound muscle action potentials from the gastrocnemius muscle and intrinsic muscles of the rat hind paw.

A notch filter for 60 Hz interference was used during recording along with the high pass filter setting of 10 Hz and low pass filter of 5 kHz. A 20 ms sweep was recorded for each 0.10 ms electrical stimulus to the sciatic nerve. As the

amplitude of the CMAP increased with each increase in stimulus intensity, the recording range was increased to maintain the peak of the CMAP on the screen. This is comparable to reducing the gain in an analog system, which prevents loss of data referred to as clipping. The range of 0.01 mA to 3.0 mA was explored to insure reaching supramaximal intensity (Daube 1996). The supramaximal stimulus is defined as the stimulus above which there is no further increase in the ampitude of the CMAP (Oh 1993; Misulis 1997). Above 2-3 mA of stimulus intensity, volume conduction can occur and thus, any CMAP's recorded are not physiologically relevant (Personal communication, R. Madison, 2003).

Method 3: Motor Unit Number Estimation (MUNE)

Upon the implementation of the motor unit number estimation (MUNE) technique, we modified the stimulatory electrode setup by discontinuing the use of the hook electrodes for stimulating the sciatic nerve. The new cathodal stimulating electrode was a platinum wire shaped into an inverted Y. It was lowered onto the nerve proximal to the repair site, positioned to maximize contact with the nerve, and held in place by a small manipulator. The anodal stimulating electrode was placed deep into the gluteal muscle adjacent to the sciatic nerve approximately 10 mm proximal to the cathode. The recording electrode was inserted percutaneously into the gastrocnemius muscle as previously described. The filters were set as in the previous muscle recording method.

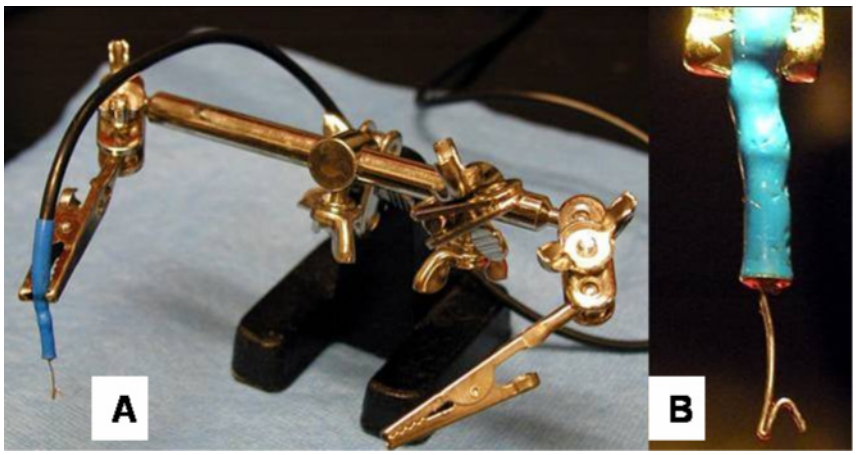

Figure 20 Cathode Stimulator Held By Manipulator

Manipulator used to hold the cathode electrode over the top of the sciatic nerve during the electrophysiological assessments. (B) magnified view of the platinum wire electrode used to stimulate the sciatic nerve proximal to the region that was repaired.

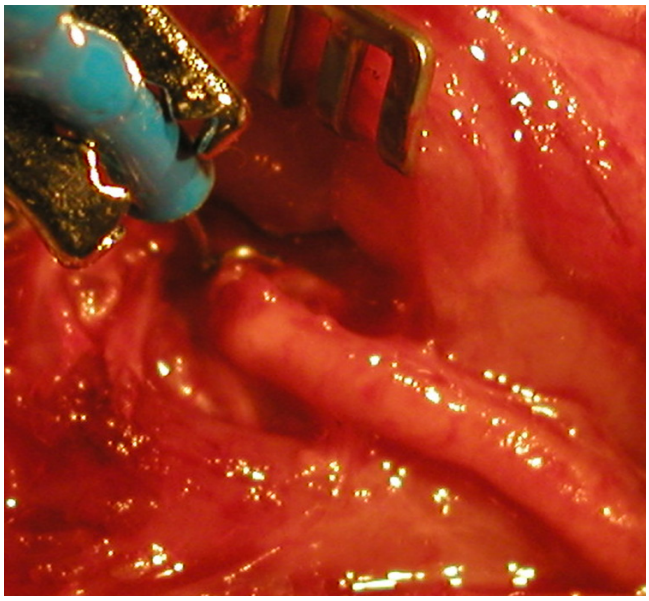

Figure 21 Stimulating Electrode Proximal to Nerve Guide

The intensity of the stimulus was increased in small increments until a small CMAP appeared on the monitor. The stimulus was increased further, in small increments, and five traces were recorded at each stimulus intensity. Between each stimulus, a 1-second delay was provided to prevent fatigue.

To facilitate analysis, an overlay of all recorded CMAPs was displayed on the monitor to allow the identification of separate and unique waveforms. As the CMAP amplitude increased with increased stimulus intensity it represents the summation of CMAPS previously identified at lower stimulus intensities (1996; Krarup, Archibald et al. 2002). For any CMAP between threshold and the supramaximal stimulus, subtracting the amplitude of the preceding CMAP gives the approximated amplitude size of a motor unit. This was performed for 5-10 distinct CMAPs above threshold. The differences in amplitudes of the individual motor CMAPs were then averaged to obtain a more accurate representation of the average motor unit amplitude. This number was then divided into the amplitude of the supramaximal CMAP to arrive at an estimate of the total number of motor units (McComas, Fawcett et al. 1971; Daube, Gooch et al. 2000; Krarup, Archibald et al. 2002). This method has been termed the statistical MUNE method since an average is calculated (Daube 1995; Shefner 2001). The statistical motor unit number estimation method has been proven more reproducible than the multiple point method, which involves moving the stimulating electrode along the nerve to obtain different wave forms (Daube, Gooch et al. 2000). When the incremental method was compared with multipoint methods in transgenic ALS mouse, the results demonstrated .95 correlation (Shefner, Cudkowicz et al. 2002). MUNE has been successfully employed in the study of peripheral nerve regeneration following entubulation repair of the median nerve using collagen tubes in adult monkeys (Krarup, Archibald et al. 2002).

The stimulus isolation unit (World Precision Instruments) uses a 5V pulse from the PowerLab main unit to trigger a constant current output with resolution of .01mA through the 10mA range. Preliminary studies performed in our laboratory have validated that this unit has the sensitivity to adjust current in increments necessary to resolve small quantal increases in CMAP amplitudes. This is necessary for MUNE. Please see the discussion section for an elaboration of the limitations of MUNE in this study.

Method 4: Compound Muscle Action Potentials

The final method used in this study was the recording of the supramaximal CMAPs of the gastrocnemius and intrinsic muscles of the foot using the same setup as before, but with the additional step of transecting and dissecting out the nerve to the biceps femoris muscle that branches from the tibial division of the sciatic nerve proximal to the repair site. The reason for removing this nerve is elaborated upon in the results and discussion sections. In addition, the sciatic nerve was stimulated distal to the repair (S2) and CMAPs were recorded from the same gastrocnemius muscle recording electrodes. Following recording of the gastrocnemius muscle CMAPs from the two stimulating sites described (S1 and S2), the distance from the nerve stimulation sites to the active recording electrode was measured with calipers and recorded. Nerve conduction velocity was calculated from the difference between the distance measurements divided by the difference in the CMAP latencies from each stimulation site.

Tissue Isolation

Following electrophysiological assessment, animals were euthanitized by intraperitoneal injection of pentobarbital (150mg/kg). The animals were transcardially perfused with phosphate buffered saline (pH 7.2) followed by 4% paraformaldehyde in 0.1 M phosphate buffer (pH 7.2). All attempts were made to minimize stress and discomfort of the animals prior to euthanasia. These methods of euthanasia are consistent with the recommendations of the Panel on Euthanasia of the American Veterinary Medical Association. The animal protocol for the proposed study was reviewed by the University of South Florida Animal Care and Use Committee and received approval #1820.

After perfusion the nerve guide was dissected free, divided into proximal, middle, and distal segments (each 3.0 mm in length), post-fixed in 1% percent glutaraldehyde and 2% percent paraformaldehyde in 0.1 M phosphate buffer (pH7.2) for 24 hours followed by 1 hour in 2% osmium tetroxide (Electron Microscopy Sciences). One 3 mm section of the contralateral mid-thigh sciatic nerve was processed in the same manner for a normal control. The nerve specimens were embedded in Araldite/Embed-812 (Electron Microscopy Sciences). Two-micrometer transverse sections were cut from the tissue blocks, floated onto glass slides (Superfrost charged), stained with toluidine blue, mounted (Permount), and cover slipped. Toluidine blue staining of peripheral nervous tissue enables visualization of myelinated axons, blood vessels, mast

cells, macrophages, and other cell types (Chamberlain, Yannas et al. 1998; Hashimoto, Suzuki et al. 2002).

Morphometric Analysis

Partially overlapping images of the entire cross section of the nerve guide/sciatic nerve were captured using a digital camera and 40x objective lens (Qcapture software, Olympus Q-color camera, Olympus BX41 microscope). The images were montaged using commercially available software (Adobe Photoshop Elements 2.0) and saved as one image of the entire cross section of the sciatic nerve (figure 22).

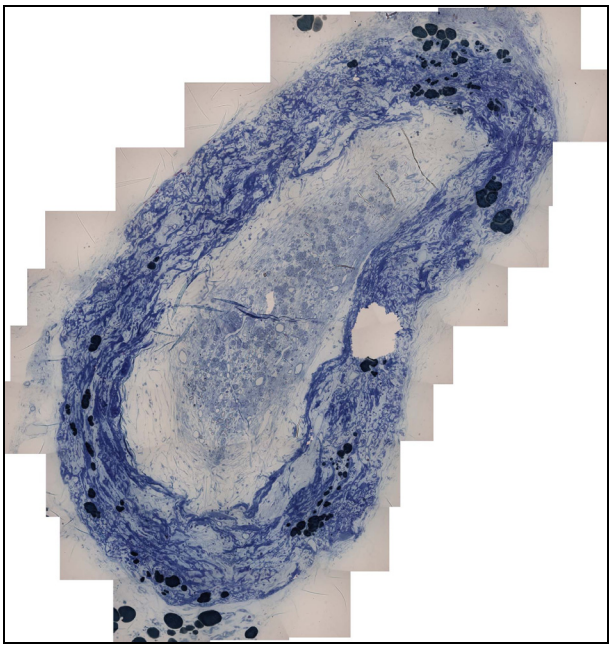

Figure 22 Montage of Nerve Guide

Twenty-four partially overlapping images (40x objective lens) digitally captured (Qcapture software, Olympus Q-color camera, Olympus BX41 microscope) from the nerve guide of an animal that underwent entubulation repair of the sciatic nerve with an empty type I collagen nerve guide 6 weeks prior to tissue harvesting. The images were montaged (Adobe Photoshop Elements 2.0) and saved as one image that incorporated the entire cross section of the sciatic nerve. Although not appreciated, due to the size of the figure above, this montage contains sufficient resolution for the operator to zoom in and identify individual myelinated axons.

The montages varied in size according to the cross sectional area of the regenerated nerve. Every myelinated axon in the images were counted (ImageJ). The image was displayed on the computer monitor and the operator moved a cross hair over an axon using the computer mouse and clicked the mouse (figure 23). The software creates a running tally and this process was repeated until all myelinated axons in the image are counted. The 40x objective lens provides magnification necessary to correctly identify myelinated axons and a field of view that is amenable to creating a montage of the entire cross section.

Nonparametric statistical analyses were performed, using Sigma Stat software to test for significant differences among groups.

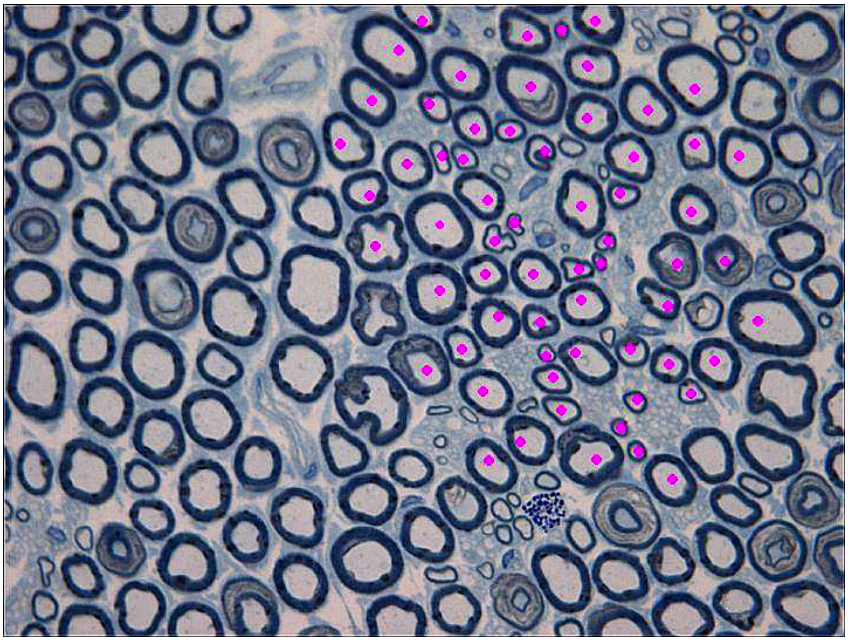

Figure 23 Axon Counting of Normal Nerve

Micrograph of normal rat sciatic nerve shows the method of counting myelinated axons using ImageJ software. A crosshair is moved with the mouse over a myelinated axon and when clicked it leaves a colored dot in the middle of the axon. This prevents recounting of any axon in the image. This micrograph captured through a (100x oil objective lens) is shown for illustration of the method we will use to count axons. The actual axon counting was performed on montages of images since they cover a larger field of view.

Axon diameters were measured (ImageJ) from three (100x oil objective) fields digitally captured from the same sections chosen for myelinated axon counting. In ImageJ the measuring scale is set by photographing an image of a micrometer with the same microscope lens and camera parameters that are used for photographing the nerve images, and then drawing a line with the computer mouse and line tool across a known distance on the micrometer image. This calibrates the pixel dimensions of the digital image to micrometers. Regions with

a high density of myelinated axons were selected for measurement. Magnification provided by the 100x oil objective lens facilitates accurate measurement of axon diameters. A straight line across the shortest distance of the axon cross section, excluding the myelin, was selected for measurement of each axon. Only axons with myelin perimeters entirely in the images were measured. Axons with double myelin rings, such as occurs when Schmidt-Lanterman clefts were in the plane of section, were excluded from measurement to facilitate a more accurate evaluation of axon diameters.

Chapter 4: Results

Introduction

The results section is organized as follows: First, general observations are discussed. Following the section on general observations, a section on descriptive morphology of both the autograft and entubulation repairs is presented. It starts with findings that are generalized to all the nerve repairs in this study and then each repair type are discussed individually. Following this section on morphology, the results from myelinated axon counts and diameter measurements are presented. Next, representative electrophysiological data are presented. Lastly, the results of the walking track and static stance analysis are presented.

General Observations

None of the rats through the course of this study demonstrated autophagia. Many presented with elongated toenails and differing amounts of phalangeal flexion abnormalities of the experimental limb. No animals that survived the initial surgery were lost during the remainder of the study, and those

that were lost due to surgical complications were replaced in order to achieve a minimum of ten rats per group. Several animals were noted to have mild heel ulcerations on the experimental limb. These lesions healed without complication or intervention. All rats presented with significant ankle contractures that limited full plantar flexion of the experimental limb.

At the six-week time point, the proximal and distal ends of the entubulation repair site were readily identified during the surgical exposure, whereas at the twelve-week time point this was more difficult. At six weeks, the intramuscular suture of the biceps femoris muscle had not been fully resorbed and was quite evident. However, at twelve weeks, there was no grossly detectable trace of suture.

To accurately identify the nerve repair site at 12 weeks we relied on anatomic landmarks such as the nerve branch from the tibial division of the sciatic nerve and the underlying gluteal musculature, to identify the collagen guide tube prior to dissection. At both the 6 and 12 week time points, the region of nerve injury and repair was covered with fibrous adhesions. The repairs that went 12 weeks appeared to have more adhesions, thus challenging the identification of the exact site of the nerve guide.

The autograft repairs were covered with fibrous adhesions, but less so than the entubulation repairs with collagen nerve guides. After careful dissection to free the nerve repair site from the adhesions, the 12-week autografts appeared

grossly as normal nerve. The junctions of the nerve graft with the proximal and distal sciatic nerve were indiscernible in most cases.

The fibrous white adhesions tethered the nerve repair to the surrounding muscular interfaces. In contrast, the nerve prior to injury was surrounded by a translucent areolar connective tissue interface, which allows the sciatic nerve mobility independent of the surrounding muscle. This tissue is necessary to prevent traction of the nerve by allowing for the nerve's longitudinal excursion during flexion and extension of the limb joints. This translucent tissue is referred to as the mesoneurium by some surgeons and investigators, however, this terminology is not universally accepted (Mackinnon and Dellon 1988). The fact that this flexible connective tissue, which is adherent to, but distinctly different from the epineurium, is present, in our opinion is indisputable. This change from a translucent mobile connective tissue prior to injury, to an adherent fibrous opaque tissue in the weeks following repair is one of the most obvious changes in the gross anatomy noted during surgical inspection. Another observation made was that once adhesions were carefully dissected from the nerve repair site, a swelling at the proximal union of the sciatic nerve and the nerve guide could be frequently identified.

The nerve to the biceps femoris muscle, which branches from the tibial division of the sciatic nerve proximal to the repair site, was most often adherent to the repair site. This has great relevance to the electrophysiological assessment. Since the stimulatory electrode was placed proximal to the nerve

repair, it stimulated the nerve to the biceps femoris along with the sciatic nerve unless the nerve to the biceps femoris muscle was carefully dissected free from this site and transected. This is elaborated on in the section devoted to electrophysiology results and in the discussion section.

Morphology

In the region of the gap repair, all the successfully regenerated nerves contained myelinated axons of smaller diameter than normal nerves (figure 24). The regenerating axons had a thinner myelin investment at all time points studied. There appeared to be a greater number of both mast cells and blood vessels in the regenerating nerves when compared to normal control nerves. Monocyte derived macrophages aggregated by the suture site, their cell membranes fused, and they became giant cells (figure 25), which phagocytose the polyglycolic acid suture. In contrast to the six week time point, where histological evidence remained of the nerve guide suture fixation, by twelve weeks, suture material had been fully resorbed.

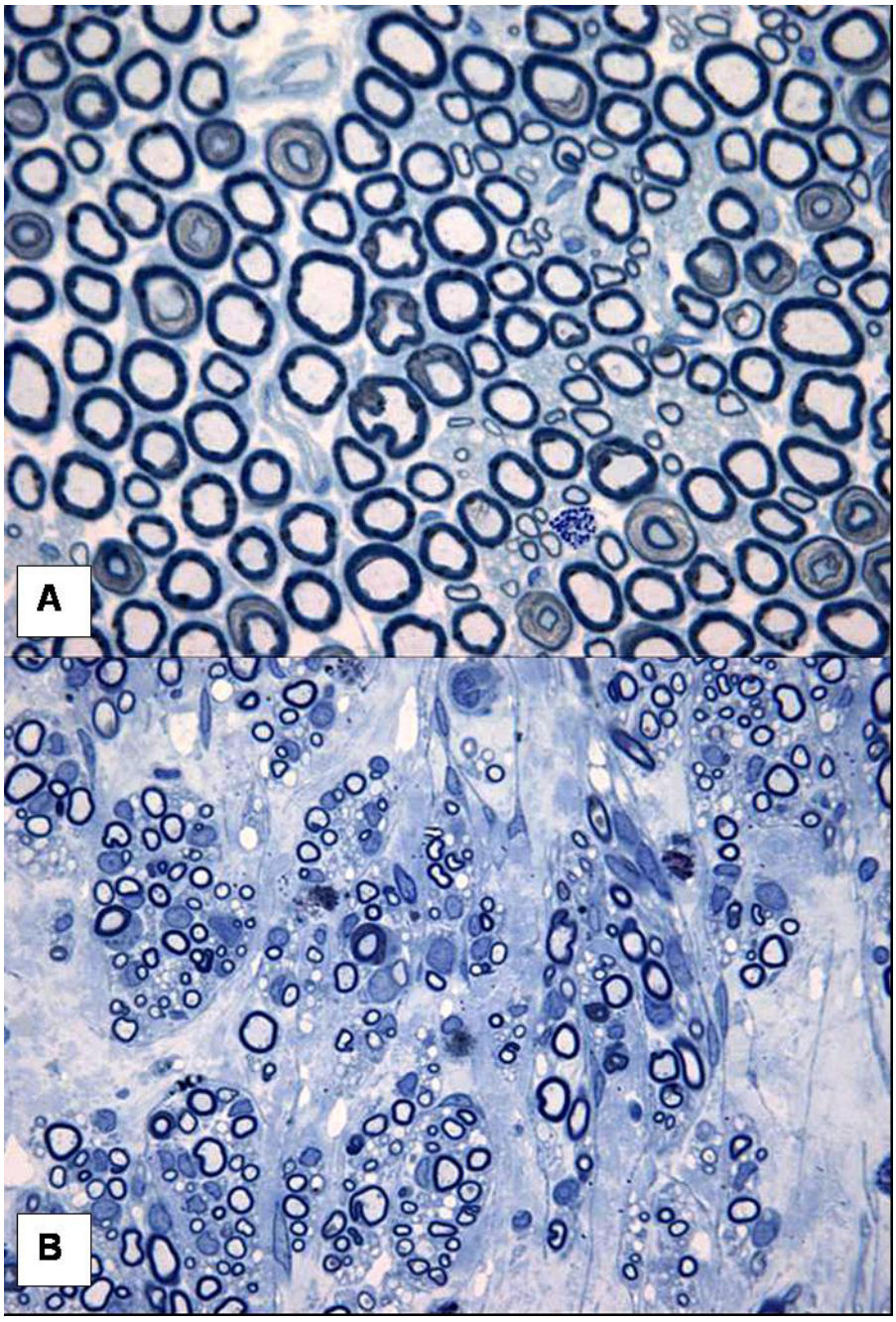

Figure 24 Normal Nerve and Regenerated Nerve In Collagen Tube

(A) Normal sciatic nerve image (B) section of the distal segment of the nerve guide without micro-guidance channels harvested 12 weeks post entubulation repair nerve. Note the significant number of cells, myelinated axons, and blood vessels in the regenerating nerve. Since the myelinated axons in the guide tube do not grow in a homogeneous fashion throughout the entire cross section of the nerve guide, they were all counted to ensure an accurate account of the nerve regeneration. The normal nerve is less cellular, has a more homogeneous distribution of myelinated axons, contains axons of larger diameter, and contains axons that are surrounded with a thicker myelin investment, as compared to the regenerated nerve.

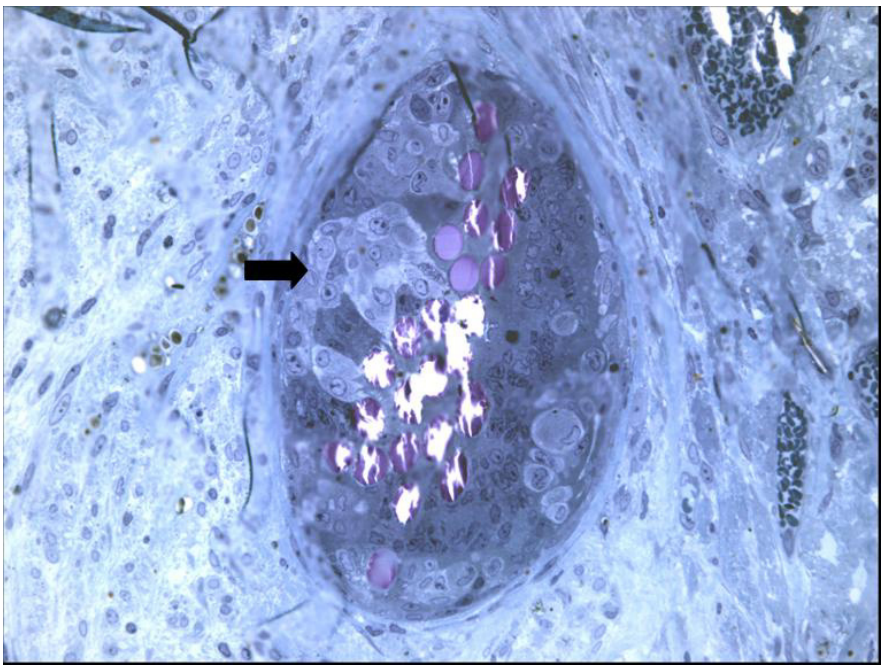

Figure 25 Suture Resorption By Giant Cells

Region of nerve guide 6 weeks post nerve repair in the process of resorption by macrophages, which fuse and become giant cells (arrow).

Nerve Regeneration in Autografts

In the mid section of nerve specimens harvested from rats that received autograft nerve repairs, there were as many as three mast cells in a single 1000x field (Figure 28). Myelin debris from axons that were present in the nerve graft prior to harvesting was still present at 6 weeks post injury/repair and was in the process of removal by Schwann cell and macrophage phagocytosis. At 12 weeks post implantation, the majority of myelin debris from the donor nerve had been cleared. In addition, there was more myelinated axons and larger myelinated axons at this later time point.

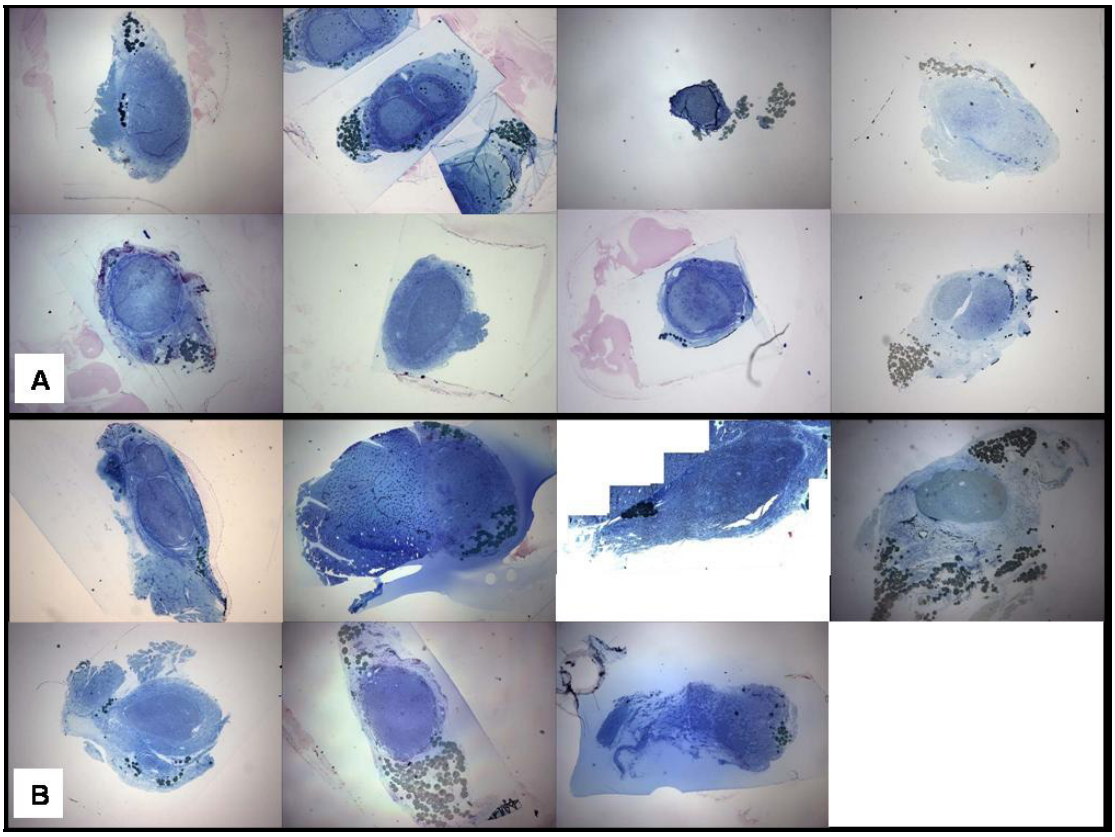

Figure 26 Autograft Nerve Repairs

Low power images of mid section of autograft nerve repairs (A) 6 weeks, (B) 12 weeks

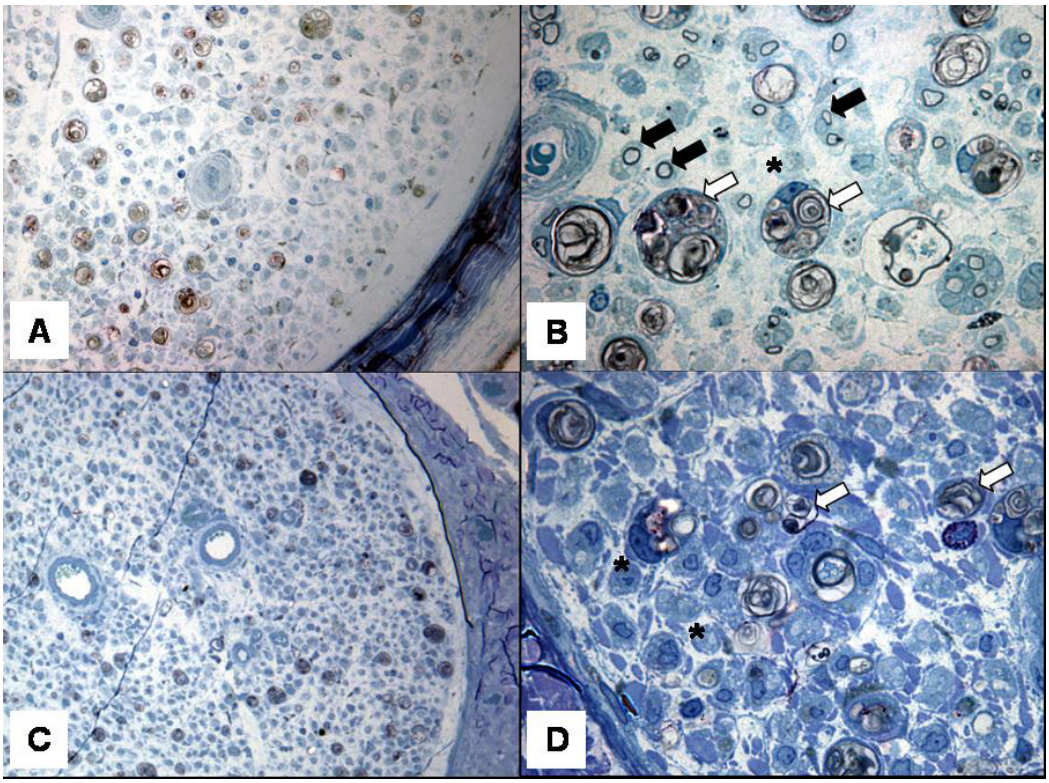

Figure 27 Nerve Regeneration in a 3 Week Autograft

(A) Low power (B) high power views of the mid-section of an autograft 3 weeks post nerve repair, showing small myelinated axons (black arrows) regenerating along Schwann cell basal lamina tubes (asterisk) that have been cleared of myelin. Ovoids of degenerating myelin remain in many of the tubes (white arrows). (C) Low power, (D) high power views of the sciatic nerve distal to the repair site show a similar distribution of empty Schwann cell tubes and those with degenerated myelin to (A & B), however, no regenerating axons can be detected in this distal region of the nerve with this staining preparation.

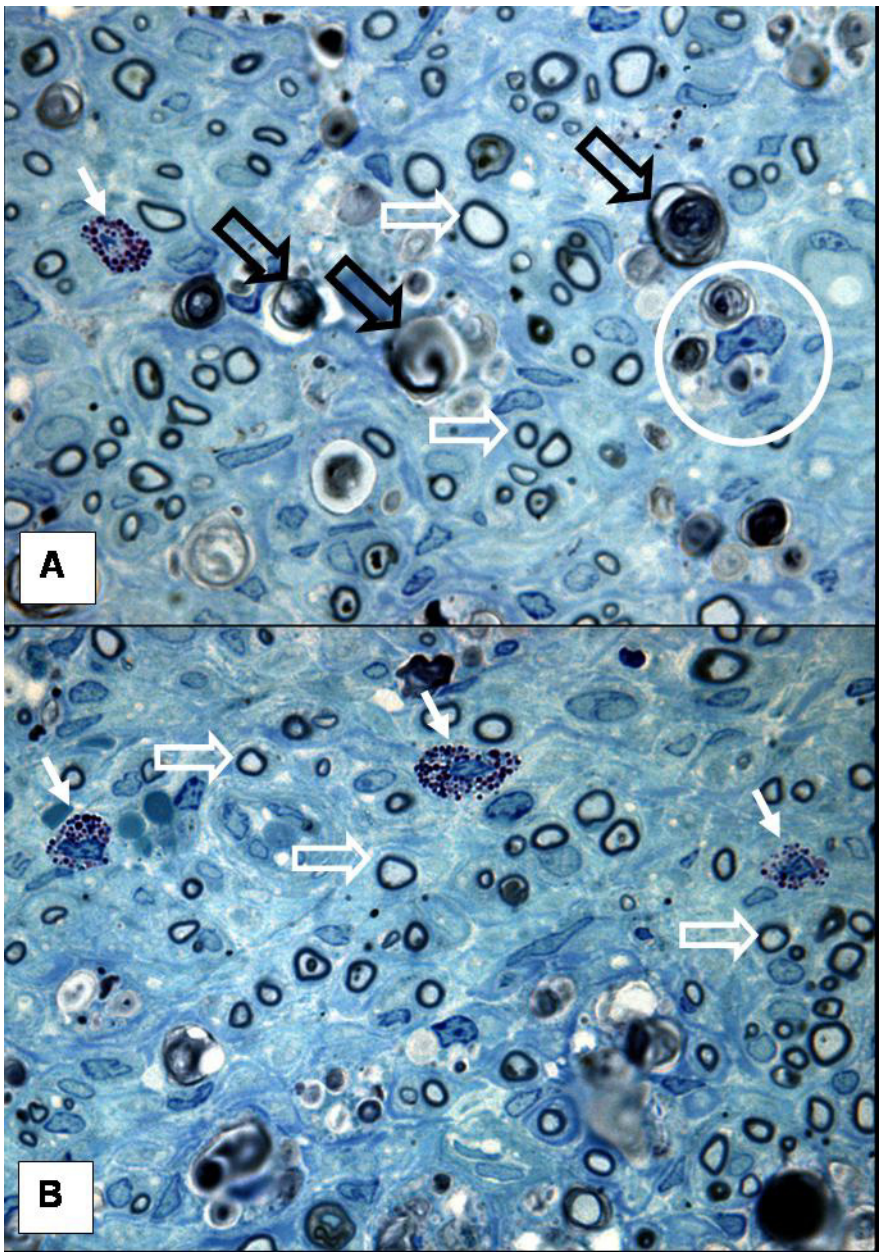

Figure 28 Nerve Autograft 6 Weeks Post Repair

Photomicrograph (100x oil objective lens) from mid section of autograft repair at 6 weeks. Myelin debris from axons that were present in the nerve graft prior to harvesting are still present at 6 weeks post injury/repair (black open arrows). Based on morphology and their relationship with degenerating axons, nuclei of a Schwann cell or macrophage (white circle) is identified and is presumably in the process of removing the myelin debris via phagocytosis. Nuclei of Schwann cells can be identified by their close proximity to newly regenerated axons, which are identified by their smaller than normal diameter and thin myelin investment (white open arrows). Their dark staining cytoplasmic granules easily identify mast cells (solid white arrows) present in this section.

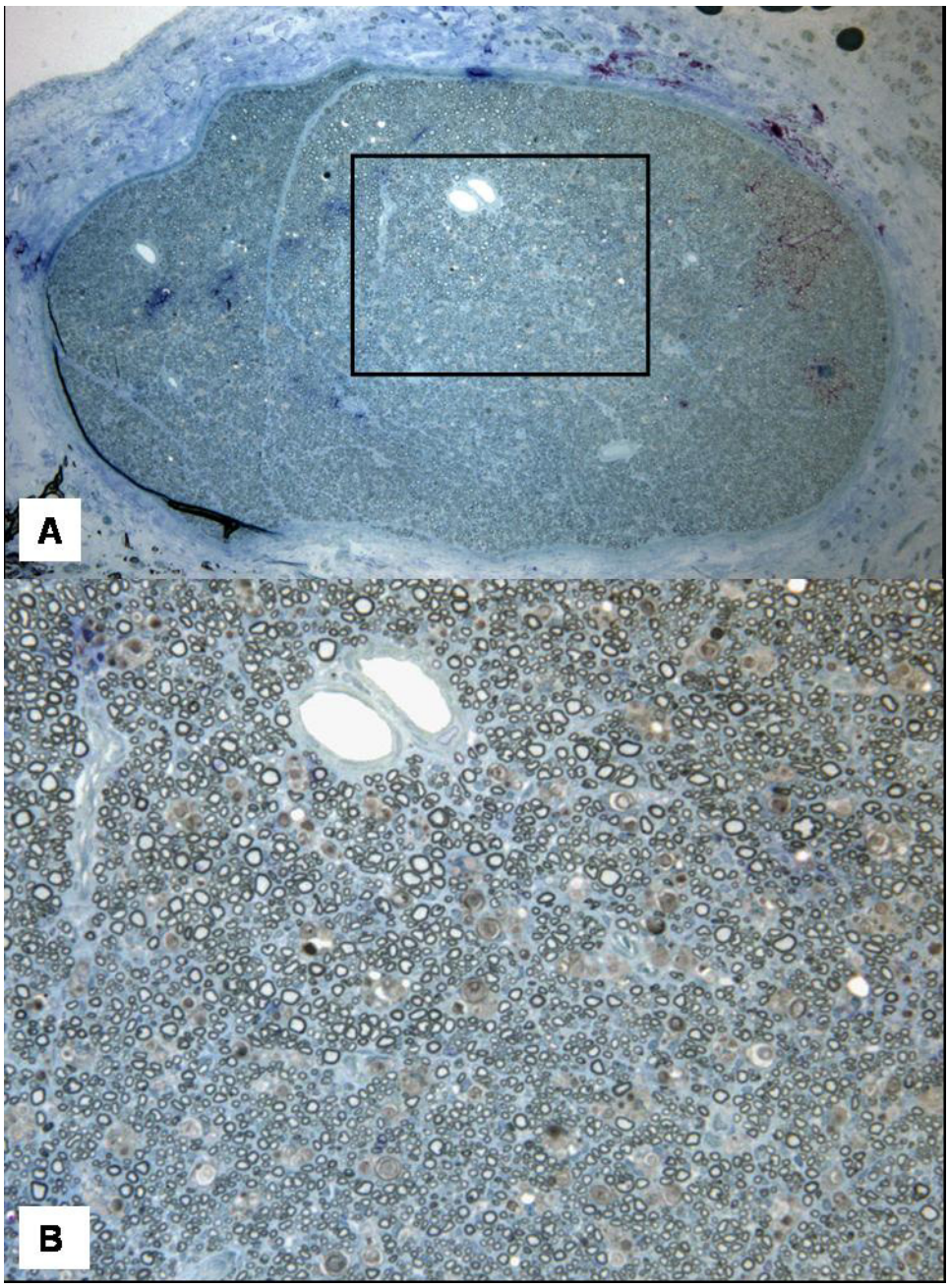

Figure 29 Autograft Nerve Repair 12 Weeks Post Implantation

(B) High magnification view of boxed region in (A). This specimen had 22,590 myelinated axons counted from a montage of this section. Note the extremely high density and uniform distribution of myelinated axons.

Axonal escape occurred at the proximal junction between autograft and sciatic nerve, as evidenced by the presence of many myelinated axons growing

outside the confines of the autograft epineurium. This was noted in several specimens harvested from the middle of the graft (figure 30).

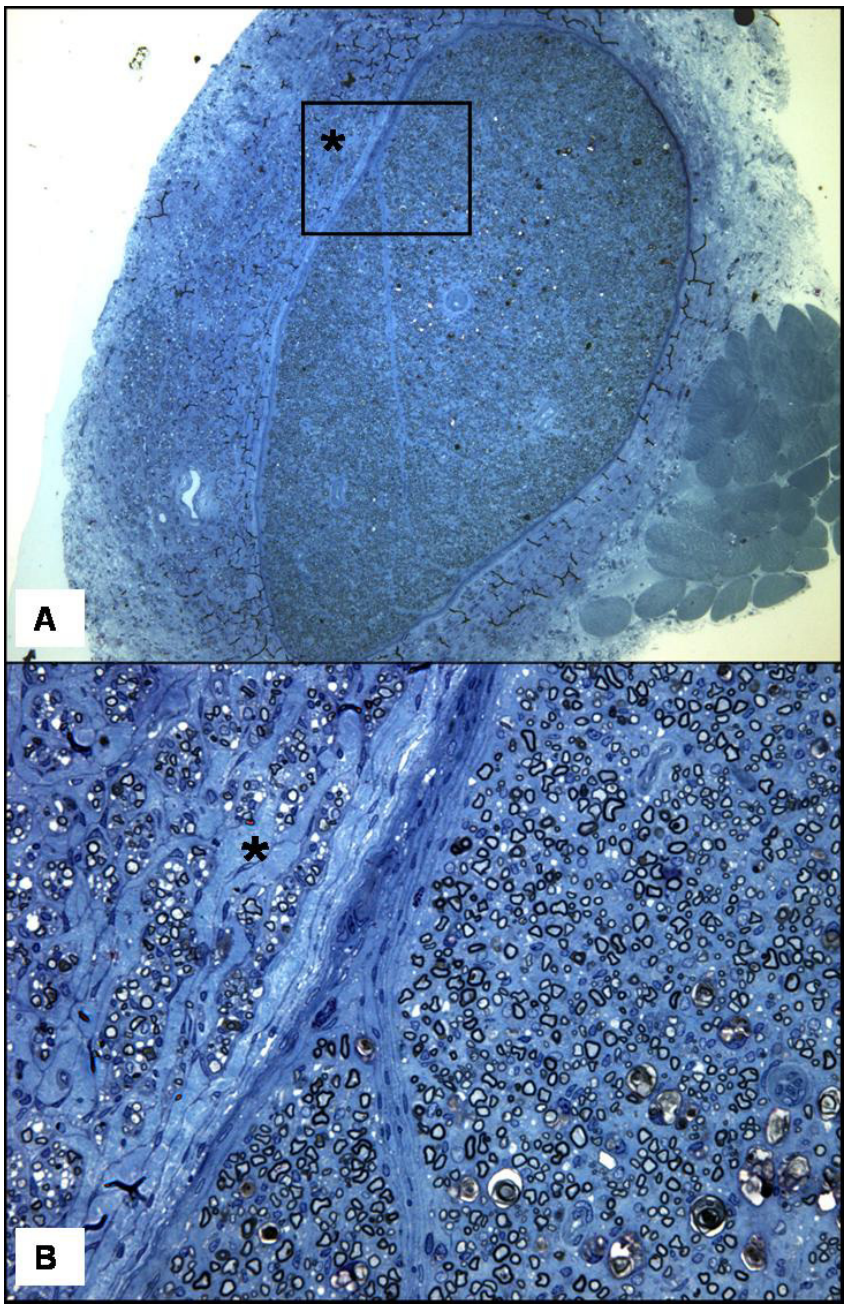

Figure 30 Autograft With Axonal Escape

(B) High magnification view of enclosed region in (A) showing many regenerated axons (asterisk) that grew outside the confines of the autograft epineurium. AG with 13,582 myelinated axons at 6 weeks. Image demonstrates axonal escape with AG repair

Empty Collagen Nerve Guides

The majority of empty collagen nerve guides had patent lumens at six, twelve, and twenty four weeks post implantation. Some had a flattened cross section, which was noted both grossly and histologically. Over time the collagen nerve guide wall became more infiltrated with cells, however, the approximate wall thickness did not appear to change to a large degree (figure 31). At the six week time point the nerve guide lumen was more sparsely occupied by regenerated nerve (axons and Schwann cells) than at twelve weeks. By 24 weeks, the area occupied by axons appeared greater than at 6 and 12 weeks, filling the nerve guide lumen. A frequent observation was the presence of mini fascicles in regenerated nerve sections (figures 32, 33).

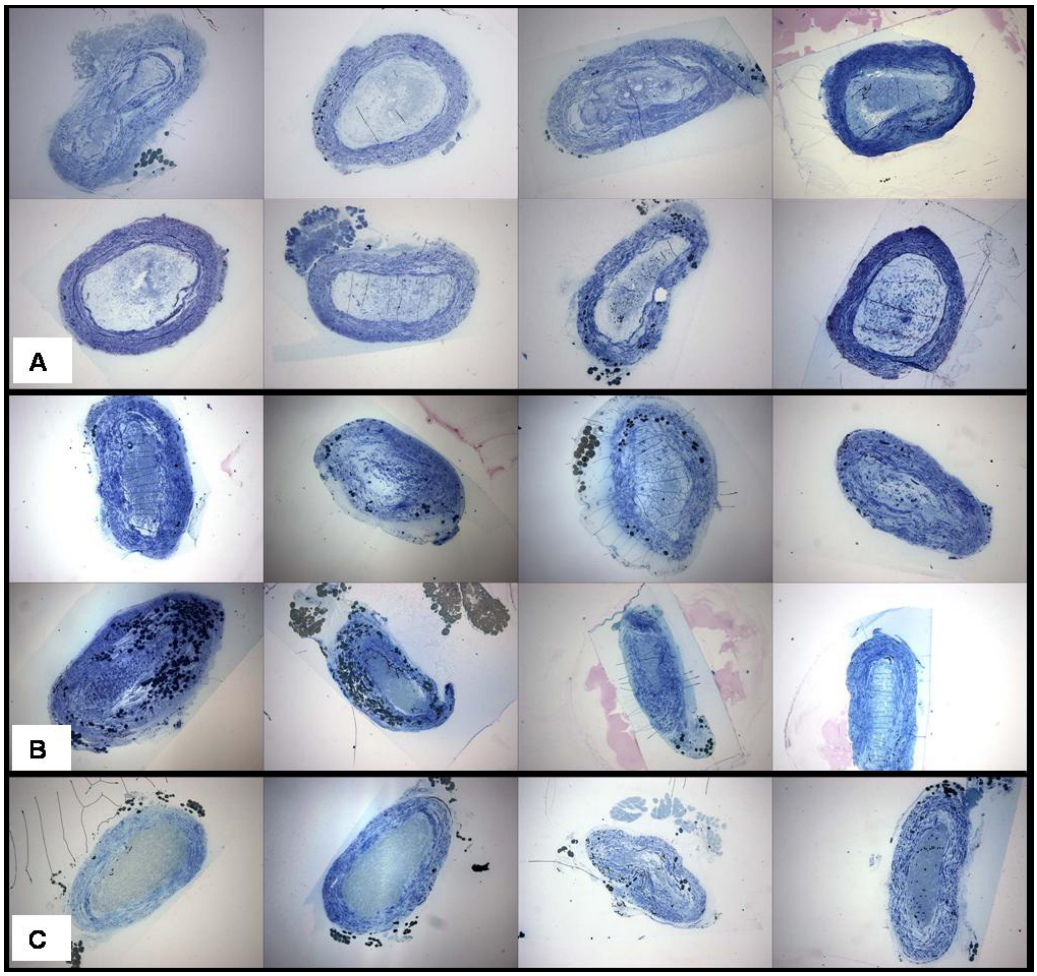

Figure 31 Low Power 6, 12, 24 Week CT Nerve Guide Sections

Low power images of mid section of empty nerve guides (A) 6 weeks, (B) 12 weeks, and (C) 24 weeks.

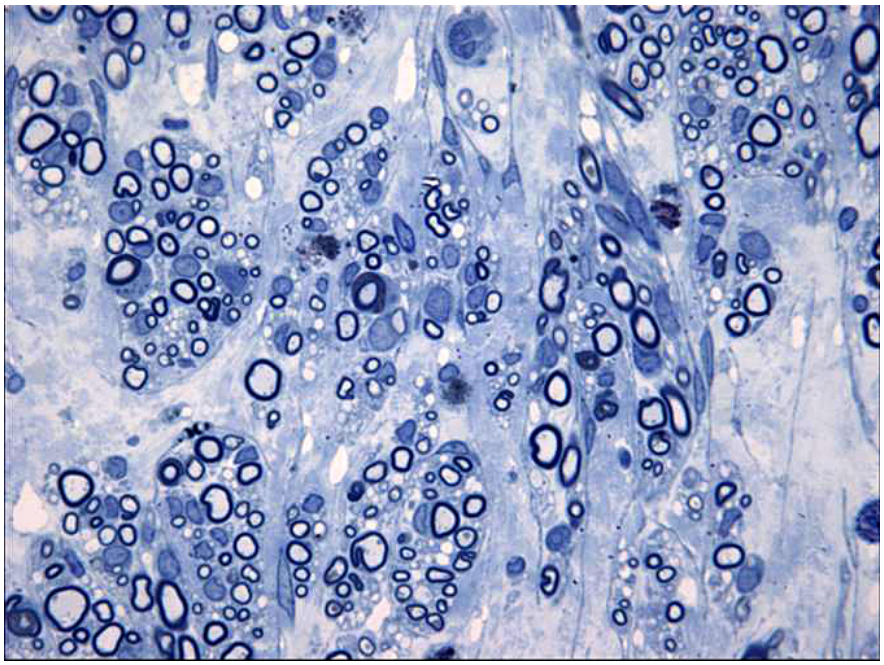

Figure 32 Regenerated Nerve in Collagen Guide

Distal segment of the collagen guide tube 12 weeks post repair with (B). Note the significant number of cells, myelinated axons, and blood vessels in the regenerating nerve.

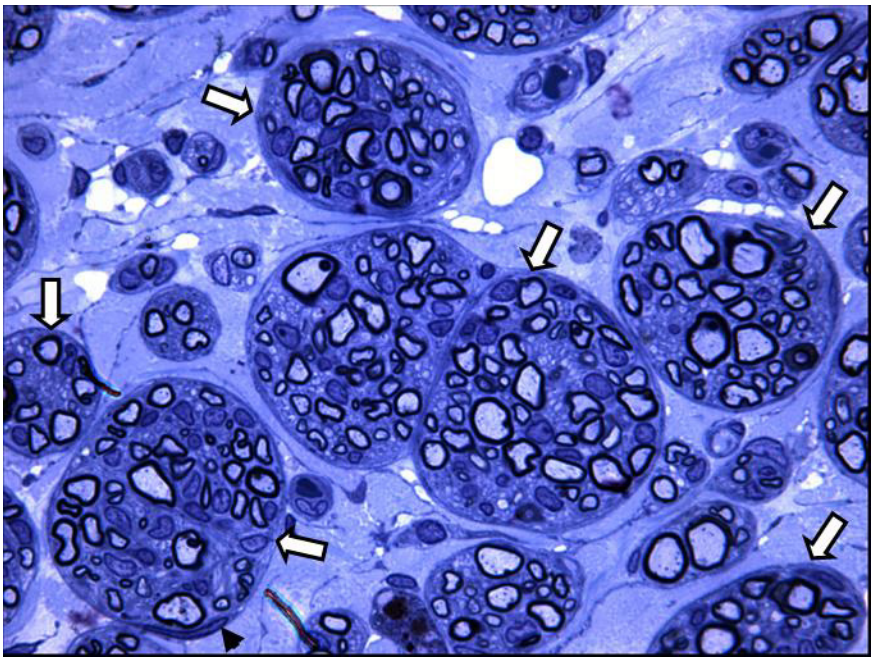

Figure 33 Minifascicles in Regenerated Nerve

High power view (100x oil objective lens) of regenerated nerve in at 12 weeks demonstrating minifascicles (open arrows), and a perineurial cell (black arrowhead) bottom left region of image.

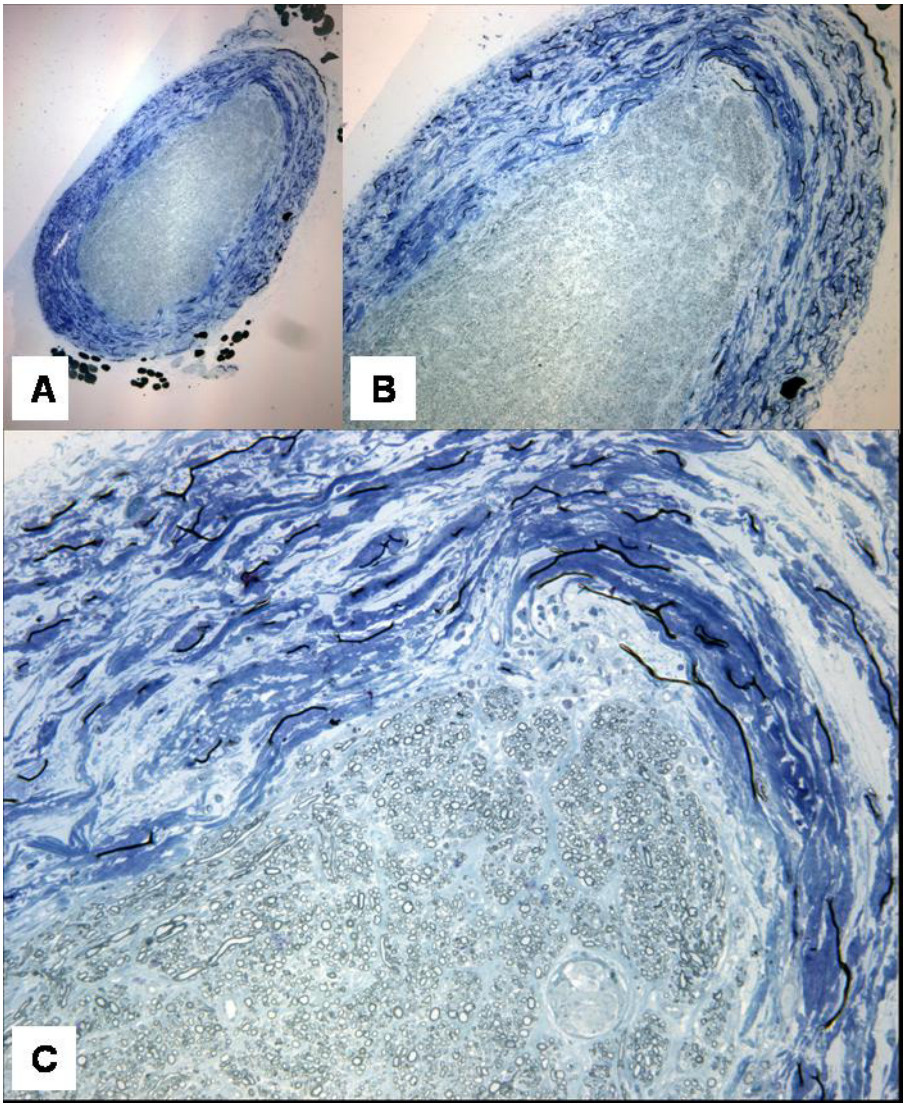

Figure 34 Regeneration in CT at 24 weeks

(A), (B), (C), low, medium, high power views respectively from a CT nerve guide specimen harvested at 24 weeks post implantation. This particular specimen had the highest number of myelinated axons (24,515) in the mid-section of the nerve guide of all entubulation repairs performed in this study. It also had more myelinated axons than the majority of the 12-week AG repairs. The myelinated axons are well distributed throughout the entire cross-section of the nerve guide lumen.

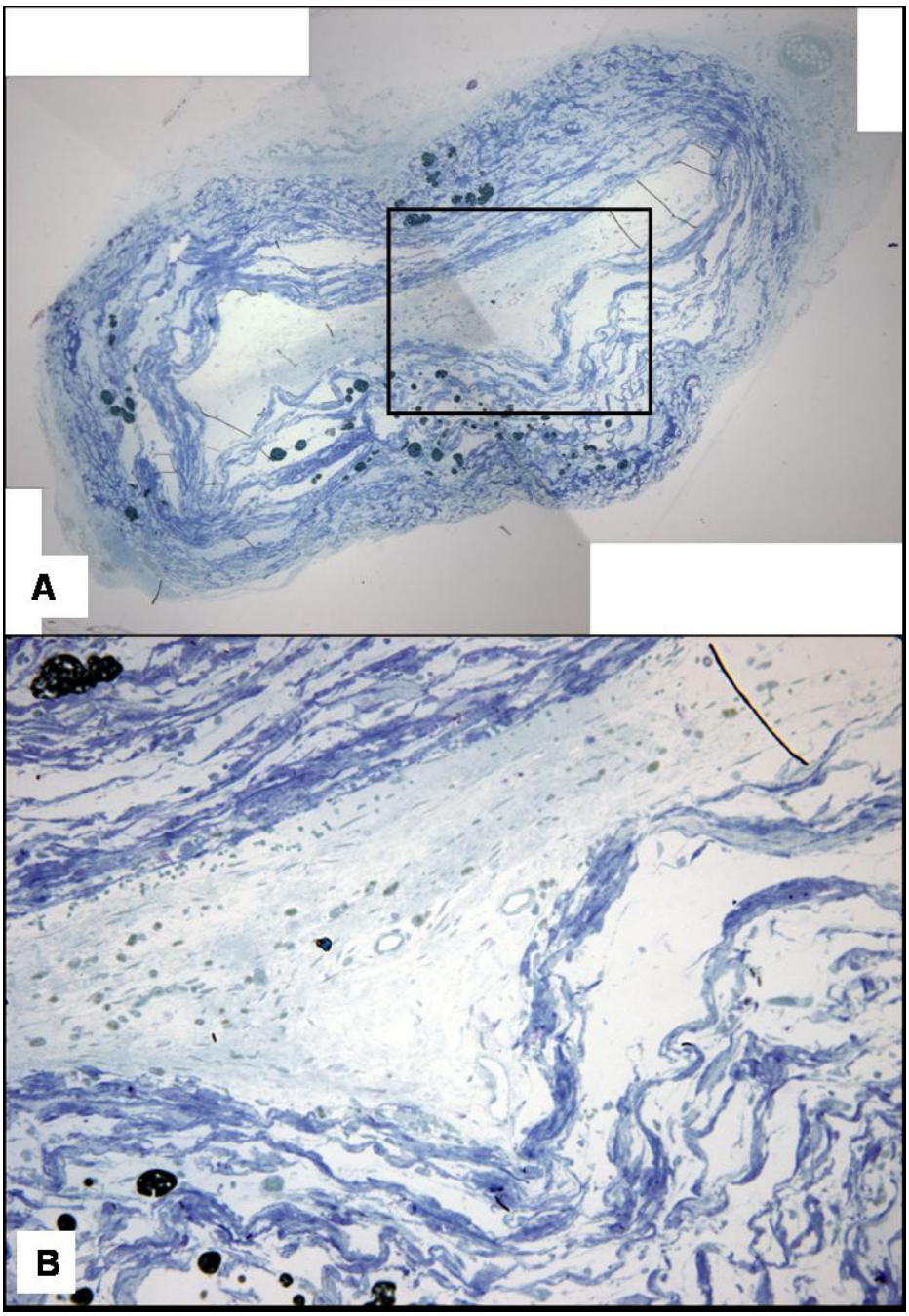

Figure 35 Failed Regeneration in CT Group

Middle section of a nerve guide 6 weeks post implantation with a flattened morphology. The lumen has been reduced, but not obliterated. No myelinated axons were identified in this specimen.

Nerve Guides with Longitudinal Microtube Channels

Regenerating axons grew through and between longitudinal collagen microtubes within the lumen of the larger collagen nerve guide. Morphology in these regenerated nerve guides was highly variable. The outer guide tube wall in some specimens was infiltrated by cells and appeared less dense than some microtubes (figure 36). Within a single nerve guide, the degree of resorption of the individual microtubes varied, as well as the axonal growth through the microtubes (figure 41, 42). Variation also existed between specimens. The number of microtubes that could be identified histologically, at 6 and 12 weeks, was on occasion, less than 5, even though we confirmed their presence prior to surgical implantation.

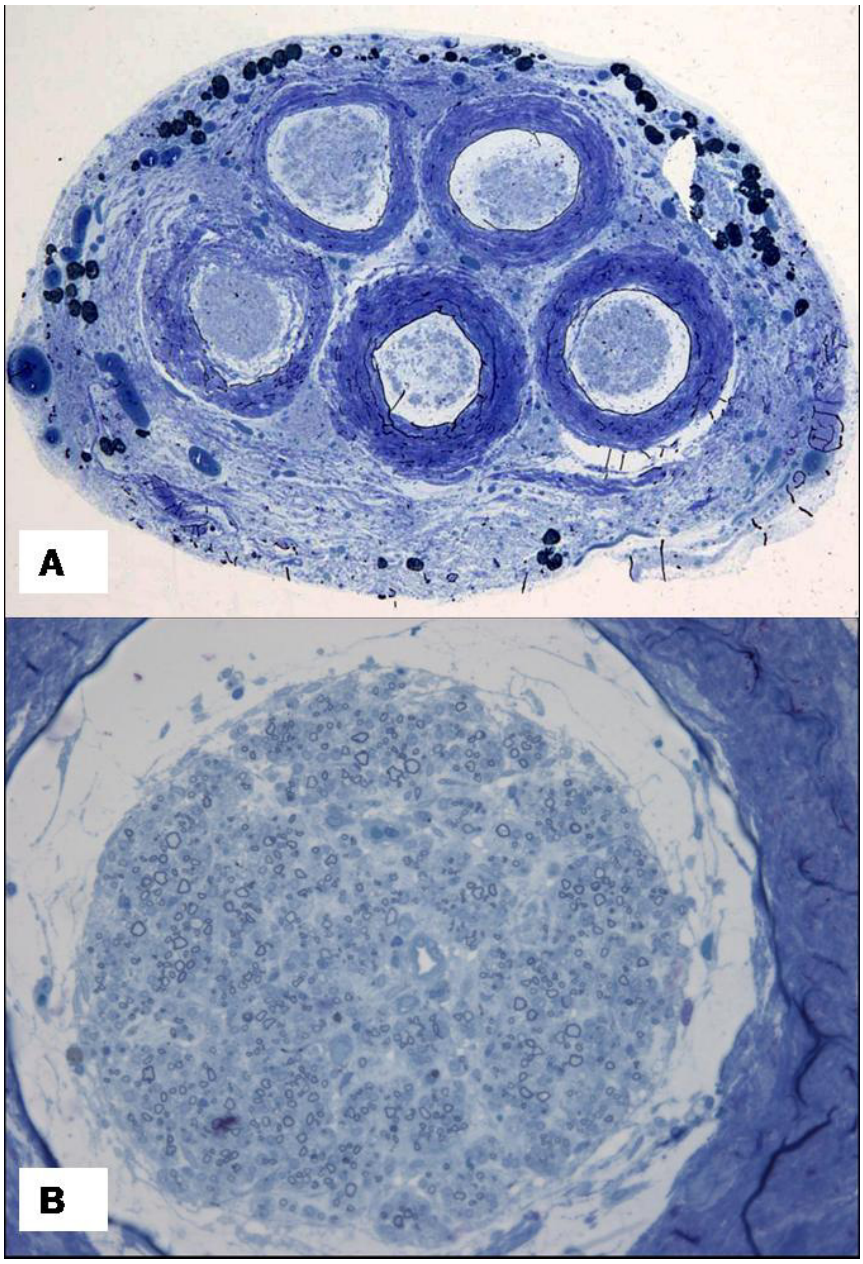

Figure 36 Microtube With Myelinated Axons

(A) Low and (B) High power micrographs of the distal segment of a nerve guide with microtube guidance channels 12 weeks after injury and repair. Note myelinated axons in a microtube that has not degraded. The original outer collagen tube has been infiltrated by cells and has been remodeled to a greater degree than the collagen microtubes.

In one particular specimen, the presence of a population of plasma cells was noted (figure 37). This was the exception, and was not observed in other

specimens. Minifasicles were observed in the regenerating nerves in some specimens of the MT group (figure 40).

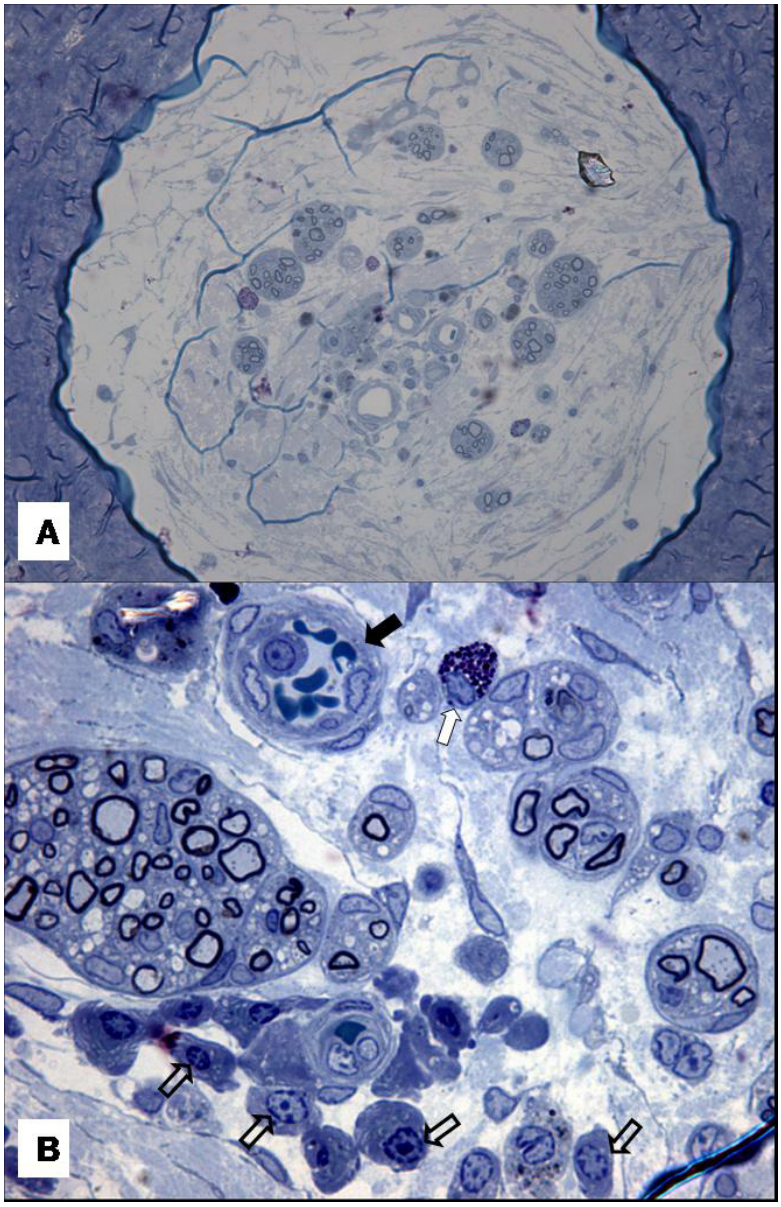

Figure 37 Regenerated Nerve with Plasma Cells inside Microtube

(A) Low power view of few regenerating axons in a microtube within a nerve guide at 12 weeks. (B) High power view from same specimen revealing a mini-fascicle containing myelinated and unmyelinated axons. Outside the borders of the fascicle are plasma cells (open arrows), which are identified by their "clock faced" pattern of dark staining heterochromatin and basophilic cytoplasm. A blood vessel containing erythrocytes and a leukocyte is present in the image. The image contains a mast cell (white arrow).

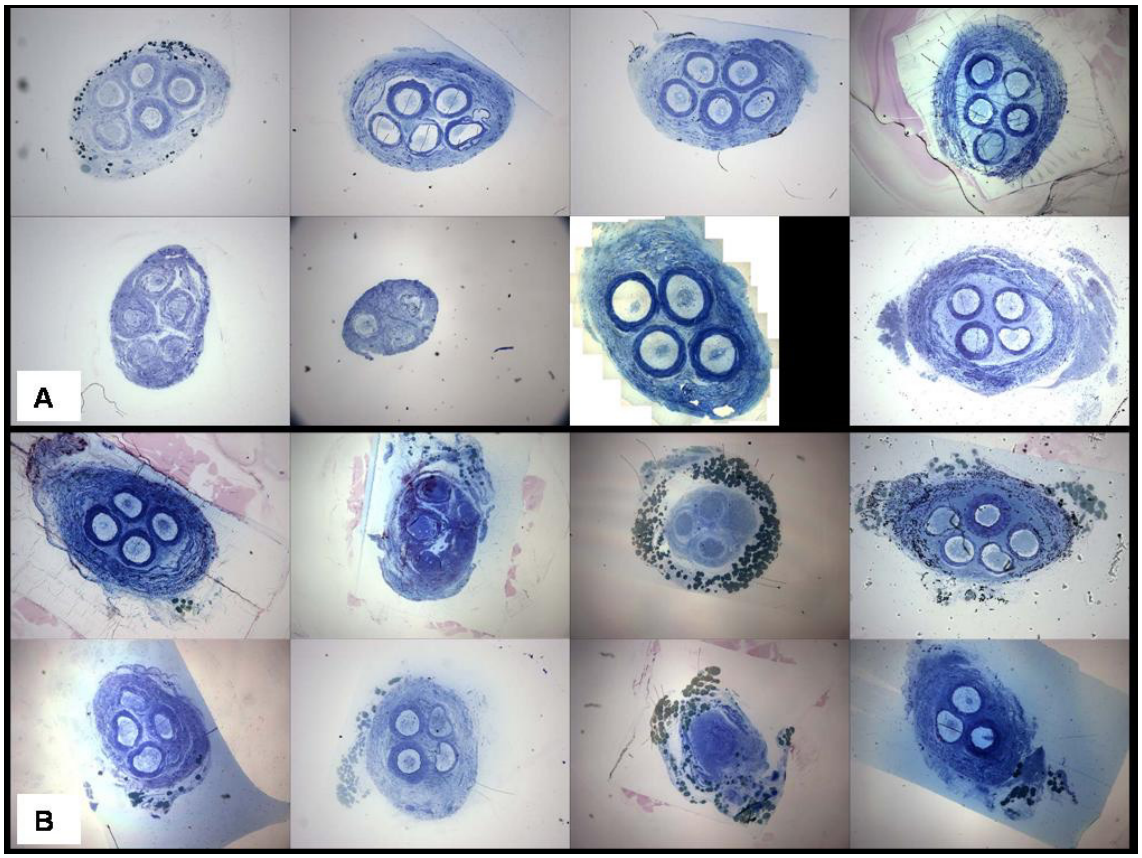

Figure 38 Low Power MT Nerve Guides at 6 & 12 Weeks

(A) Sample middle sections from 6 week MT group. (B) Sample middle sections form the12 week MT group

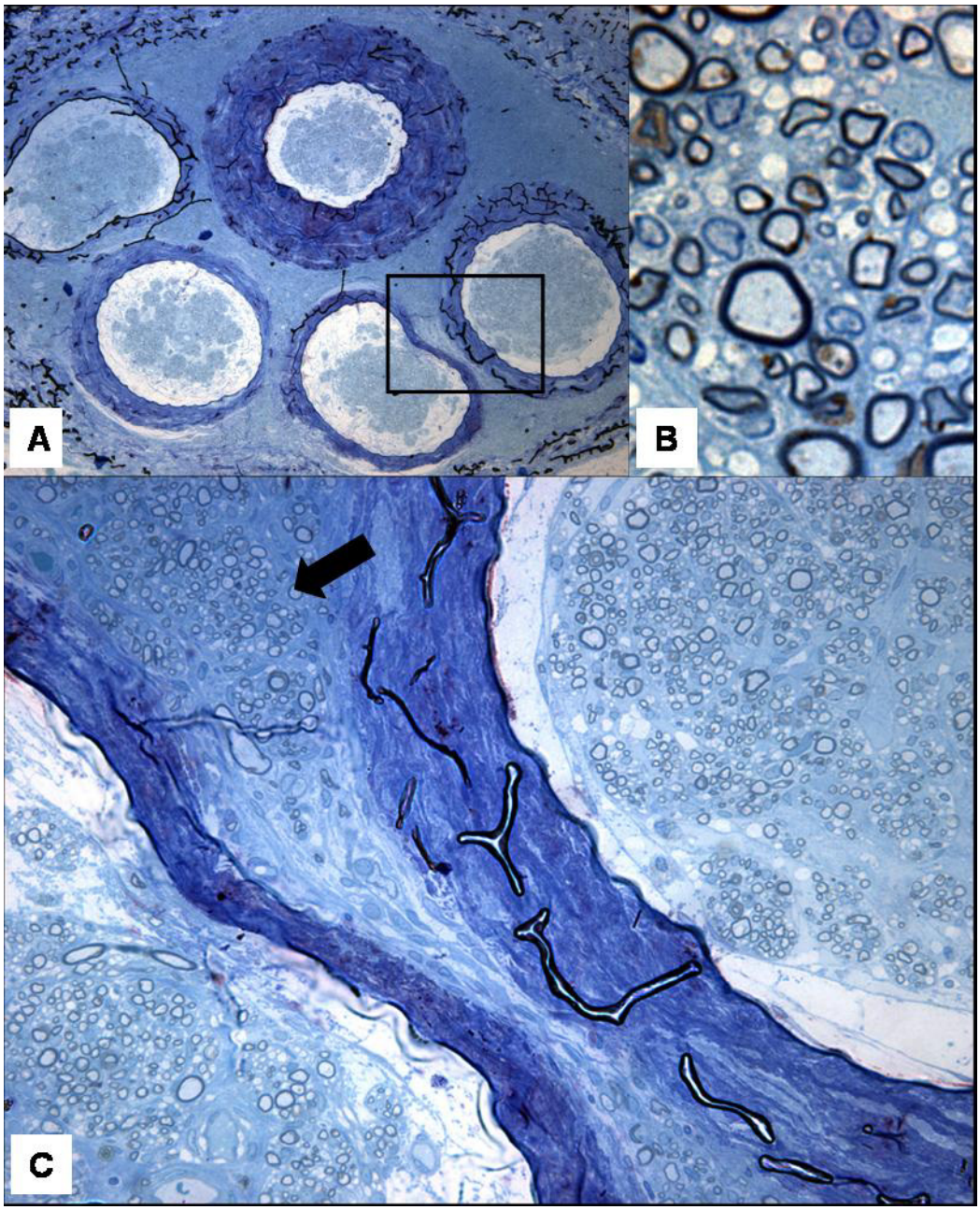

Figure 39 Axons Regenerating In and Between Microtubes

(A) MT nerve guide specimen harvested 12 weeks post implantation. (C) magnified view of enclosed region in (A) demonstrates dense axon growth in and between (arrow) two microtubes. (B) High magnification (100x oil objective lens) showing well myelinated axons from this specimen.

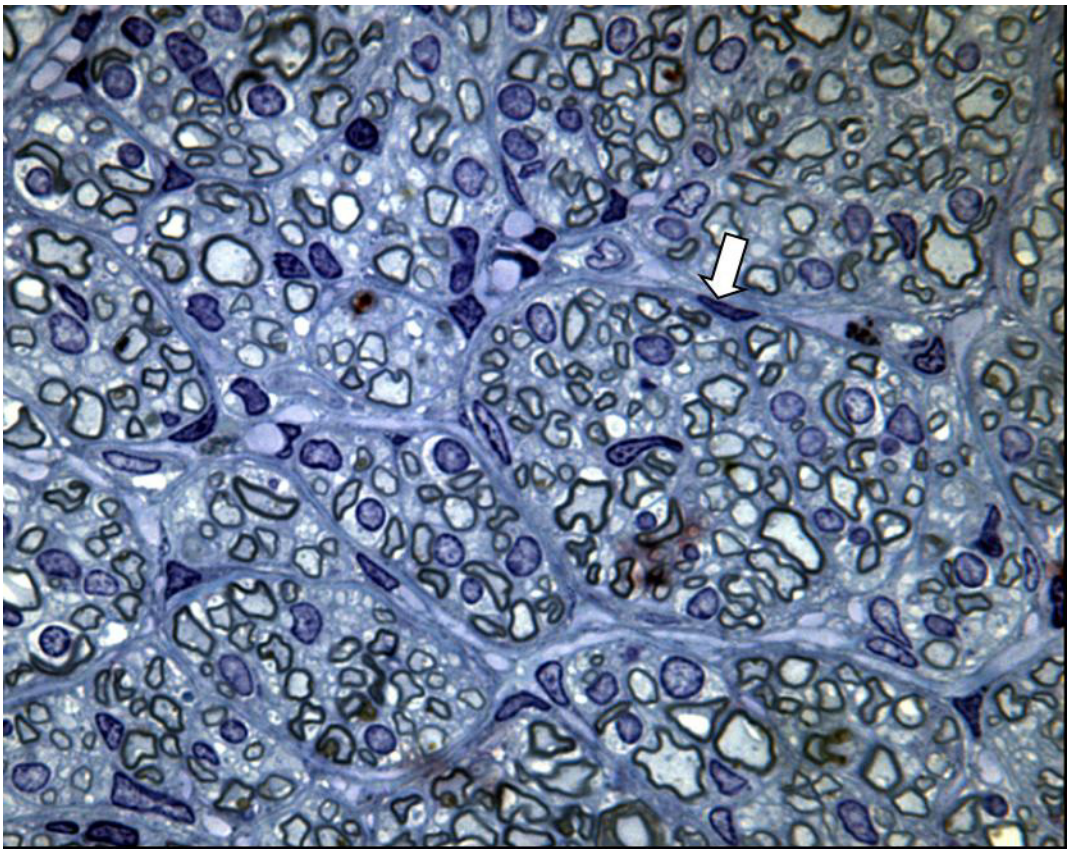

Figure 40 MT Nerve Guide at 12 Weeks Fasicular Morphology

A12 week MT specimen with 9994 myelinated axons and a highly fascicular morphology. Perineurial cells (arrow).

Variability in nerve guide resorption also existed among different sections of the same nerve guide. In one particular specimen from the 6 week MT group, the proximal section had evidence of only 2 microtubes, and the middle section had only 4 microtubes. The distal section had 3 intact microtubes, 1 microtube that was largely resorbed and at the same time partially collapsed, and a region where a tube may have existed but remnants were not detectable (figure 41). In a failed repair from the 6 week MT group, the microtubes were highly infiltrated

by cells, and highly resorbed. They also contained fibrotic tissue without the presence of axons (figure 43).

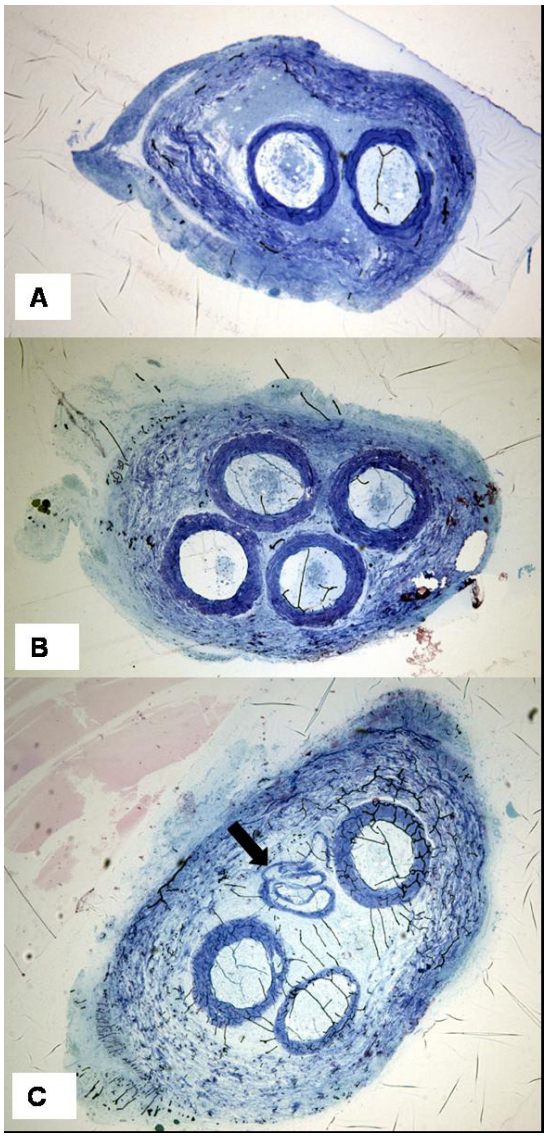

Figure 41 Variable Resorption of Microtubes Proximal to Distal

(A) proximal, (B) middle, (C) distal sections of a 6 week MT demonstrating variability of microtube morphology. Upon implantation there were 5 collagen microtubes, however, at the six week time point there are only 2 identifiable microtube present proximal section, 4 in the middle section, 4 in the distal (one collapsed, arrow). In the distal section, the wall thickness of each microtube is different. There are many axons in the proximal section. The middle section has only 275 myelinated axons.

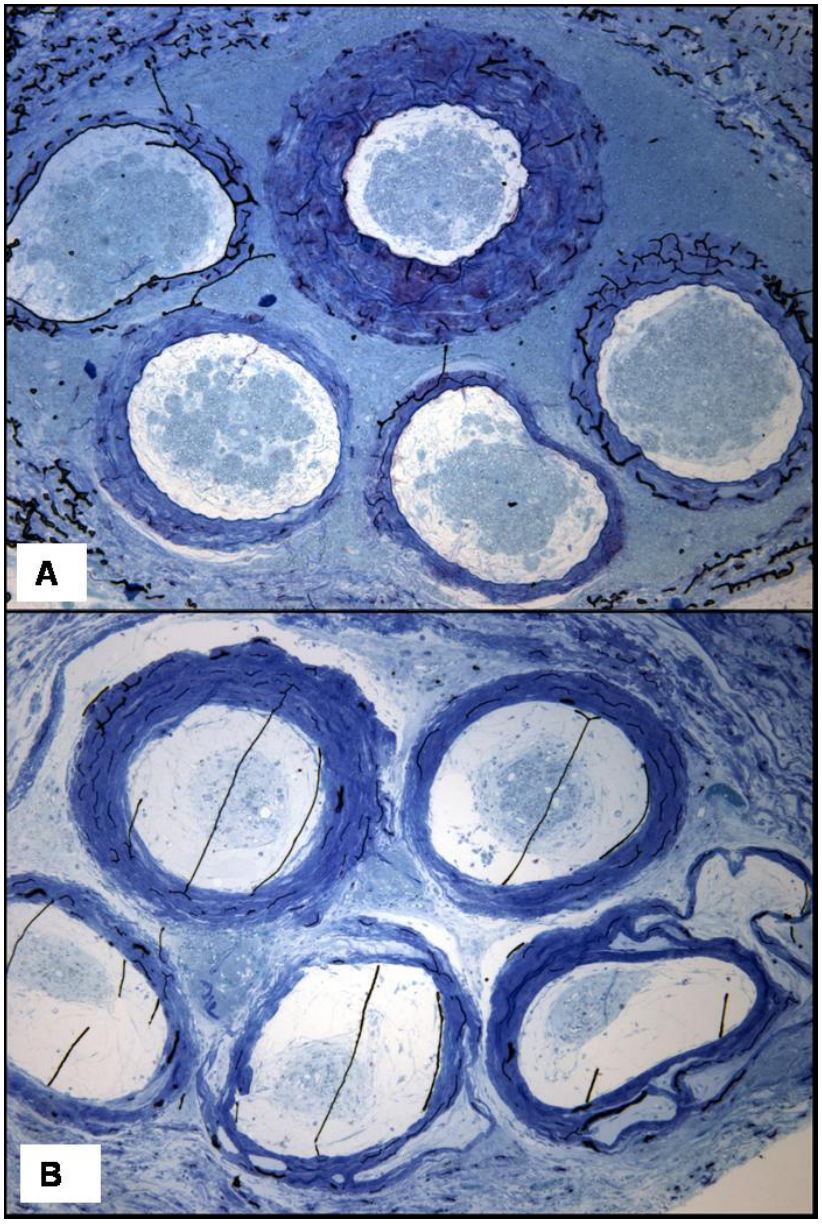

Figure 42 Microtube Variability

(A) Nerve guide section from 12 week MT group. (B) Nerve guide section from 6 week MT group. These two specimens although from two different time points show remarkably similar microtube morphology; each of the 5 microtubes are visible within the outer guide tube and have a variable wall thickness. This particular 12-week specimen was one with very successful regeneration (12,905 myelinated axons in mid-section of nerve guide), where as this 6 week specimen had particularly poor regeneration (186 myelinated axons in mid-section of nerve guide).

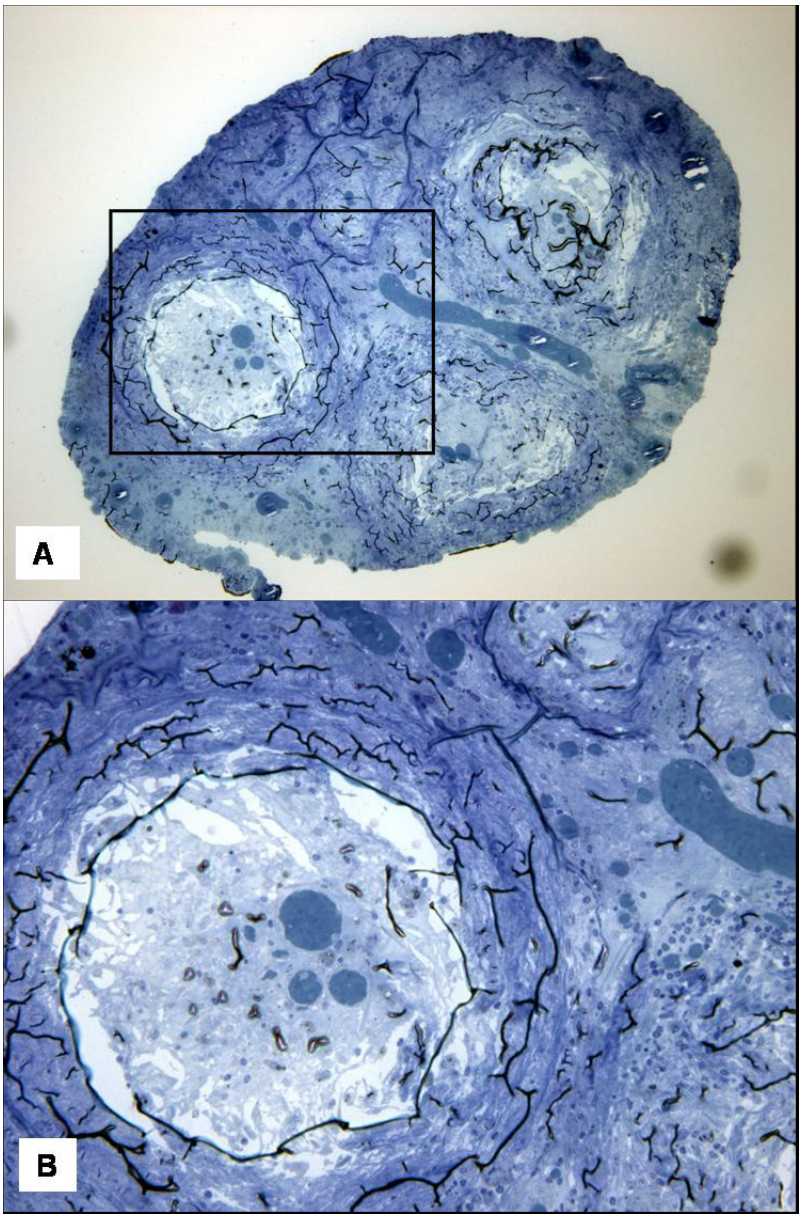

Figure 43 Failed MT Nerve Guide

This specimen had no visible axons in the nerve guide at 6 weeks post nerve repair.

Nerve Guides with Longitudinal Filaments Channels

Axonal regeneration was highly variable at both 6 and 12 weeks in nerve repairs with nerve guides containing longitudinal collagen filaments. Intraluminal filament position was highly variable and there was little resorption or cellular infiltration of the solid collagen filaments (figure 45). In some specimens axons and cells grew between the filaments (figure 45), but in others axons grew in regions outside a grouping of filaments (figure 46).

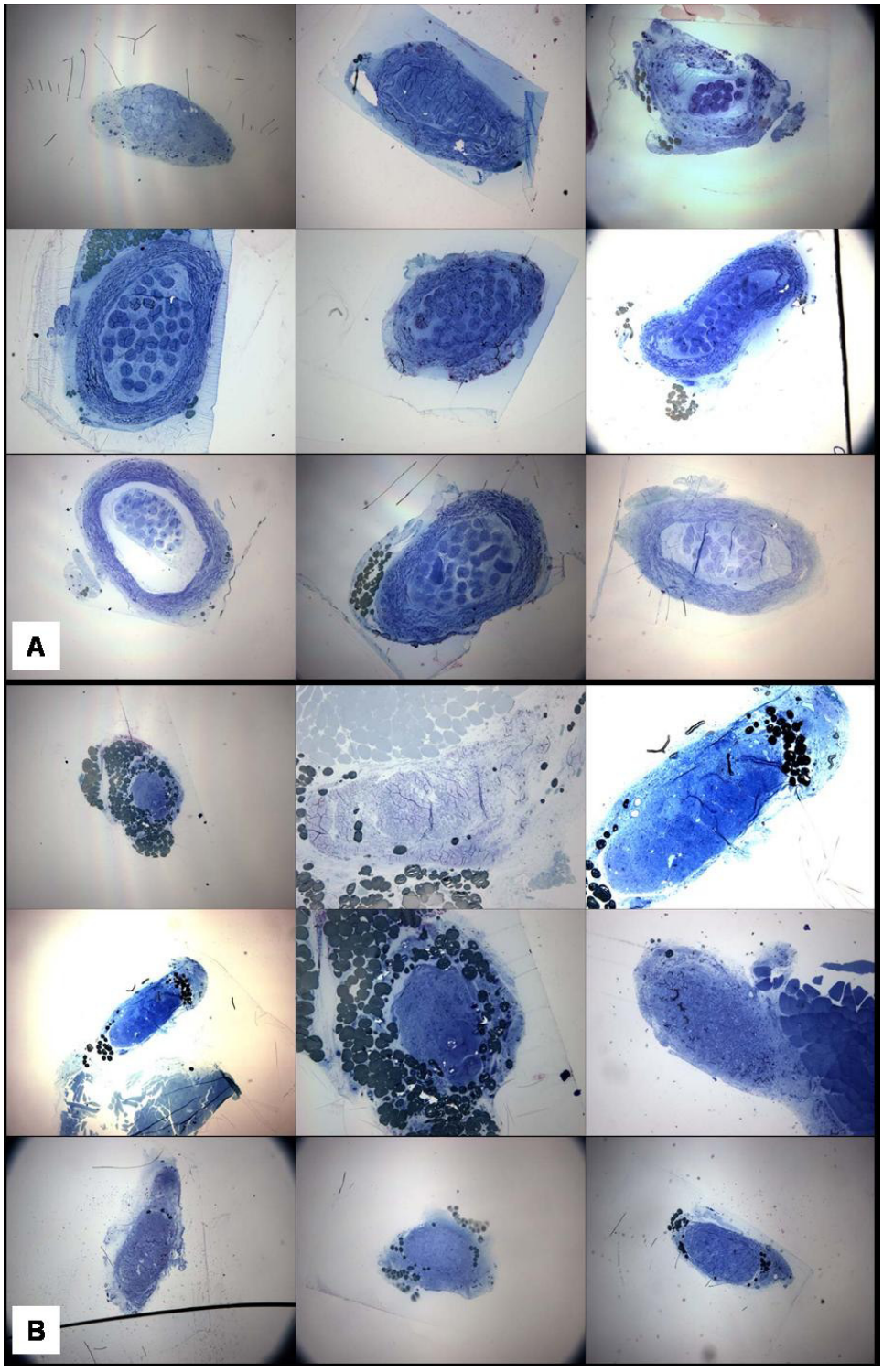

Figure 44 Nerve Guides with Filaments at 6 & 12 Weeks

Low power images of mid section of nerve guides with longitudinal filaments (A) 6 weeks, (B) 12 weeks.

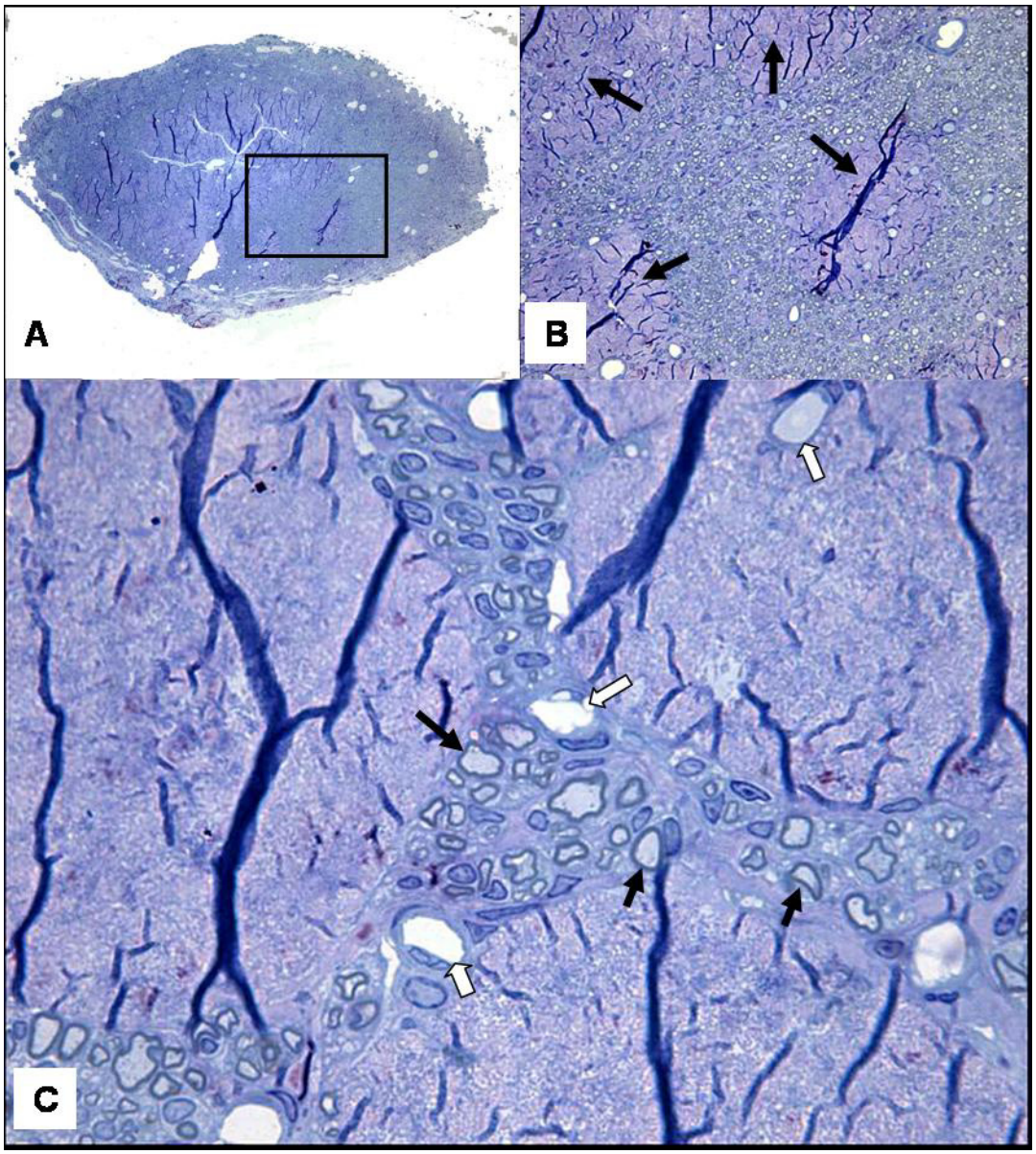

Figure 45 Nerve Guide With Filaments

(A) Low, (B) medium, and (C) high power images of a cross section of a nerve guide that contained filaments, 12 weeks after injury and repair. (B) High power image from enclosed region in image (A). The collagen filaments show little cell infiltration or degradation (black arrows in image B). Note myelinated axons (black arrows in image C) in the spaces in between the collagen filaments that have not degraded and the significant number of blood vessels (open white arrows) that have infiltrated the nerve guide. The nucleus of an endothelial cell is bulging into the vessel lumen. Some of the blood vessels have infiltrated the collagen filaments but most occupy the space outside the filaments. Although there is a filament in this image (B) that is surrounded by myelinated axons, this was not the trend. Most filaments aggregated and axons grew around them.

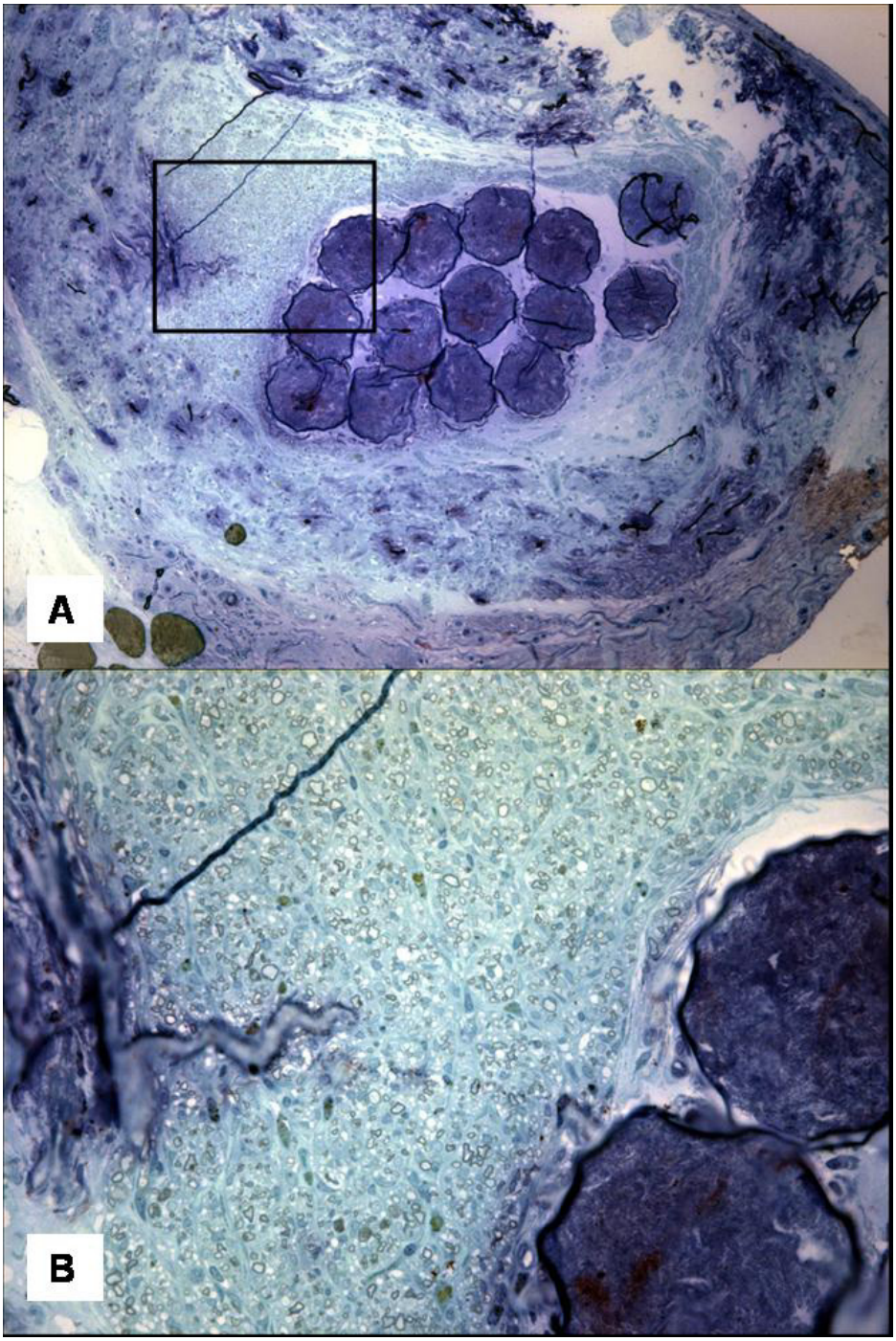

Figure 46 Myelinated Axons Growing Outside Region Of Filaments

(A) Low power image of a nerve guide middle section with filaments from rat 171 at 6 weeks demonstrates that filaments did not attract axons to grow in the channels between them and that a very large population of axons exists outside the region of the filaments. In this specimen there exists 2292 myelinated axons. (B) High power image from the boxed region enclosed in (A).

There were several specimens in which the individual filaments maintained an equal distribution within the outer nerve guide, thus providing the maximal surface area permitted by this design (figure 47). These specimens did not have the greatest number of axons. In fact, certain specimens in which the filaments aggregated, and axons grew in regions outside the filaments, had the greatest axon counts of the MF groups. This was not a trend. There were specimens with aggregated filaments that had little or no axons. In some, the aggregated filaments occluded the area available for axon growth while in others small numbers of axons grew between the filaments (figures 50, 51). In specimens that had evenly dispersed filaments, the filaments were not equal in diameter. Some appear approximately twice as large as others do (figure 47).

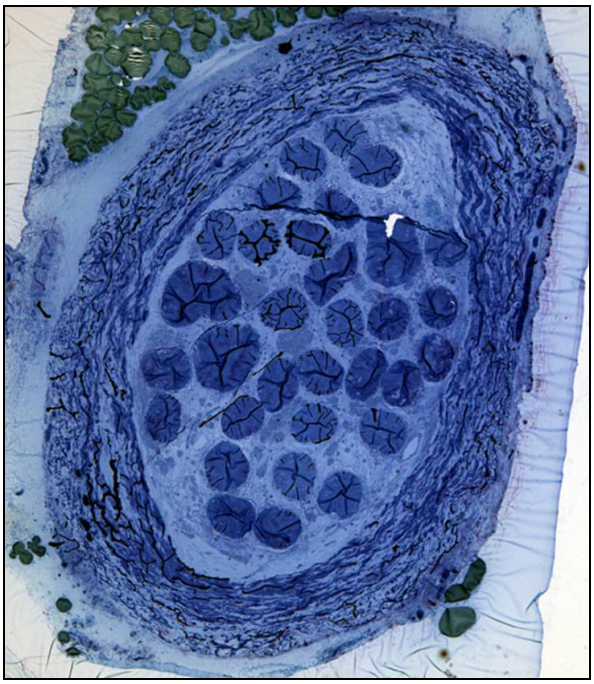

Figure 47 Nerve Guide Image Demonstrating 32 Separate Filaments

Nerve guide section containing 32 distinct and separate filaments. The myelinated axon count was 1681. Though this nerve guide contained filament of even spacing, regeneration was marginal.

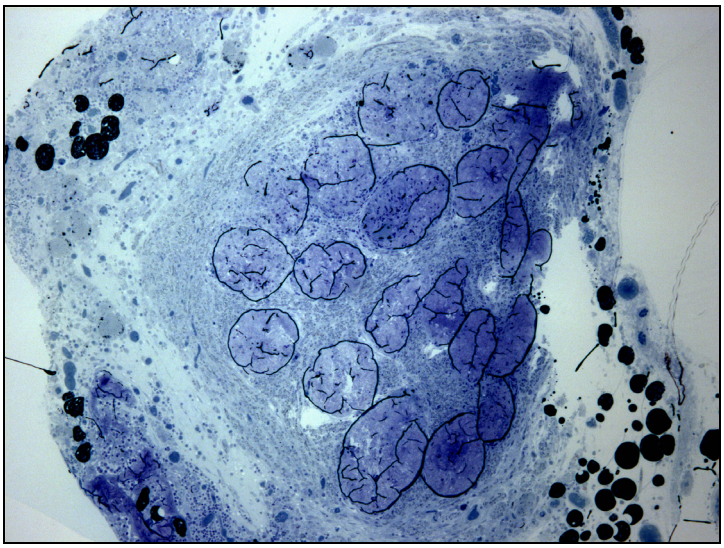

Figure 48 Nerve Guide Filaments And Many Axons At 6 Weeks

This specimen had the greatest number myelinated axons (3334) of all of the MF nerve guides at 6 weeks. Some filaments maintained a fair degree of separation, and there were axons growing between them, while other filaments contacted each other.

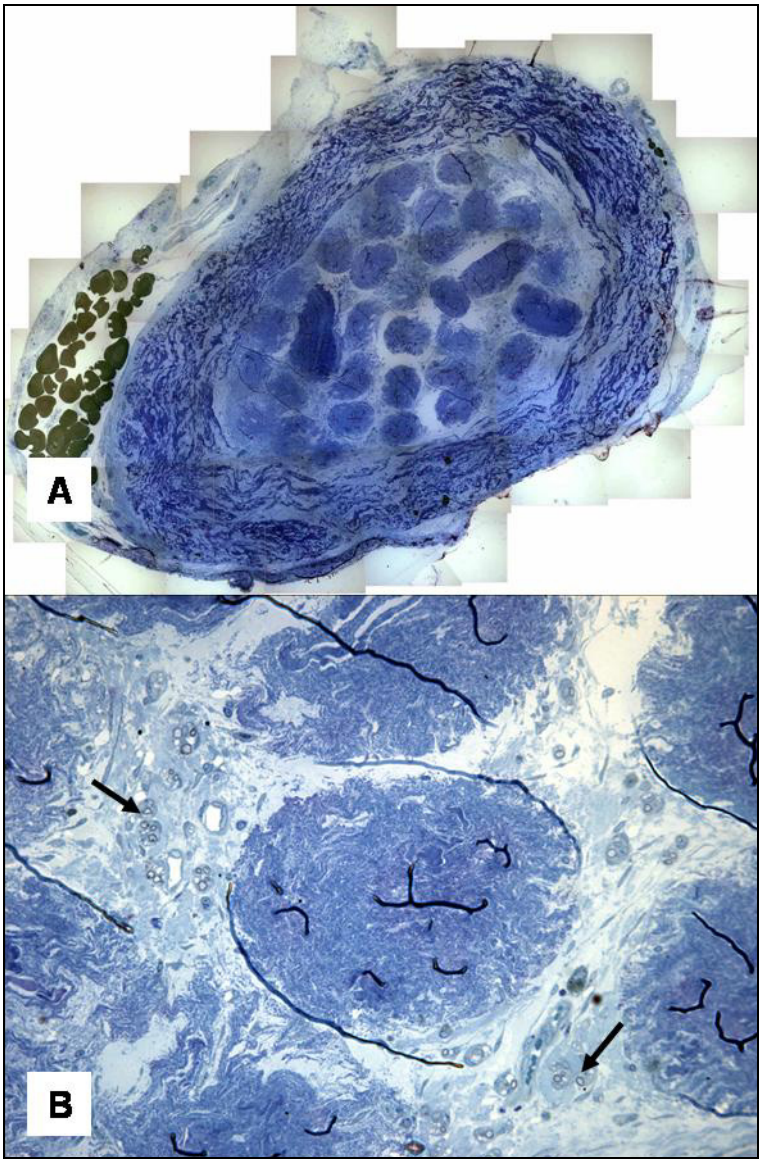

Figure 49 Nerve Guide With Filaments and Few Axons at 6 Weeks

(A) Montage from 6 week MF specimen. The filaments are separate and distinct. (B) reveals poor regeneration, few myelinated axons (black arrows) present in spaces between filaments. Total number of myelinated axons in this specimen is 393.

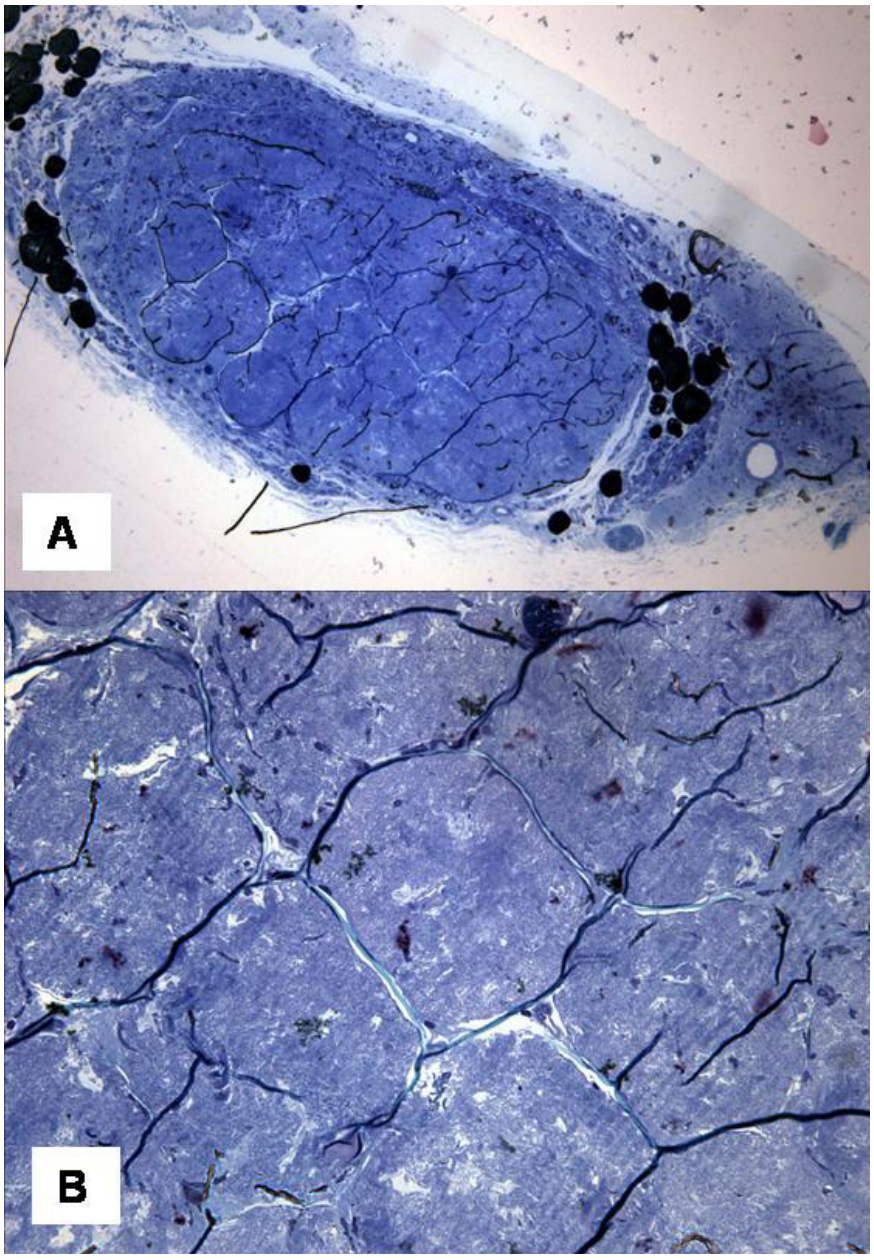

Figure 50 Aggregated Filaments & Failed Regeneration

In this 12-week MF specimen, the filaments appear to have swollen and aggregated obliterating space for axon growth. There are no axons in this section and little cellular infiltration of the filaments has taken place.

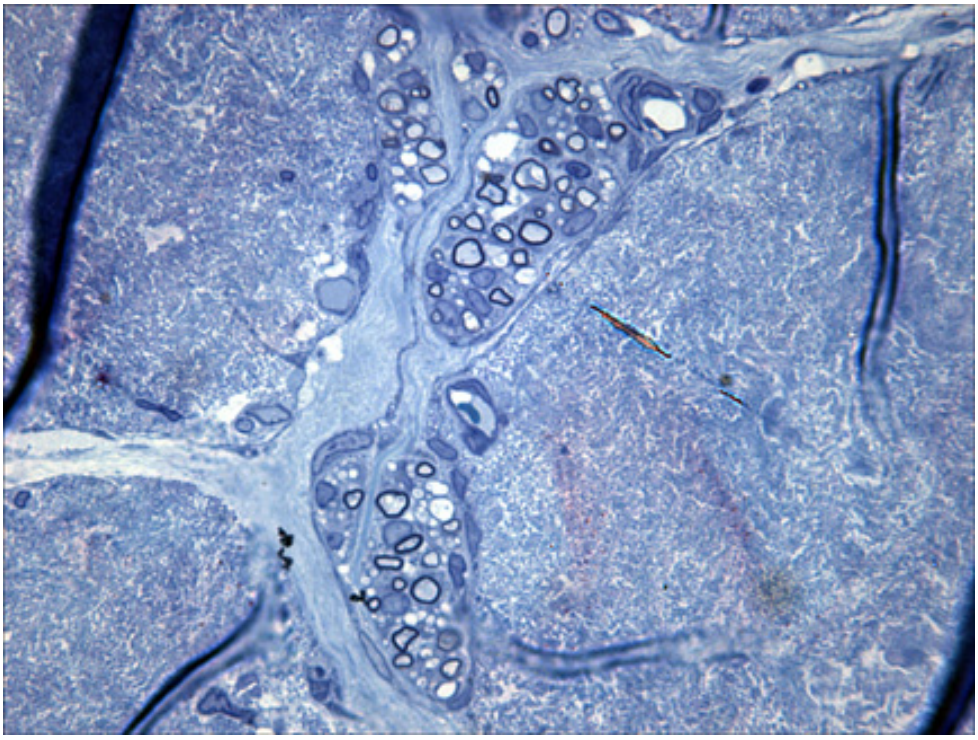

Figure 51 Small Number of Axons In between Filaments

At 6 weeks post implantation this MF nerve guide specimen has few myelinated and unmyelinated axons growing axons between filaments

Myelinated Axon Counts and Statistical Analyses

The montage technology worked successfully. It allowed us to count myelinated axons from the entire cross section of the nerve specimen. Although labor intensive, it proved critical for providing accurate evaluation of nerve regeneration through nerve guides with such varied morphology. Sample montage images from each nerve repair group and the normal control are displayed in figures 52 and 53.

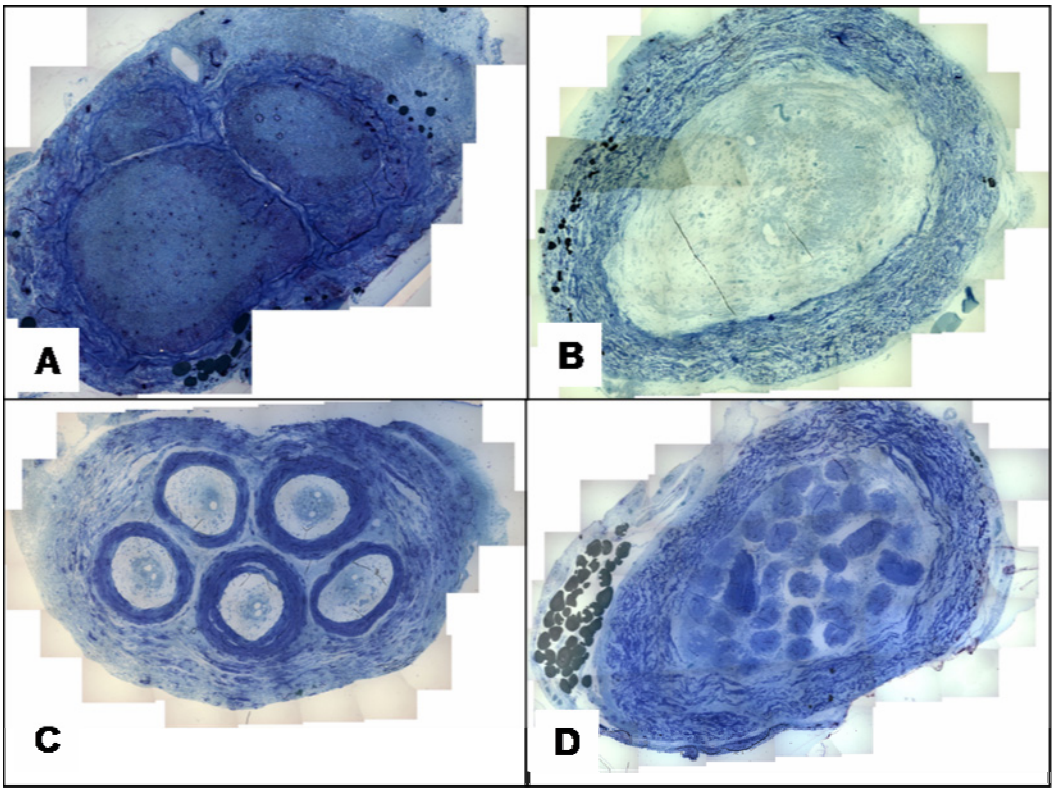

Figure 52 Nerve Repair Montages

Montages from each nerve repair group. (A) AG, (B) CT, (C) MT, (D) MF.

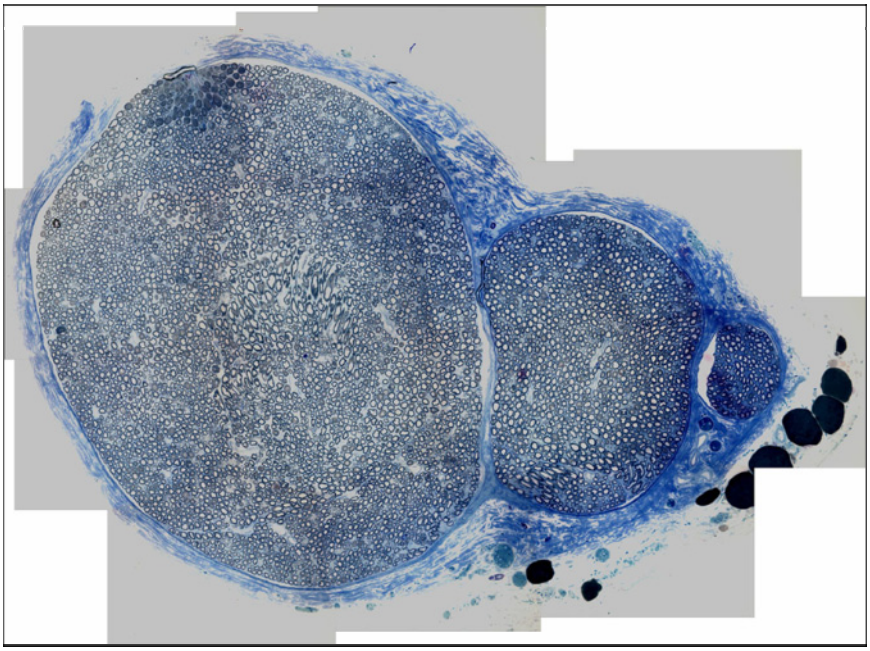

Figure 53 Normal Control Montage

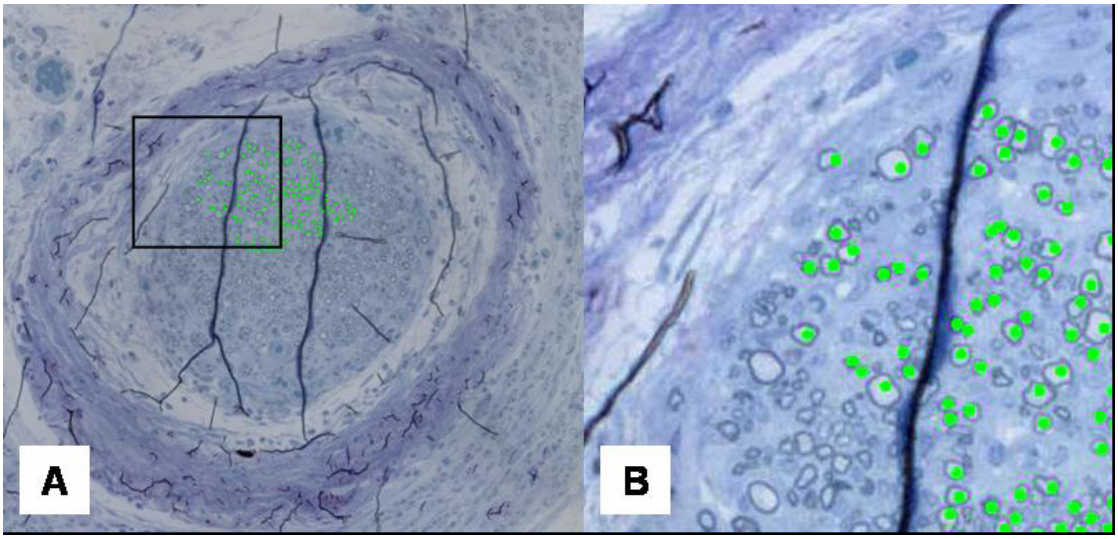

Figure 54 Partially Counted Nerve Guide

(A) Partially counted nerve area from a montage of a nerve guide with microtube channels 12 weeks after repair. Counted, myelinated axons are marked by dots. (B) Magnified view of region enclosed in (A).

Descriptive statistics of myelinated axon count are discussed and summarized in Table number 2 and Figure number 55 below. Following these are the results from the inferential statistical analyses.

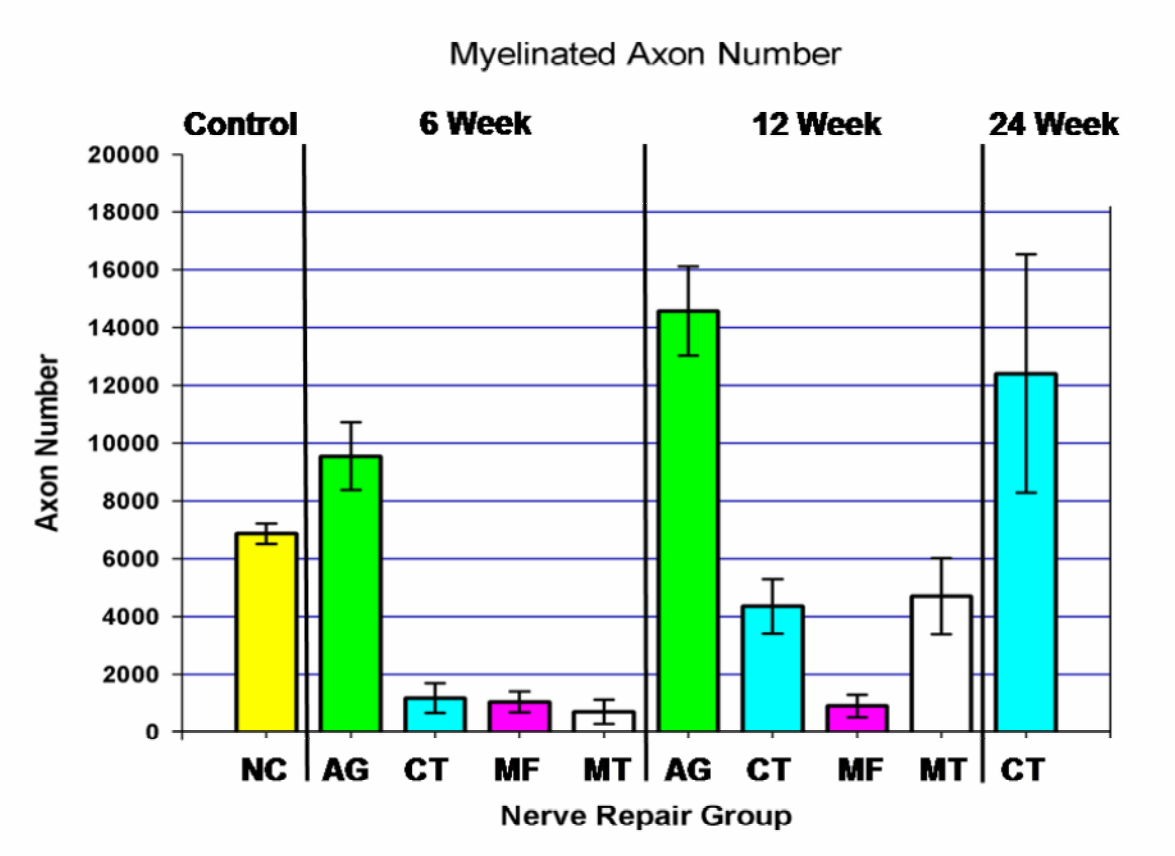

Figure 55 Number of Myelinated Axons After Post Nerve Repair

The mean number of myelinated axons in the middle section of the repair site increased from 6 weeks to 12 weeks in each repair group except MF. Differences between groups are considered significant with $P < 0.05$. At 6 weeks, AG has significantly more axons than CT, MF, and MT. There is no significant difference in the number of myelinated axons between CT, MT, and MF. At 12 weeks, AG has significantly more myelinated axons than CT, MT, and MF. Both CT and MT have significantly more myelinated axons than MF. There is no significant difference between the MT and CT group at 12 weeks. CT group at 24 weeks is not significantly different from the AG at 12 weeks. At both 6 and 12 weeks, only the AG had significantly more myelinated axons than the normal control.

Table 2 **Myelinated Axon Counts Raw Data**

6 week	6 week	6 week	6 week	12 week	12 week	12 week	12 week	24 week	Normal Control
AG	CT	MF	MT	AG	CT	MF	MT	CT	NC
9,201	2,354	0	2,172	12,712	9,384	0	4,521	22,515	6,031
12,694	0	3,334	0	9,133	1,272	0	744	21,486	4,279
13,582	36	82	222	13,715	4,444	103	3,477	9,812	7,430
11,168	485	159	0	22,590	4,280	10	5,055	6,459	5,920
8,393	5,108	393	0	14,277	3,213	1,050	11,923	1,756	7,640
0	2,048	913	3,951	21,412	2,947	4,789	9,994		7,318
10,106	135	1,681	0	14,026	1,755	0	2,115		7,234
9,881	527	220	275	13,667	4,174	255	24		7,852
10,031	1,084	2,292	193	9,538	2,179	2,696	575		7,687
10,425	0	1,632	186		9,842	464	4,957		7,327
						0	12,905		
						1,520	166		
						935			

At 6 weeks, the mean number of myelinated axons in the midsection of the AG repair was 9548. There was one complete failure (0 myelinated axons) out of 10 animals (n = 10). The AG repair at 6 weeks had myelinated axon counts ranging from 0 to 13,582. One specimen had a 0 axon count. The specimen containing the fewest number of myelinated axons in the 6-week AG group, had 8393 myelinated axons. The mean number of myelinated axons in the midsection of the entubulation nerve guide repairs (CT, MF, MT) was 1,178, 1,051, and 700 respectively (n = 10 in each group). In the 6-week time point, the myelinated axon counts ranged from 0 to 5108 in the CT group, 0 to 3334 in the MF group, and 0 to 3951 in the MT group. Each of the 6-week entubulation repair groups had at least 3 animals that contained fewer than 100 axons in the

mid-section of their nerve guides, and each group had at least one complete failure (0 myelinated axons). In the MT group only 2/10 (20%) had myelinated axon counts greater than 2000, and the rest, 8/10 (80 %), had axon counts less than 300. In fact, 4/10 (40%) had 0 myelinated axons in the MT group at the 6 week time point. In the MF group 6/10 (60%) had counts greater than 300, 2/10 (20%) had counts greater than 2000,

At 12 weeks, there were no failures among the AG group. The mean myelinated axon number was 14,563, and the number of myelinated axons ranged from 9,133 to 22,590 (n = 10). There were no obvious failures in the 12 week CT group, which had a mean of 4,349 myelinated axons and counts that ranged from 1,272 to 9,842 (n = 10), and the 12 week MF group had a mean of 909 with a range from 0 to 4,789 (n = 10). The 12 week MT group had a mean myelinated axon count of 4,705 with counts that ranged from 24 to 12,905.

In the CT group that went 24 weeks the mean myelinated axon count was 12,406 with a range from 1,756 to 22,515. The two highest counts in the 24 week CT group (22,515 and 21, 486) were almost identical to the 2 highest counts in the 12 week AG group (22,590 and 21,412). Although the AG repairs more consistently contained greater numbers of regenerated axons at 12 weeks, the empty collagen tube was capable of not only sustaining regeneration across a 10 mm gap but at a longer time point (24 weeks for CT verses 12 weeks for AG) regeneration was similar to the autograft, based on myelinated axon number.

Nerve Guides (CT, MF, MT) at 6 Weeks

Analyses of data included all specimens (i.e. specimens with 0 axon counts and extremely low counts, such as those with <100 axons). Myelinated axon counts from the mid section of the nerve guides in the 3 entubulation repair groups (CT, MF, MT) failed tests for normality (P=<0.001). Kruskal-Wallis One Way Analysis of Variance (ANOVA) on Ranks (a nonparametric comparisons test for 3 or more groups) was performed on the results of the myelinated axon counts. The null hypothesis was that the axon counts were not drawn from populations with different medians. The alternative hypothesis was that the myelinated axon counts were drawn from populations with different medians. More specifically, the number of myelinated axons in the nerve guides with guidance channels would be greater than that of the empty collagen nerve guide. We failed to reject the null hypothesis. There was no statistically significant difference in the number of myelinated axon between the three entubulation repair groups at six weeks (P = 0.488).

Mann-Whitney Rank Sum Tests were also performed to compare the myelinated axon counts from each microguidance channel nerve guide repairs to the empty collagen tube (CT) independently. First, the six-week axon counts from the CT group were compared to the MT group. The difference in the median between the CT group and the MT was not statistically significant (P = 0.344). Next the CT group was compared to the MF group and there was no

statistically significant difference (P = 0.970). At 6 weeks there is not a significant difference in the number of myelinated axons between the MT and MF group (Mann-Whitney Rank Sum Test, P = 0.307).

Nerve Guides Verses Autografts at 6 Weeks

Kruskal-Wallis One Way ANOVA on Ranks followed by Dunn's Method of Multiple Comparisons versus Control was used to test for significant differences in myelinated axon counts from all entubulation nerve repair groups and the autografts at 6 weeks. The ANOVA on ranks revealed a statistically significant difference (P = 0.001). The multiple comparisons test revealed statistically significant differences between each of the entubulation repairs and the autograft repairs at 6 weeks (P < 0.05). All the entubulation repairs with collagen nerve guides (CT, MF, MT) had significantly fewer myelinated axons than the AG group at 6 weeks.

Nerve guides at 6 Weeks Verses Normal Control

Kruskal-Wallis One Way Analysis of Variance on Ranks was used to test for significant differences in myelinated axon counts between the entubulation repair groups and the normal sciatic nerve control. There was a statistically significant difference between these repair groups and the normal control (P = 0.001). Dunn's method of Multiple Comparisons versus the Normal Control group was performed to isolate the groups that differed significantly. Each of the

6 week entubulation repair groups (CT, MT, MF) had myelinated axon counts were significantly less than the normal control axon counts ($P < 0.05$).

Nerve Guides (CT, MF, MT) at 12 Weeks

As in the 6-week time point, the null hypothesis was that there is no difference in the number of myelinated axons in the mid section of the nerve guide between the different entubulation repairs. The alternative hypothesis was that the number of myelinated axons in the nerve guides with guidance channels would be greater than that of the empty collagen nerve guides.

The myelinated axon counts from the mid section of the nerve guides in the 3, 12-week entubulation repair groups (CT, MF, MT) failed tests for normality ($P = < 0.001$). Kruskal-Wallis One Way Analysis of Variance (ANOVA) on Ranks was performed on the results of the myelinated axon counts. There was a statistically significant difference between groups ($P = 0.002$). Dunn's Method of Multiple Comparisons procedure followed. Both the CT and MT groups have significantly more myelinated axons than the MF group at 12 weeks ($P < 0.05$). The mean myelinated axon number in the MT group is larger than the CT group but this difference was not statistically significant. Additionally, a Mann-Whitney test was run to compare the 12-week MT group to the 12-week MF group. The MT group had significantly more myelinated axons than the MF group ($P = 0.008$).

Nerve Guides Verses Autografts at 12 Weeks

Kruskal-Wallis One Way ANOVA on Ranks was used to test for significant differences between the number of myelinated axons in the mid section of the entubulation nerve guide repairs and the AG nerve repairs at 12 weeks. The differences in median values between groups are significantly difference ($P = 0.001$). Dunn's Method of Multiple Comparisons versus Control was used to isolate differences between groups with the autograft assigned as the control. All of the entubulation repairs (CT, MF, MT) had significantly fewer myelinated axons in the mid section of the repair site than did the AG repairs ($P < 0.05$).

Nerve guides at 12 Weeks verses Normal Control

Kruskal-Wallis One Way ANOVA on Ranks was used to test for significant differences between the number of myelinated axons in the all the entubulation nerve repairs at 12 weeks as compared to the normal control sciatic nerve. There were significant differences ($P = < 0.001$). Dunn's Method of Multiple Comparisons verses Control Group followed. Both the CT and MF groups had fewer myelinated axons than the normal control sciatic nerve ($P < 0.05$).

Analysis of Groups Over Time

There was a trend of increasing number of myelinated axons group over time. In order to test if a significant difference in groups existed over time

Kruskal-Wallis One Way ANOVA on Ranks was performed on the CT groups of 6, 12, and 24 weeks. This was the only repair type with a 24 week survival time (n=5). The difference in medians was statistically significant (P = 0.002). Dunn's Method of Multiple Comparisons revealed a statistically significant difference between the 6 week CT group and the 12 week CT group, the 6 week CT group and the 24 week CT group ($P < 0.05$). No statistically significant difference existed between the 12 week CT group and the 24 week CT group.

Each nerve repair group was analyzed across the 6 week and 12 week time periods to see if there was a statistically significant increase in the number of myelinated axons with in each group over time. The 12 week CT group had significantly more myelinated axons than the 6 week CT group (Mann-Whitney Rank Sum Test, P = 0.006). The 12 week MT group had significantly more myelinated axons than the 6 week MT group (Mann-Whitney Rank Sum Test, P = 0.008). The difference between the 6 and 12 week MF groups was not significant (P = 0.438). The 12 week AG group had significantly more myelinated axons than the 6 week AG group (t-test, P = 0.018). The Bonferroni approximation to correct for multiple comparisons was not indicated since results were reported for within group comparisons across time only.

Nerve Repair Versus Normal Control Across Time Periods

Both the 6 week and 12 week AG groups had significantly greater number of myelinated axons than the normal control (Kruskal-Wallis One Way ANOVA on

Ranks, $P < 0.05$). The only entubulation repair to have a mean number of myelinated axons greater than the normal control was the 24 week CT group. This difference, however, did not reach statistically significance (Mann-Whitney Rank Sum Test, $P = 0.358$). In other words, by 24 weeks the number of myelinated axons in the CT group was not significantly different from the normal control.

Post Hoc Analyses

Both the data from the 6 week groups and from the 12 week groups were subjected to further analysis using different cut offs for inclusion in the statistics, based on the notion that including the "failures" may somehow skew the results and cause us to miss an important trend. Cut offs of 100, 500, 1500, and 2000 axons were tested. Only nerve guides with axon counts greater than those cut offs were included in the statistical comparisons. There was essentially no change in the results when using variable cut offs for statistical analyses.

Myelinated Axon Diameters

Images captured with the digital camera and 100x oil objective lens provided the resolution necessary for measurements of axonal diameter. ImageJ software leaves a line and number designation on each measured axon (figure 56). This feature enabled us to be certain that each axon was measured but once. The toluidine blue stained, osmicated, sections enabled us to readily discern myelinated from unmyelinated axons in regenerating nerves (figure 57). Tables 3 and 4 summarize the diameter results, and they are displayed graphically in Figures 58 and 59.

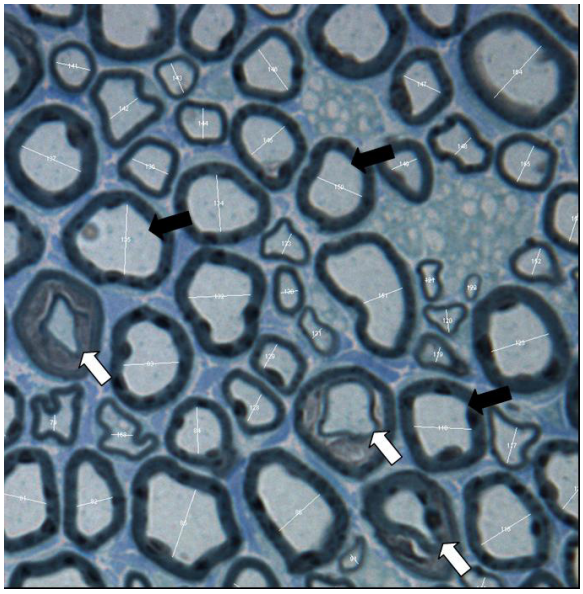

Figure 56 Axon Diameters of Normal Control

Cropped image (100x oil objective lens) of normal nerve. The axonal diameter was measured from all the myelinated axons (black arrows) from digital images captured through the 100x oil objective lens excluding any axons that are not completely within the field, and any axons that have double myelin rings (white arrows), which occur at Schmidt-Lanterman clefts. Non-circular and distorted axons were measured across their shortest diameter to avoid inflating estimates of axon size.

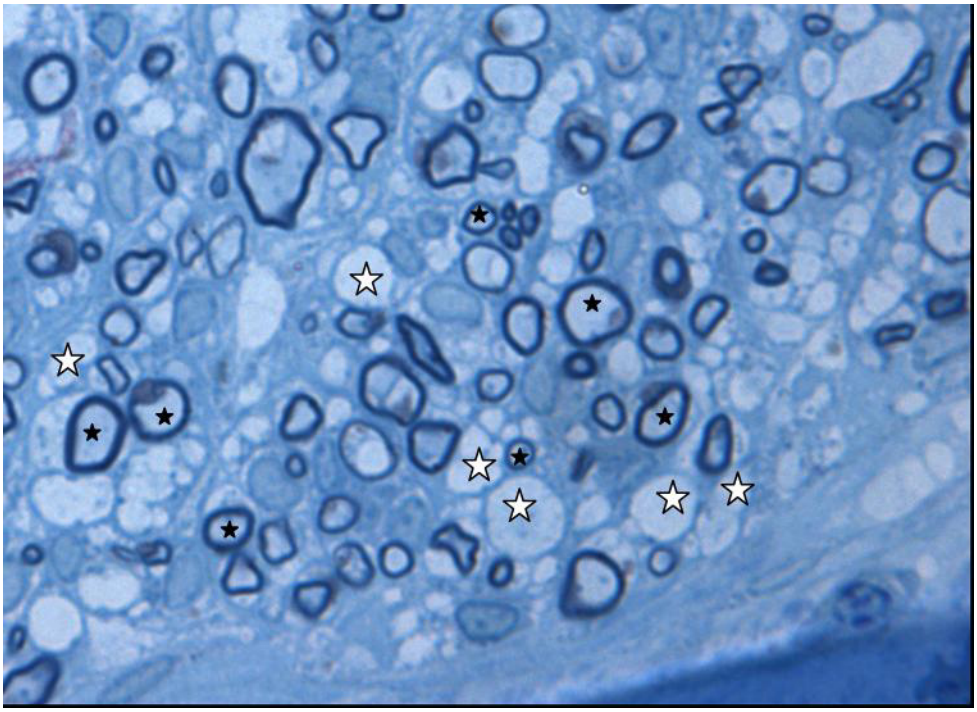

Figure 57 Regenerated Nerve, Myelinated versus Unmyelinated Axons

Cropped image (100x oil objective) from a nerve guide specimen (6 week MT group), which shows the contrast of myelinated (black stars) and unmyelinated (white stars) axons. This contrast was sufficient for counting and measuring myelinated axons in regenerated nerve sections.

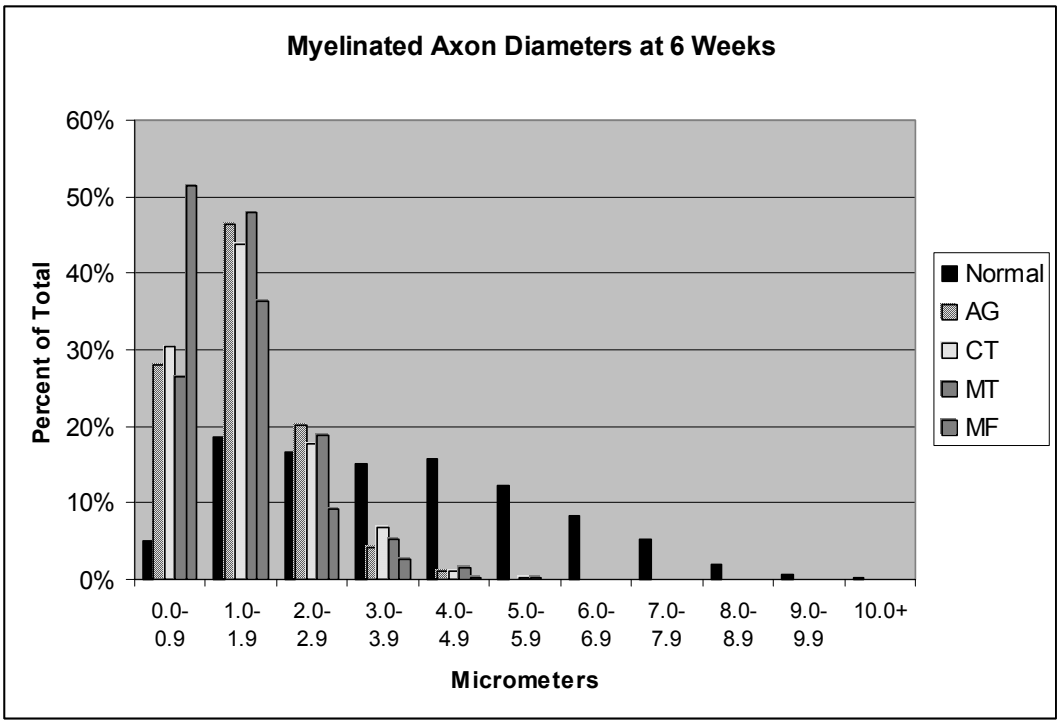

Figure 58 **Histogram of Myelinated Axon Diameters at 6 Weeks**

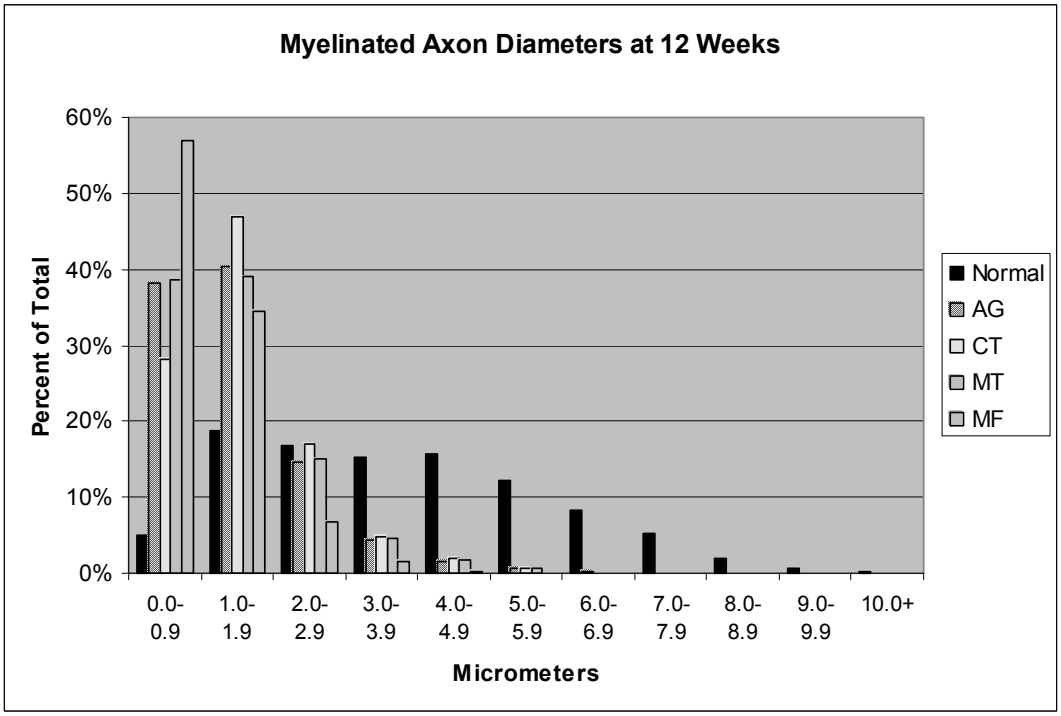

Figure 59 **Histogram of Myelinated Axon Diameters at 12 Weeks**

Table 3 **Myelinated Axon Diameters at 6 Weeks**

Micrometers	Normal	AG	CT	MT	MF
0.0-0.9	5%	28%	30%	27%	51%
1.0-1.9	19%	46%	44%	48%	36%
2.0-2.9	17%	20%	18%	19%	9%
3.0-3.9	15%	4%	7%	5%	3%
4.0-4.9	16%	1%	1%	1%	0%
5.0-5.9	12%	0%	0%	0%	0%
6.0-6.9	8%	0%	0%	0%	0%
7.0-7.9	5%	0%	0%	0%	0%
8.0-8.9	2%	0%	0%	0%	0%
9.0-9.9	1%	0%	0%	0%	0%
10.0+	0%	0%	0%	0%	0%
Mean	**3.83 µm**	**1.53 µm**	**1.54 µm**	**1.56 µm**	**1.21 µm**

Table 4 **Myelinated Axon Diameters at 12 Weeks**

Micrometers	Normal	AG	CT	MT	MF
0.0-0.9	4.9%	38.1%	28.1%	38.6%	57%
1.0-1.9	18.7%	40.3%	47.0%	39.1%	34%
2.0-2.9	16.7%	14.7%	16.9%	15.1%	7%
3.0-3.9	15.2%	4.3%	4.8%	4.7%	2%
4.0-4.9	15.8%	1.5%	1.9%	1.7%	0%
5.0-5.9	12.3%	0.7%	0.7%	0.7%	0%
6.0-6.9	8.3%	0.3%	0.0%	0.1%	0%
7.0-7.9	5.2%	0.0%	0.0%	0.0%	0%
8.0-8.9	2.1%	0.0%	0.0%	0.0%	0%
9.0-9.9	0.6%	0.0%	0.0%	0.0%	0%
10.0+	0.2%	0.0%	0.0%	0.0%	0%
Mean	**3.83 µm**	**1.40 µm**	**1.56 µm**	**1.42 µm**	**0.99 µm**

Regenerated nerves in all repair groups, at both the 6 and 12 week time points, contained myelinated axons with a mean diameter significantly less than the normal control sciatic nerve ($P < 0.05$, multiple comparisons versus control, Dunnett's method). There was no significant difference in the mean axon diameter between repair groups at the 6 week time point ($P = 0.298$, power is

0.100, One Way ANOVA) or 12 week time point (P = 0.063, power is 0.402, One Way ANOVA).

All the nerve repair groups had similar percentages myelinated axons in the each diameter range (Figures 58, 59). At least 70% of the myelinated axons in the 12-week repair groups were less than 2.0 μm (Figure 59). This was in contrast to normal nerve, which has less than 24% of myelinated axons less than 2.0 μm. Each repair group except the MF group has less than 1% of myelinated axons greater than 5.0 μm at 12 weeks post repair. The MF group had no myelinated axons 4.0 μm or greater in diameter. In the CT group, there was an increase in mean myelinated axon number over time, as previously stated; however, the percentage of axons in each diameter range is similar (Figure 60). The exception was at 24 weeks, there were 0.3% of the myelinated axons in the 6.0 to 6.9 μm range while at earlier time points all axons were smaller in diameter than 6.0 μm in the CT repair group. The AG had 0.3% of the myelinated axons in the 6.0 to 6.9 μm at the 12-week time point.

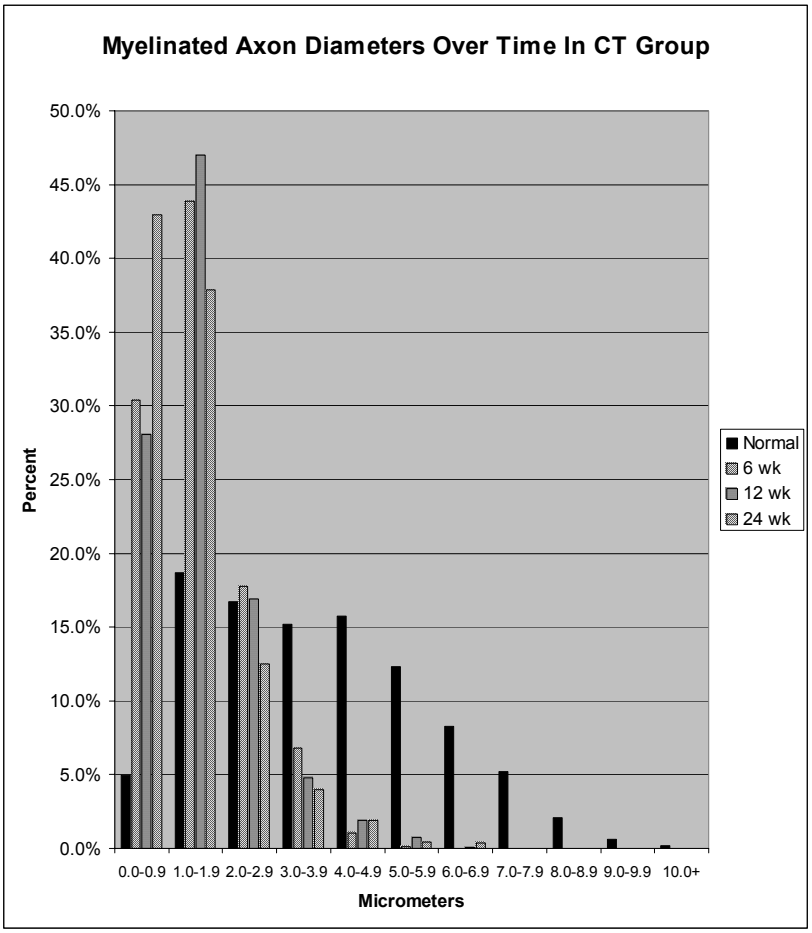

Figure 60 **Myelinated Axon Diameters Over Time CT Group**

Table 5 **Myelinated Axon Diameters Over Time CT Group**

Diameter	Normal Control	6 wk CT	12 wk CT	24 wk CT
0.0-0.9	4.9%	30.4%	28.1%	43.0%
1.0-1.9	18.7%	43.9%	47.0%	37.9%
2.0-2.9	16.7%	17.8%	16.9%	12.5%
3.0-3.9	15.2%	6.8%	4.8%	4.0%
4.0-4.9	15.8%	1.0%	1.9%	1.9%
5.0-5.9	12.3%	0.1%	0.7%	0.4%
6.0-6.9	8.3%	0.0%	0.0%	0.3%
7.0-7.9	5.2%	0.0%	0.0%	0.0%
8.0-8.9	2.1%	0.0%	0.0%	0.0%
9.0-9.9	0.6%	0.0%	0.0%	0.0%
10.0+	0.2%	0.0%	0.0%	0.0%

Electrophysiology

Axons grew across the repair site in specimens from each group as evidenced by the recording of extracellular nerve action potential recordings of the sciatic nerve distal to the repair. In addition, there was electrophysiological evidence from each group that axons not only crossed the repair site but also grew back to reinnervate intrinsic muscles of the foot. Nerve conduction velocity across the repairs site was calculated in several specimens and found to be significantly lower than normal. The presence of a clean CMAP shift following a change in stimulus location, which is necessary for calculation of NCV, in general, was more consistently recorded from animals that received autograft repair than entubulation repair

As stated previously, several electrophysiological evaluation methods were used to determine return of function in different nerve repair groups. Below, are representative data from each method along with the results of experiments that allowed us to understand how errant action potentials cause interference patterns during gastrocnemius muscle recordings.

Compound Nerve Action Potentials

Figures 61 and 62 are images of the computer screen from electrophysiological experiments in which evoked CNAPs were recorded with two sets of hook electrodes placed on either side of the repair site. In each pair of images, the top image was derived from the sciatic nerve 12 weeks post repair,

and the bottom image was derived from the normal contralateral sciatic nerve. These images demonstrate conduction of nerve action potentials across the repair site. In each example, the magnitude of the action potential from the repaired nerve was less than that of the contralateral normal nerve. Unfortunately, in many cases, further analysis was not possible due to the size and proximity of the stimulus artifact, which obscured a portion of the CNAP.

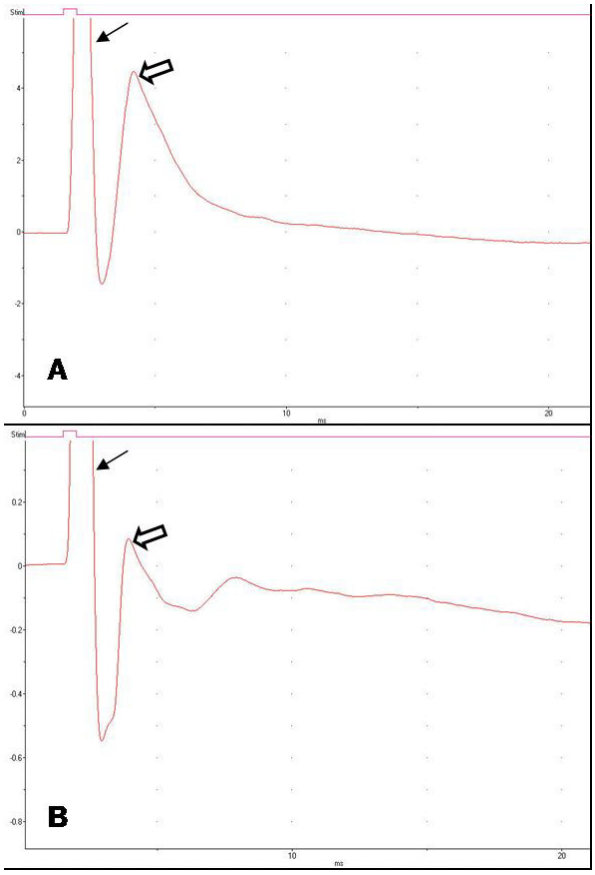

Figure 61 Compound Nerve Action Potentials CT Group

Representative Electrophysiological Trace. (A) Normal sciatic nerve extracellular action potential tracing. (B) Recording from nerve repaired with empty nerve guide (CT) 12 weeks prior. The stimulus artifact is large (solid arrow) and obscures a portion of the nerve action potential (open arrow). This specimen had 9,384 myelinated axons counted from the middle of the repair site.

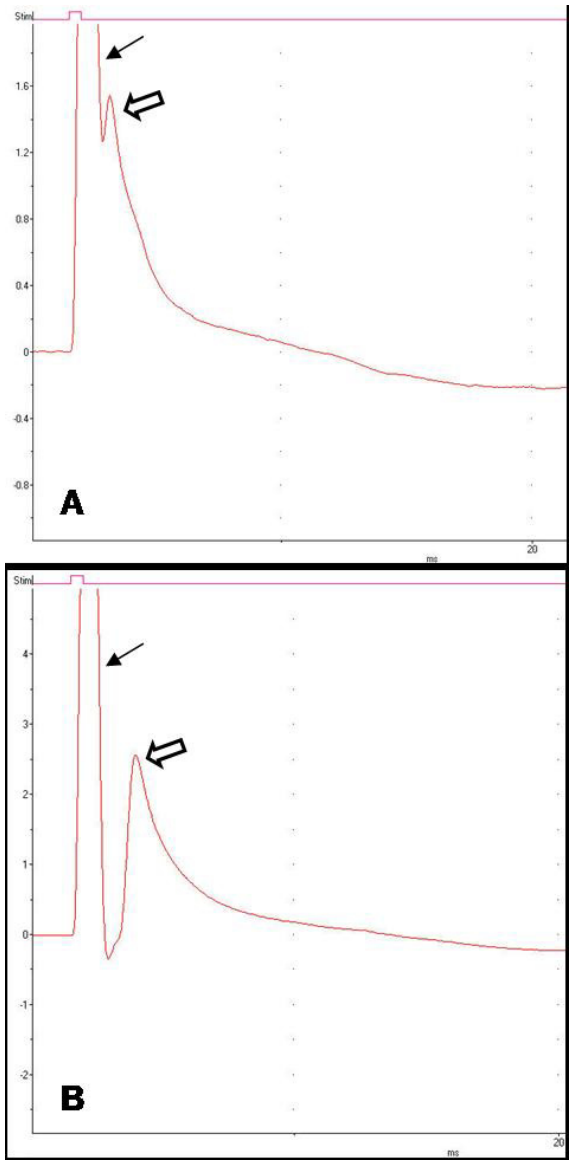

Figure 62 Compound Nerve Action Potentials MT Group

Representative Electrophysiological Trace. (A) Normal sciatic nerve extracellular action potential tracing. (B) Recording from a nerve repaired with a MT nerve guide 12 weeks prior. The stimulus artifact is large (solid arrow) and obscures a portion of the nerve action potential (open arrow). This specimen had 4,521 myelinated axons counted from the middle of the repair site.

Compound Muscle Action Potentials and Anatomy

Figures 63, 64, and 65 illustrate the results from two experiments performed on a normal rat to determine the electrophysiological contribution to

the gastrocnemius muscle recordings of a large branch of the tibial division of the sciatic nerve, which we now know innervates the biceps femoris muscle (accessory head, anterior head & posterior head). Two experiments were performed and are described below. It is noteworthy that the biceps femoris muscle is superficial to and completely covers the lateral head of the gastrocnemius in the Lewis rat. These experiments demonstrated that when uncoated needle recording electrodes were inserted percutaneously into the normal gastrocnemius muscle, by passing the needle through the biceps femoris, and the sciatic nerve was stimulated in gluteal region, the recorded CMAPs were a summation of both the gastrocnemius and the biceps femoris. Stated differently, the distinct gastrocnemius CMAP was obscured by combining with biceps femoris CMAP. The CMAP's from both muscles are in phase because the stimuli reaching each muscle were traveling through a normal nerve, which have approximately the same conduction velocity.

Figure 63 shows the results of experiment 1 (normal left hind limb), in which the sciatic nerve was stimulated with the platinum wire electrode in the exposed gluteal region. Recordings were taken from the gastrocnemius muscle and 3d metatarsal space prior to and after transection of the nerve branching from the tibial division of the sciatic nerve, proximal to where the nerve repair site would be in an operated rat, during stimulation of the sciatic nerve in the gluteal region. The amplitude of the gastrocnemius CMAPs dropped by approximately half when the sciatic nerve branch to the biceps femoris was cut while the

amplitude of the CMAPs recorded from the 3d metatarsal space did not change in magnitude. This result indicated that the muscle innervated by this sciatic nerve branch was contributing to the magnitude of the amplitude of the electrodes that were targeted for the gastrocnemius muscle. Recordings from muscle in the foot were not affected by the nerve that branched from the sciatic nerve proximal to the precise site that is transected and repaired in the animals in this study; they were innervated by nerves that branched from the sciatic nerve distal to the repair site.

Next, the sciatic nerve was transected in the same location that is used in the rats that receive entubulation repair. The nerve was stimulated and CMAPs were recorded after transection of the sciatic nerve

Experiment 2 (normal right hind limb): Recordings were taken from the gastrocnemius muscle and from the 3d metatarsal space during stimulation of the sciatic nerve in the exposed gluteal region. The sciatic nerve was transected at the same location as in animals that entubulation repair was performed. This left the nerve branching from the tibial division of the sciatic nerve, intact since it was proximal to the lesion site. When the sciatic nerve was stimulated in the gluteal region, the gastrocnemius recording electrodes record a large CMAP, but the electrodes in the 3d metatarsal space record none. If the electrodes that were set up to record gastrocnemius CMAPs was only recording potentials from the gastrocnemius muscle there should have been no CMAPs following transection of the sciatic nerve. Our conclusion is, the CMAP must have been

recording from another muscle. The likely contributor is the biceps femoris, which lies superficial to the gastrocnemius on its lateral aspect. It is this muscle that the uncoated electrode passed through in order to reach the gastrocnemius. When the nerve branching from the tibial division of the sciatic nerve is subsequently cut, there is no longer a recorded CMAP from this electrode set up.

The results of these two experiments systematically demonstrate the contribution of the proximal tibial division of the sciatic nerve to the biceps femoris muscle in the normal rat during percutaneous bare needle electrode recordings of the gastrocnemius with the G2 electrode placed subcutaneous in the region of the gastrocnemius and sciatic nerve stimulation in the gluteal region.

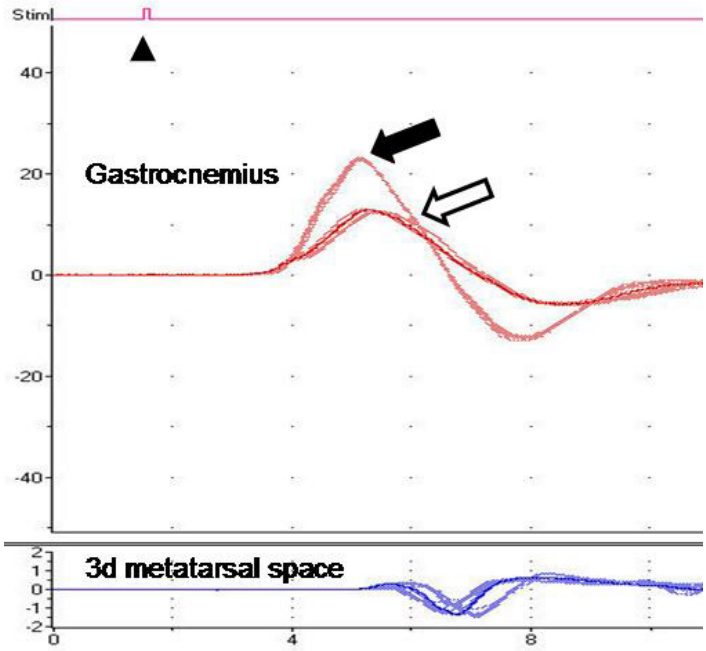

Figure 63 Normal Gastrocnemius CMAP & Biceps Femoris

Experiment #1 Normal Rat Left Hindlimb. Overlay of CMAPS prior to (solid arrow) and after (open arrow) transection of proximal tibial division of the sciatic nerve with percutaneous needle electrode insertion to gastrocnemius muscle. Prior to cutting tibial nerve: the CMAP has a peak of 23.28mV occurring at 5.15ms, after the nerve is cut the CMAP peak is 12.95mV peak at 5.30ms. Notice the deviation from baseline (3.4ms) and the peak of the CMAP under both conditions occurs at approximately the same time (latency) in these normally innervated muscles. There is not a similar change in peak amplitude on lower channel (3d metatarsal space) because the tibial nerve, a terminal division of the sciatic nerve originates distal to the region used for the entubulation repair groups, continues as the lateral plantar nerve as it enters the foot and innervates the musculature of the foot

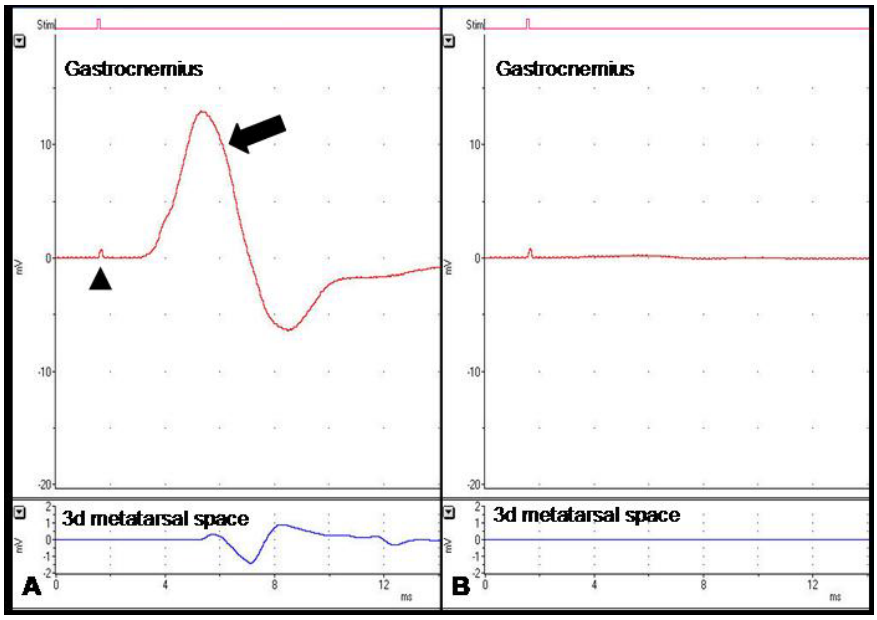

Figure 64 Gastrocnemius CMAP Cut Sciatic Nerve

(A) CMAP of normal gastrocnemius (arrow) top trace) and 3d metatarsal space (bottom trace) after transection of the proximal tibial division of the sciatic nerve. The arrow head points to the stimulus artifact. (B) Absence of CMAPs on both channels recorded immediately after transection of the sciatic nerve at the site used in animals that receive entubulation repair.

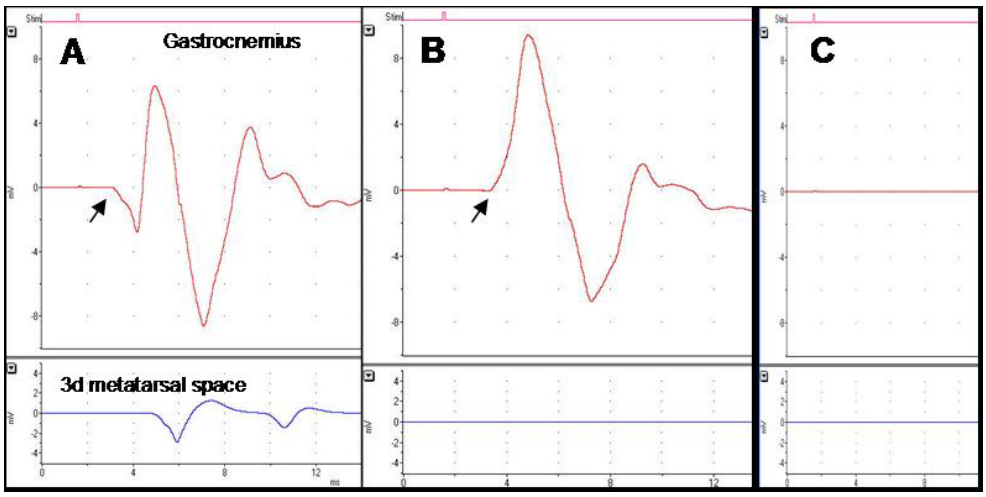

Figure 65 Electrophysiology Experiment Two

The Sciatic nerve is cut first, and then the nerve to the biceps femoris is cut in a normal Lewis rat. (A) Before cutting sciatic nerve, a CMAP (top channel) is recorded from gastrocnemius electrodes and from the 3d metatarsal space (bottom channel). (B) After sciatic nerve is cut (distal to branching of the nerve to the biceps femoris muscle). Note there is still a recorded CMAP on the top channel even after sciatic n. is cut, however there is no CMAP recorded on bottom channel (3d metatarsal space.) (C) Recordings taken after the nerve to the biceps femoris is cut showing that are no longer CMAPs.

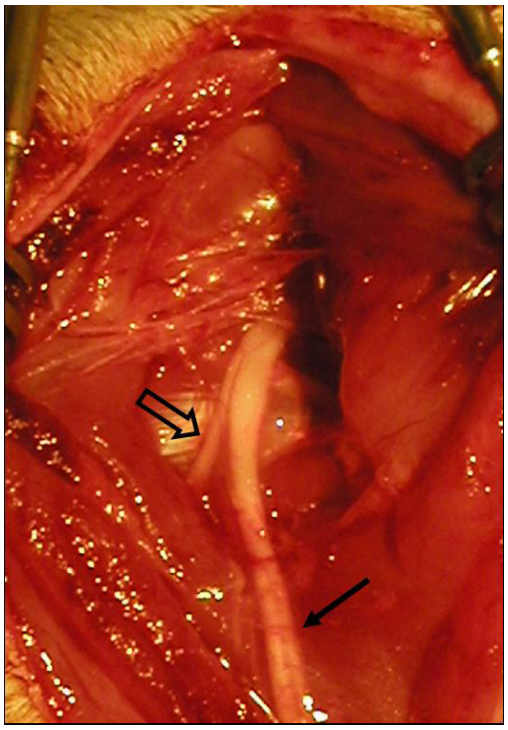

Figure 66 Anatomical Study & Nerve Branch to Biceps Femoris

Rat sciatic nerve in gluteal region and posterior thigh (solid arrow) displaying a large nerve (open arrow) that branches from its tibial division. This nerve innervates the biceps femoris.

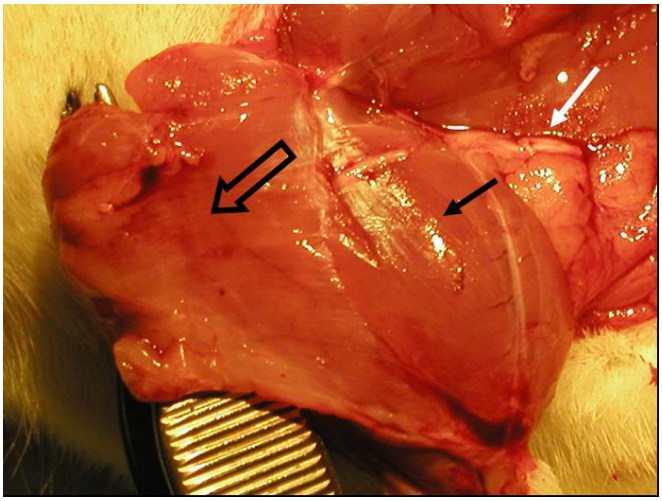

Figure 67 Anatomical Study Rat Hindlimb Musculature

This Figure shows the relationship of the gastrocnemius (solid black arrow) and the biceps femoris (open arrow). The biceps femoris muscle is transected and reflected to display the gastrocnemius. Prior to the dissection, the biceps femoris completely covered the lateral head of the gastrocnemius. The gastrocnemius muscle (lateral and medial heads) are innervated by muscular branches (white arrow) of the tibial nerve.

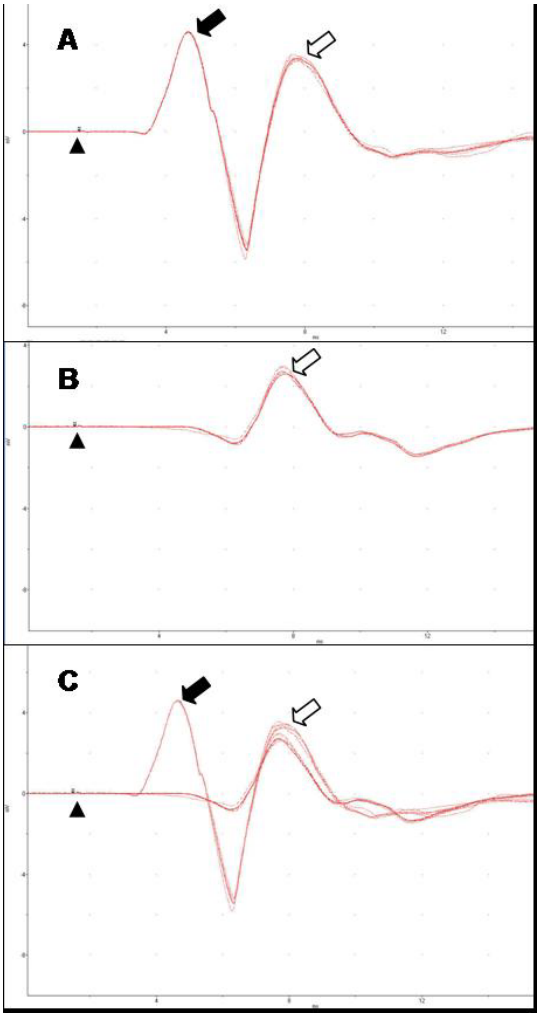

Figure 68 CMAP's From Gastrocnemius & Biceps femoris

These recordings are from the specimen from the 12week CT group with the greatest number of myelinated axons (9,842) in the nerve guide midsection. CMAPs recorded from the gastrocnemius prior to (A) and after (B) cutting the nerve to biceps femoris. (A) CMAPs recorded from percutaneous needle electrodes in gastrocnemius muscle image prior to nerve transection (showing 2 peaks: 1st (solid arrow) with a latency to peak of 3.124ms, 4.58mV max, amplitude 9.986mV. Second peak (open arrow) in the top image has a latency of 6.3, 3.36mV max, 4.52mV Amplitude (Max-Min) (B) is a CMAP after nerve to biceps femoris was cut. Latency to peak is 6.2ms, 2.75mV max, 4.13mV amplitude. (C) Is the overlay of both recordings (A) and (B) showing that the second peak is from the gastrocnemius muscle. The regenerated axons have reinervated the muscle and the latency is longer relative to the peak from the biceps femoris peak.

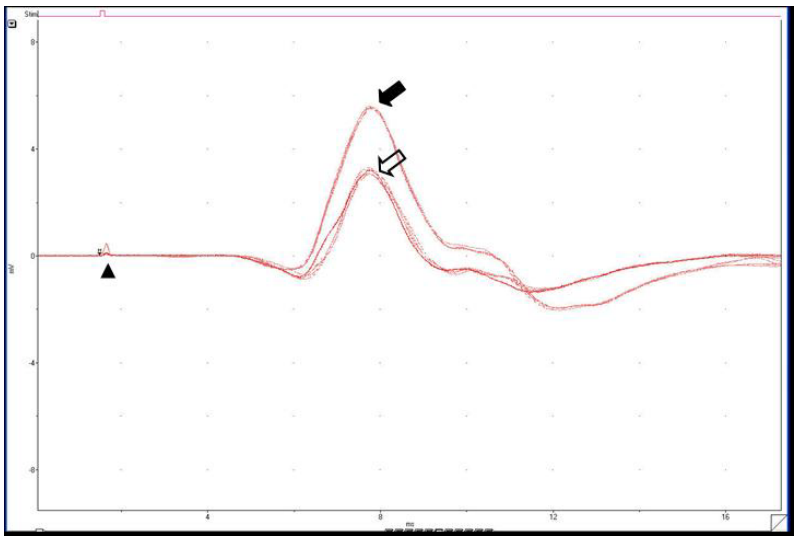

Figure 69 Gastrocnemius CMAP and G2 Electrode Position

This Figure illustrates the affect of G2 electrode placement on amplitude in a specimen from the 12 week CT group that contained the greatest number of myelinated axons (9,842) in the nerve guide midsection. It is an overlay of several CMAPs recorded with the G2 electrode placed subcutaneously over the gastrocnemius (smaller amplitude, open arrow), and several CMAPs recorded with the G2 electrode place subcutaneously over the lateral malleolus (larger amplitude, solid arrow).

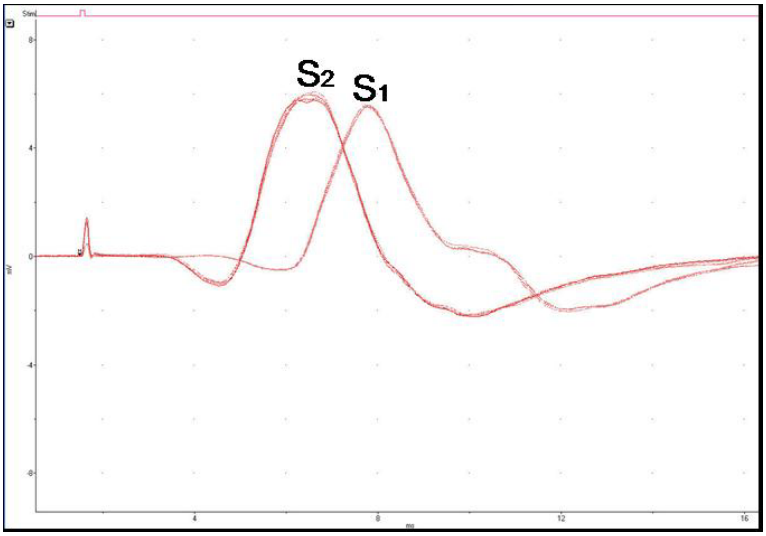

Figure 70 Shift of CMAP Latency From S1 to S2

CMAPs recorded from the gastrocnemius muscle of a specimen from the 12 week CT group. The shift from S1 to S2 shows the decrease in latency when the stimulating electrode is moved from the sciatic nerve in the gluteal region (S1) to the sciatic nerve in the thigh (S2) distal to the nerve repair. Measurements of the inter-electrode distances were recorded and used to calculate conduction velocity across the repair site. S1 latency to peak = 6.28ms, S1 to G1 distance = 51mm. S2 latency to peak = 5.125ms, S2 to G1 distance = 29mm. NCV = 19.1 m/s. This specimen had 9,842 myelinated axons in the midsection of the repair.

Table 6 Nerve Conduction Velocities 12 Weeks Post Repair

Normal Control	AG	CT	MF	MT
52 m/s ± 8 (n=7)	20 m/s ± 6 (n=2)	17 m/s ±2 (n=3)	-	-

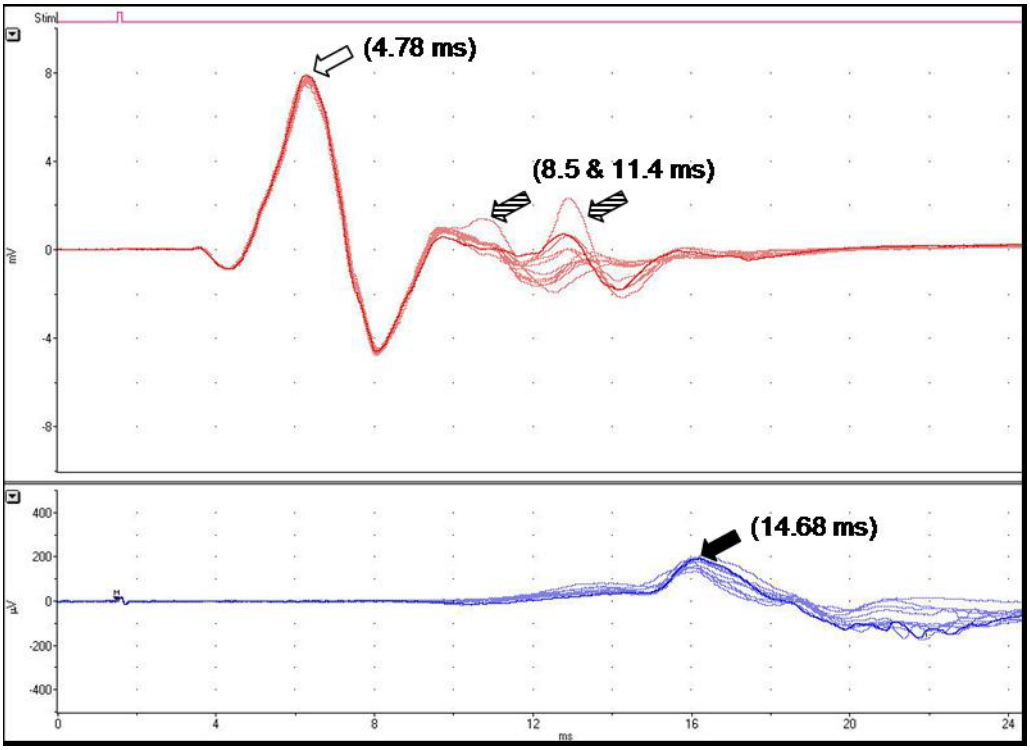

Figure 71 CMAP in 1st Metatarsal Space in 12 Week MT Group

On the top channel the 1st large CMAP (open arrow) is likely from the normally innervated biceps femoris and was recorded unintentionally. One or both of the later peaks (striped arrows) on this same channel are likely CMAPs recorded from the gastrocnemius muscle. Their latency's to peak amplitude (8.5 & 11.4ms) and the magnitude of their amplitudes are more indicative of CMAPs from immature regenerated nerve. Initially the recording electrode was in the 3d metatarsal space, and no CMAP was recorded upon stimulation of the sciatic nerve in the gluteal region. Because of the observation of active 1st toe abduction/adduction by this animal when it was in the static stance photography box, a needle electrode was inserted into the 1st metarsal space and a CMAP (solid black arrow on bottom channel) was successfully recorded. This is the rat from the MT group with the greatest number of myelinated axons (12,905) in the mid-section of the repair.

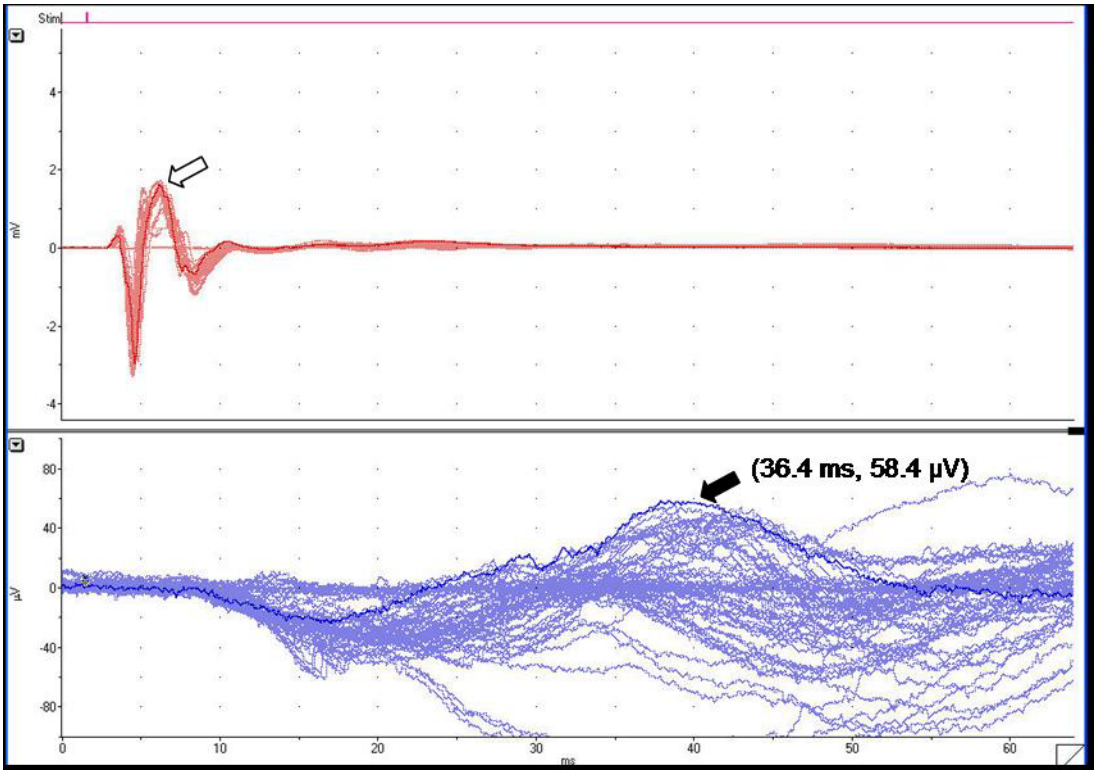

Figure 72 Late CMAP in Foot

R86 12 wk MF group had only 103 myelinated axons counted in mid-section of nerve guide yet there is a CMAP (solid black arrow) in the foot. It has a long latency (36.4ms) indicative of poorly myelinated axons, which have reduced conduction velocities relative to normal. The CMAP is of small amplitude (58.4µV) indicating few and small motor units, which is in turn indicative of few axons reaching and forming functional synaptic connections with this muscle group. The top channel scale (open arrow pointing to large CMAP) is in millivolts where as the bottom is in microvolts to enable viewing this small amplitude CMAP recorded from the foot.

Motor Unit Number Estimation (MUNE)

Recordings were taken in manner conducive to MUNE analysis, however this method was discontinued and the analysis was not performed. The reasons for this are elaborated upon in the discussion. Figure 74 is simply provided to demonstrate how the examiner would display recorded CMAPs prior to the analysis described in the methods section.

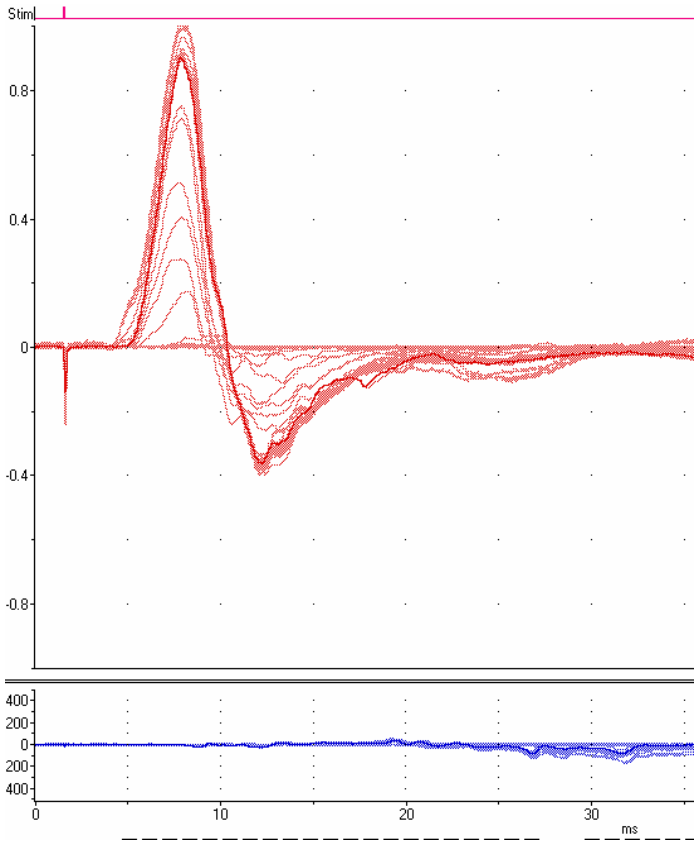

Figure 73 Motor Unit Number Estimation (MUNE)

Overlay of multiple compound muscle action potentials (CMAPs) recorded following electrical stimulation (in incremental intensities) of the sciatic nerve proximal to the repair site. The traces on the top channel were recorded with monopolar needle electrodes inserted into the gastrocnemius of an animal in the 12-week MF group. The trace in the lower portion of the Figure shows small CMAP's in the intrinsic muscles of the foot in the same animal, indicating successful reinnervation to the intrinsic muscles of the foot.

Functional Assessments

Sciatic Function Index

At 12 weeks there is a significant difference in the SFI between groups (P = 0.040), however the power of the test is only 0.484, which is well below the desired value of 0.800. There is no significant difference among these groups (P

< 0.050) when pairwise multiple comparisons procedures are performed (Student-Newman-Keuls Method).

Table 7 Mean Sciatic Function Index From Walking Tracks

	AG	CT	MT	MF
SFI prior to nerve injury/repair	**-5.6**	**-8.6**	**-7.79**	**-7.67**
SFI at wk 1	**-84.22**	**-83.69**	**-80.55**	**-80.62**
SFI at wk 6	**-82.32**	**-79.85**	**-76.69**	**-82.19**
SFI at wk 12	**-78.17**	**-77.06**	**-78.57**	**-86.60**

Figure 74 Normal & 1 Week Walking Tracks

(A) In the normal rat each toe leaves a distinct ink print. The toes are abducted and the body weight is distributed among all of the toes during walking. (B) Walking track from an animal 1 week after nerve injury and repair shows a consistent full print length and a reduced toe spread relative to normal. Distinct toe prints cannot be delineated because the ink runs together when the animal's toes are in full adduction.

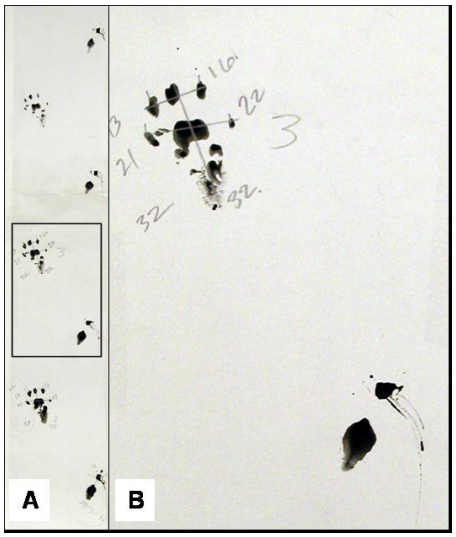

Figure 75 Walking Track From Rat With Flexed Toes

(A) Walking tracks from a rat from 12 weeks after autograft repair. (B) Magnified view of enclosed region in (A). This rat maintained its toes in full flexion both in static standing and during walking. Note that toe spread cannot be measured from the operated hindlimb and reduced print length observed is an artifact due to the toes being curled under the forefoot. This specimen had 13,715 myelinated axons in the middle of the repair site.

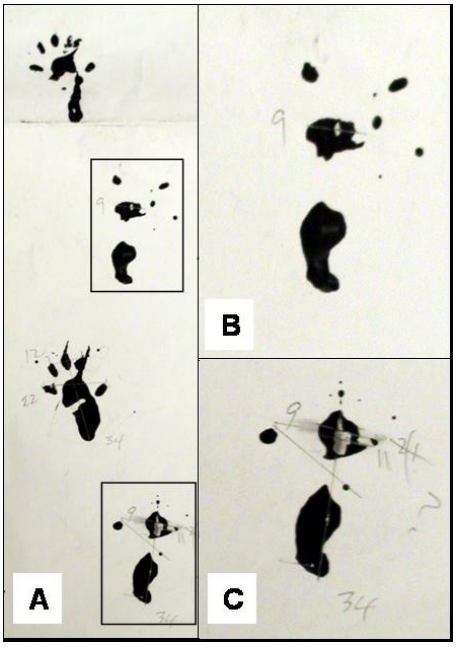

Figure 76 Walking Track From CT Group at 12 Weeks

(B) & (C) are from the enclosed regions in (A). This particular specimen had 9842 myelinated axons in the middle of the repair site, indicating a good probability of functional return, yet this is difficult to gauge from these prints because the ink is not uniformly distributed on the paper.

Static Stance Analysis

The static stance box allowed us to observe the functional result of nerve injury and regeneration from a unique vantage point. Because of noting 1st toe abduction in one particular specimen (Figure 79) we decided to modify the recording of CMAPs in the feet to include the 1st and 2nd metatarsal spaces instead of only the 3d metatarsal space. The results of the SSI are summarized in table 8.

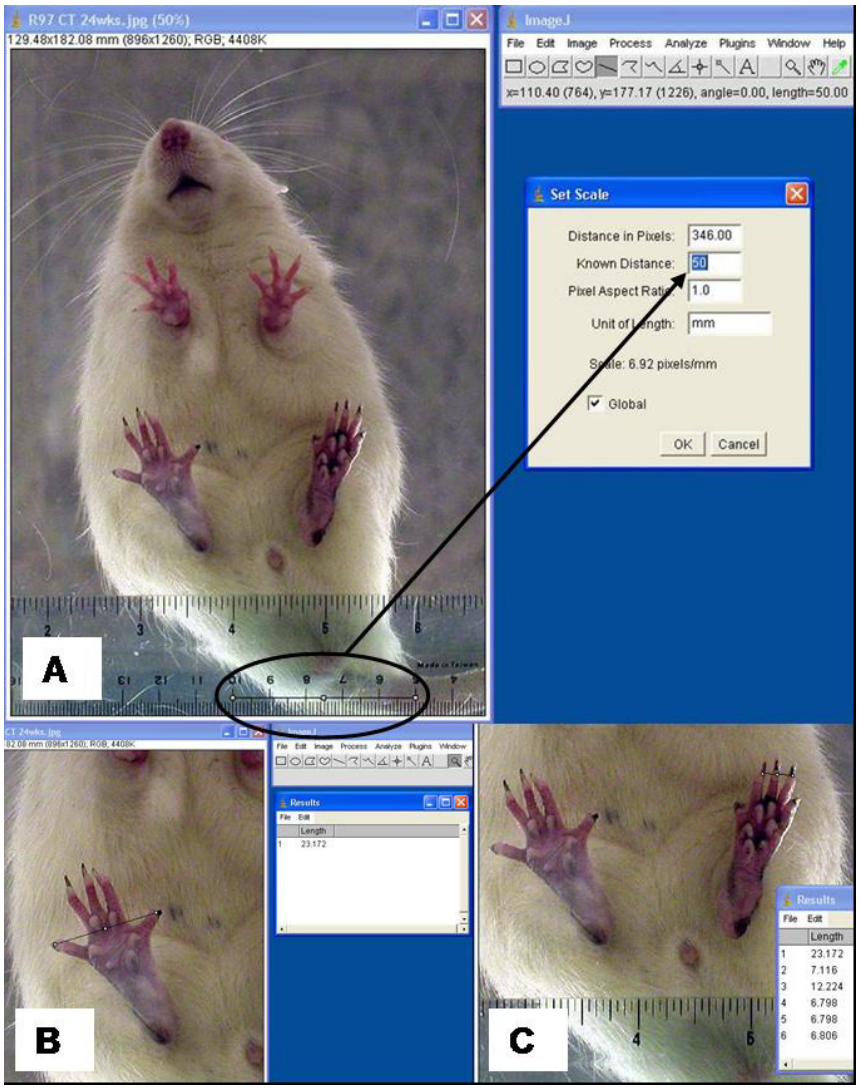

Figure 77 Setting Scale For Toe Spread Measuremens With ImageJ

Screen captures of digital image taken from static stance photography box and imported into ImageJ software. This rat is one from the CT group that went 24 weeks. (A) Shows calibration of scale from metric scaled ruler, which is included in the image. A line is drawn across a 50 mm (encircled region) of the ruler and entered as a known distance (arrow) that equals the computer derived distance of 346.00 pixels. (B) Shows measurement of the normal 1-5th toes spread, (C) demonstrates measurement of intermediate toe spread in the operated limb.

Table 8 Mean Static Stance Index (Percent of Normal Toe Spread)

	AG	CT	MT	MF
6wk	51.20	43.60	39.32	37.45
12wk	47.32	61.61	42.36	37.97
24wk		61.43		

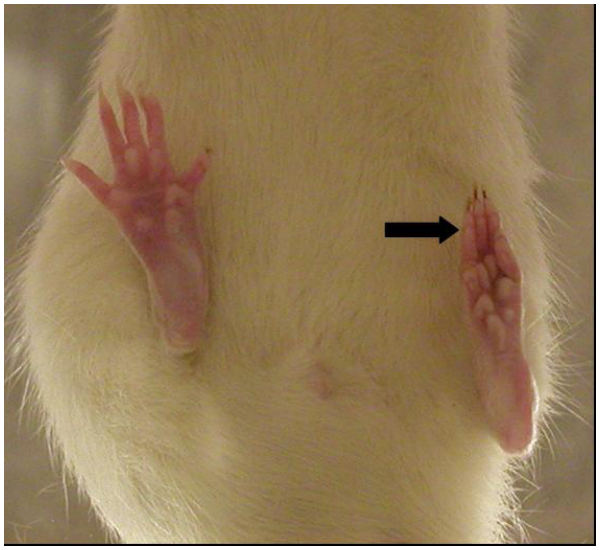

Figure 78 Typical Foot Posture 1 Week After Nerve Injury & Repair

Unoperated foot shows normal abducted position of each digit, where as the operated foot (arrow) shows foot posture without toes in adduction at 1-week post nerve injury repair.

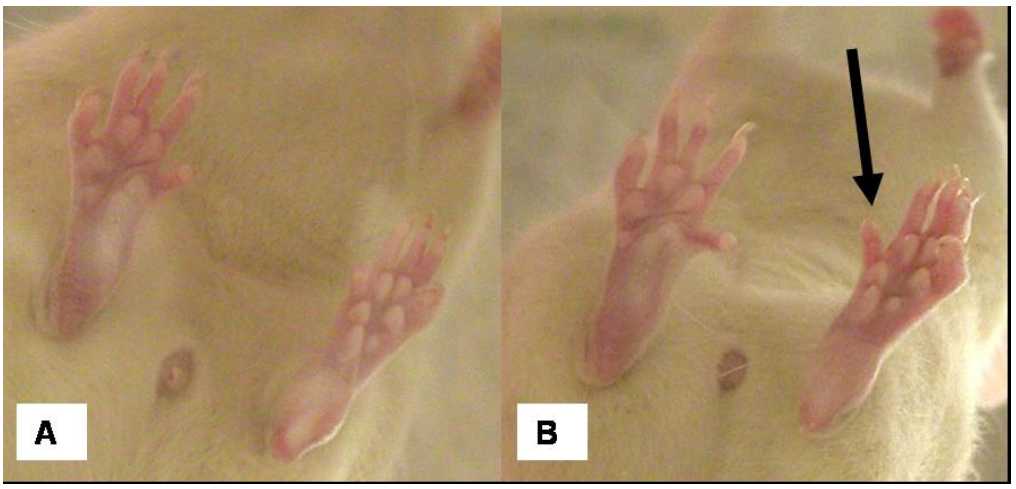

Figure 79 Static Stance Photo Movement of Digit

Two images of the same rat taken moments apart. This rat had sciatic nerve repair with a guide tube with guidance channels 12 weeks prior to these images being captured. The image on the left shows the1st toe (arrow) is not abducted. Image on the right shows the 1st toe (arrow) in abduction. This rat actively abducted its toe when it stood on its hind limbs. This movement widened the animal's base of support to facilitate balance, demonstrating a coordinated movement from a reinnervated muscle group.

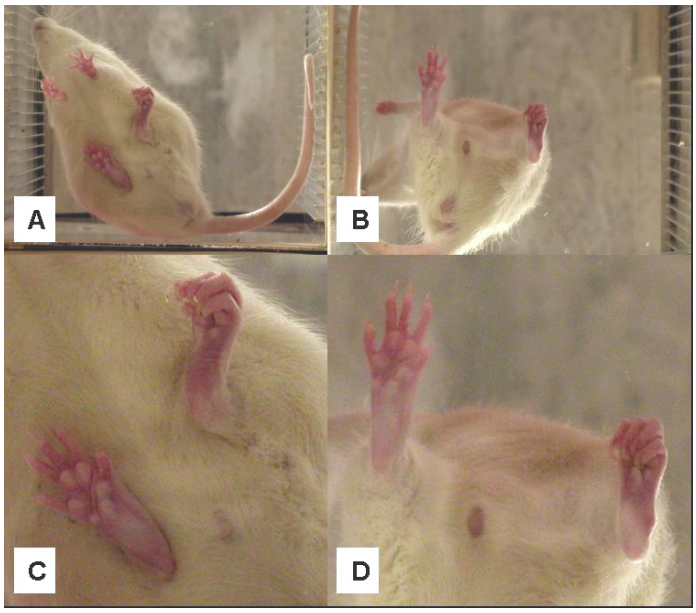

Figure 80 Digital Flexion Abnormality in Operated Limb

Example of an animal with toe flexion abnormality in the operated limb (AG group at 12 weeks). Images on bottom of Figure are close up views of the image above, (A & C) the rat is in quadrupedal stance, (B & D) it is standing on its hind limbs only. This foot posture prevents accurate toe spread measurements from either walking tracks or static stance photos. This particular rat had 13,715 myelinated axons in the middle of the autograft at 12 weeks.

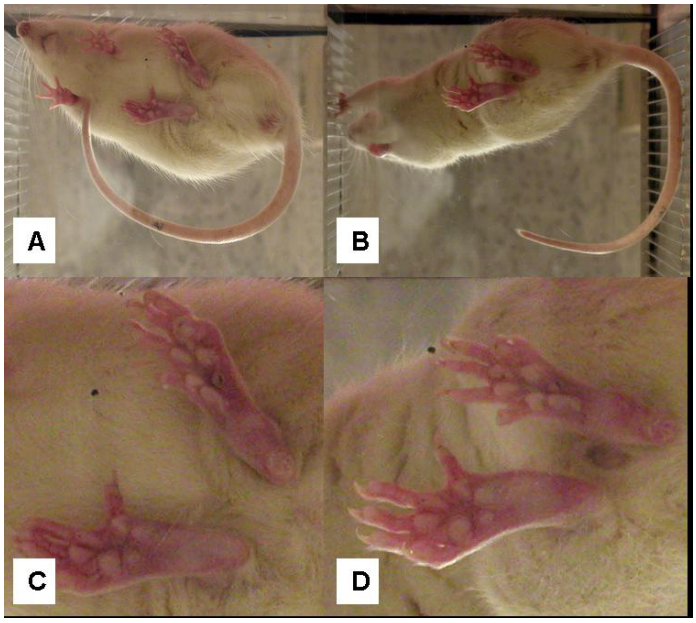

Figure 81 Autograft With Return Of Toes Spread At 12 Weeks

All images from same animal, (A) & (C) in quadrupedal stance, (B) & (D) in bipedal stance. This rat received autograft repair 12 weeks prior to these images being taken and shows excellent return of toe abduction.

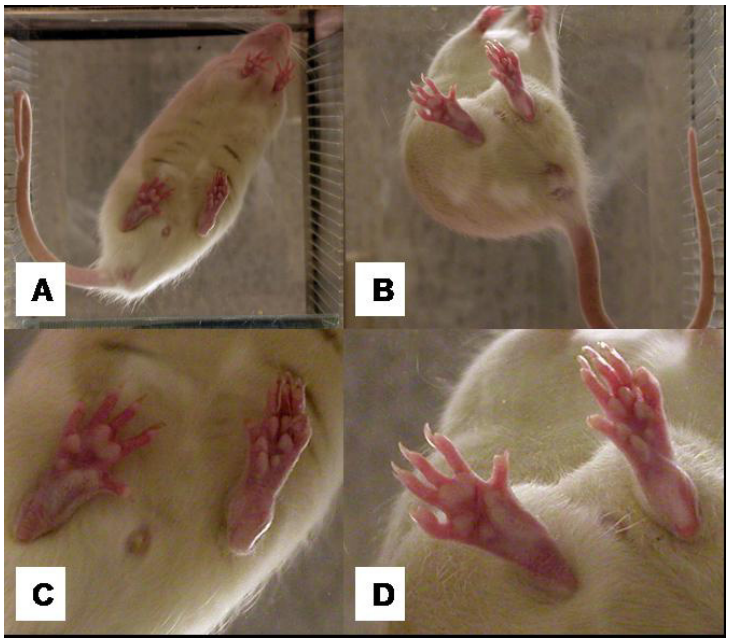

Figure 82 Toes Spread Return (MT Repair Group at 12 Weeks)

All images from same animal, (A) & (C) in quadrupedal stance, (B) & (D) in bipedal stance. This rat received MT nerve guide 12 weeks prior to these images being taken. There is evidence of return of toe spread that increases somewhat when the animal transfers more weight onto the hind limbs in bipedal stance. This particular rat had 12,905 myelinated axons in the mid-section of the nerve guide at this time point. This was the highest axon number in the MT group.

The five rats in the 24-week CT group were chosen to examine if a relationship existed between the number of axons counted and the score from the SSI using 1-5th toes spread measurements. Amongst these five animals there appeared to be was no correlation (summarized in table 9 and Figure 83). The specimen with the highest number of myelinated axons had flexion deformities of all the digits of the experimental hindfoot (Figure 80), which made accurate measurement of toes spread impossible. The specimen with the fewest myelinated axons had the largest 1-5th toe spread. This large toe spread may have represented contracture and not active toe abduction. The three rats with

intermediate axon numbers demonstrated no correlation with the toe spread measured from static stance images.

Table 9 **24 Week CT Static Stance Index, Axon Number, Foot CMAP**

Rat#	Group	Weeks	Axons	% normal 1-5th TS	CMAP in foot
1	CT	24	22,515	Deformity	Yes
2	CT	24	21,486	53.04	Yes
3	CT	24	9,812	32.03	Yes
4	CT	24	6,459	63.62	Yes
5	CT	24	1,756	97.04	Yes

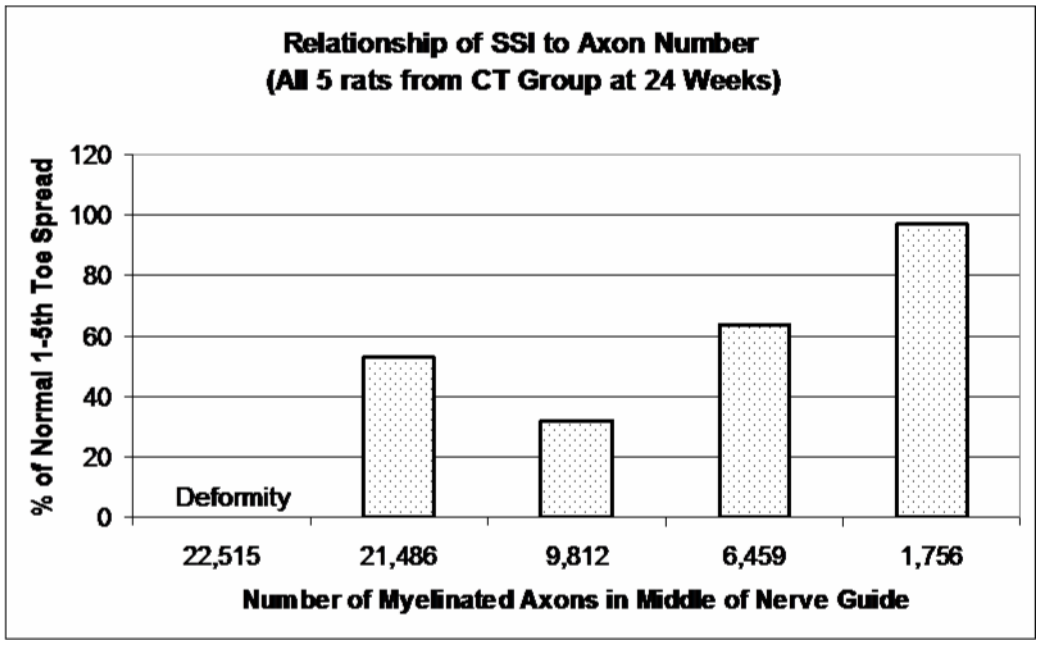

Figure 83 **SSI Plotted Against Axon Number**

Chapter 5: Discussion

Autografts are the preferred method of repair for gap injuries and our data verified their efficacy. In the present study, the mean number of myelinated axons in the middle of the autograft increased by 45% from the 6 to the 12 week time point, and at both time points the myelinated axon number was much greater than the normal control. These data are in contrast to Chamberlain et al., who, using similar histological assessment methods, found no significant difference between myelinated axon counts at 6 weeks, 30 weeks, and 60 weeks in Lewis rats that underwent a 10 mm autograft repair (Chamberlain, Yannas et al. 1998; Chamberlain, Yannas et al. 1998). In that study, the orientation of the autograft was not reversed, unlike the present study, because of the desire to optimize fascicular alignment. This may account for their autograft reaching a greater number of myelinated axons than ours at the 6 week time point and then reaching a plateau.

In newly regenerated peripheral nerve, many more axons occupy the nerve segment distal to the injury site than occupy the nerve segment proximal to the injury site. This is true for both autograft and entubulation repair of peripheral nerve and occurs because the parent axon branches into several neurites, each of which may elongate and take a different path (Dohm, Streppel et al. 2000). If

a neurite reestablishes an appropriate peripheral contact, in time, the axon's supernumerary branches are eliminated (Mackinnon, Dellon et al. 1991).

The autografts in this study, and previous animal studies, represent an idealized nerve graft in many ways. They are not directly comparable to clinical autografts. The size of the autograft is a perfect match in these studies, and a second surgical site is unnecessary to obtain the graft. Unlike the clinical nerve autograft, which may reside out of the body for 90 minutes prior to implantation, our autografts do not leave the surgical site. The presumption is that in our autograft model the majority of Schwann cells in the autograft survive, and in the clinical autograft the majority of Schwann cells die. It is the presence of live Schwann cells that give the autografts in this study a major advantage over the entubulation repair groups. Schwann cells provide an endogenous source of growth factors, NGF, BDNF, CNTF, which enhance both neuronal survival and growth (Ho, Coan et al. 1998; Lee, Yu et al. 2003). Several studies of nerve gap repair have shown that living Schwann cell laden grafts are superior to acellular grafts at promoting nerve regeneration (Evans 2000; Hadlock, Sundback et al. 2001).

Although the present design of microtube or filament guidance channels provide greater surface area for cell migration than empty tubes they cannot compare to the much greater surface area provided by an autograft. The remnant basal lamina Schwann cell tubes of the autograft not only provide a much greater surface area than the fabricated nerve guides provide, but they are

the ideal substrate for neurite growth cone adhesion and elongation. Even when an autograft is repeatedly frozen and thawed, killing the resident Schwann cells, the basal lamina supports axon growth and Schwann cell migration (Ide 1983). The basal lamina contains laminin, type collagen IV, fibronectin, and heparin sulfate proteoglycans (Laurie, Leblond et al. 1982), and each of these macro molecules has a proven ability to promote neurite outgrowth from dorsal root ganglia, *in vitro* in the presence of nerve growth factor (Chernousov, Stahl et al. 2001). Moreover, these molecules enhance regeneration across nerve gaps when they are added to the lumens of nerve guides (Madison, Da Silva et al. 1988; Woolley, Hollowell et al. 1990; Zhang, Oswald et al. 2003).

Schwann cells that have lost contact with axons, like those in the autograft at the time of initial implantation, undergo proliferation. Proliferation and migration is far greater when Schwann cells adhere to laminin or fibronectin as compared to type I collagen, and both of these molecules are present in the Schwann cell basal laminae of the autograft (Ahmed and Brown 1999) (Vleggeert-Lankamp, Pego et al. 2004). When fibronectin is manipulated into a fibrillar macromolecule, it accelerates Schwann cell migration and directional guidance via alignment and binding of cytoskeletal F-actin filaments (Ahmed and Brown 1999).

When autografts cannot be used, a biomaterial graft may be a good alternative (Keeley, Atagi et al. 1993). In addition to avoiding the comorbidity of the harvest site necessitated by autograft repair, entubulation repair using

biomaterial tubes offers a mechanical feature, a cuff to surround the nerve stumps, which appears to decrease the axonal escape that can occur at the autograft suture line. The composition and architecture of the biomaterial guide should contribute to the degree of regeneration and functional recovery (Madison, Da Silva et al. 1988). Many design cues can be derived by analyzing features of the autograft. An overall goal of the project (phases I, II, and III) was to systematically determine the effects of the nerve guide parameters of permeability, architecture, adhesive molecules, and growth promoting molecules on regeneration following entubulation repair of a peripheral nerve gap injury, in order to build the final prototype for repair of a median nerve lesion in the monkey. The focus of the present study was studying the effects of different nerve guide architectures.

The present study demonstrated that axons grow through type I collagen nerve guides that contain guidance channels, as evidenced by the histological data. Regenerating axons reestablish synaptic contact with peripheral targets as evidenced by the presence of evoked gastrocnemius muscle CMAPs. There is return of motor function in the limb that underwent nerve repair as demonstrated by the partial return of toe spread in some animals. Although the data demonstrated that nerve guides with longitudinal channels could be used for the repair of peripheral nerve gap injuries, they were not significantly better than empty tubes.

Heparin was incorporated into the nerve guides to provide a binding site for bFGF and laminin for the Phase III rat in vivo study on the effect of bioactive molecules on nerve regeneration. To ensure that inclusion of exogenous bioactive molecules were the only variables between phase II and phase III, heparin was incorporated into the type I collagen matrix of the nerve guides fabricated for this study (phase II, guidance channels).

The effect on nerve regeneration of type I collagen (5.0% heparin) nerve guide as compared to a pure type I collagen nerve guide was not tested in this study. Although it is known that specific heparin binding peptides benefit aspects of nerve regeneration, it is unclear how heparin alone effects regeneration in collagen nerve guides. The presence of heparin may be beneficial to regeneration in that if may temporarily bind soluble peptide growth factors released by Schwann and mast cells, and aid nerve regeneration by concentrating these factors, which may otherwise diffuse out of the tubular nerve guide. For FGF to bind to its high affinity receptor it must first be bound to either heparin or heparan sulfate, and FGF-heparin complex is more resistant to degradation than FGF alone (Tyrrell, Ishihara et al. 1993; Ishihara, Shaklee et al. 1994).

We are not the first to use heparin as a delivery molecule. Recently, heparin was used successfully to bind and deliver a variety of peptides, both growth factors and adhesive molecules, to enhance embryonic chick dorsal root ganglia neurite outgrowth in a three-dimensional matrix (Sakiyama, Schense et

al. 1999). It also has been used to improve regeneration across a 13 mm rat sciatic nerve gap (Lee, Yu et al. 2003)

Myelinated Axon Number

At the 12 week time point recovery of MT group was clearly superior to the MF group. Although the mean number of myelinated axons in the mid section of the nerve guide was higher in the MT group (4705) than the CT group (4349) this difference did not reach statistical significance. In fact, 80% of the CT group had axon counts greater than 2000 compared to only 67% in the MT group. None of the rats from the 12 week CT group had axon counts greater than 10,000 (n = 10) while in the MT group 1 rat had a myelinated axon count of 11,923, and another had a count of 12,905. These numbers are within the range of those observed for the AG group.

If endogenous fibrin matrix from the wound site fills the lumen of both a nerve guide with microtubes and one without microtubes there may be a “wash out” effect of the “greater” surface area provided by the collagen microtubes. In type I collagen/heparin composite nerve guides, Schwann cells migrate into the graft ahead of neurite growth cones, and lay down an extracellular matrix that the growth cones can more easily advance upon (Madison and Archibald 1994). Schwann cells may migrate through the fibrin matrix and “not see” the specific advantage of the surface area provided by the biomaterial nerve guide. It may be that the main advantage of a nerve guide with type I collagen guide tubes is

structural stability and not surface area for cell migration, in that it may prevent collapse of the guide tube during the early critical regeneration phase. Although the empty nerve guides may have appeared more flattened than the guides with microtubes, they did not collapse to a degree that their lumens were obliterated and therefore the benefit of the microtubes could not be revealed over a gap length of only 10 mm.

Perhaps, they will provide more obvious benefit to a longer gap repair, where an empty guide tube may be more susceptible to kinking. This may be especially true if nerve repair is performed near or across joints. The elbow provides an example of a vulnerable peripheral nerve site (Mackinnon and Dellon 1988; Hunter, Schneider et al. 1997). The ulnar nerve at the elbow has no muscular covering and lies in the boney groove between the medial epicondyle of the humerus and the olecranon of the ulna. If the ulnar nerve is injured at this site and is subsequently repaired, it may benefit from a nerve guide that has specific structural architecture to prevent lumen collapse. Under these conditions, the true benefits of this architecture may reveal itself. This is unlike the present model where the nerve guide is placed in the rat's mid thigh, away from forces that would cause it to kink and obliterate the lumen. This location is also well protected by the overlying hamstring muscles, unlike the superficial location of the ulnar nerve at the elbow. In the well protected sciatic nerve environment of the rat mid-thigh, factors other than architecture, such as growth

factors and adhesive substrate likely are the predominant factors influencing successful regeneration across a nerve deficit.

Variability

The nerve guides rapidly absorb saline, which is applied to rehydrate the nerve guides prior to implantation. This causes swelling, which in the case of the microtubes appears to press them against each other and the outer tube in a manner that is beneficial in that it prevents the microtubes from moving laterally and the patency of the tubes is maintained. The collagen filaments however, swell, aggregate, and do not appear to offer a benefit to maintaining the patency of the nerve guide lumen.

There was considerably less within group variability in the results of the myelinated axon counts in the CT group when compared to either nerve guide group with guidance channels. Perhaps more cumulative variability exists with the more elements that are added to a nerve guide. Since there were more parts in the nerve guides with guidance channels as compared to the empty nerve guides (32 more parts in the MF group, and 5 more in the MT group) there is likely greater variability in the nerve guides before they are ever put in the animals, variability that exists simply due to the manufacturing process.

In this study, every attempt was made to minimize manufacturing variability by utilizing strict standards (outlined in the methods section), which

included using nerve guides from the same lot (manufactured on the same day without altering machine calibration settings).

Another reason for variability in the results of the axon counts from nerve guides with guidance channels may be the movement of the guidance channels within the lumen of the outer nerve guide. This is not tightly controlled once the nerve guides have been implanted. Several times during the initial surgeries, immediately prior to implantation, filaments or microtubes partially slid out of the outer nerve guide. We were able to slide them back in without difficulty prior to completion of the surgeries. No nerve guides in which microtubes or filaments slid completely out during preparation for implantation were used in the study. They were discarded immediately and a sterile replacement was used instead.

If the proximal and distal sciatic nerve stumps are not sutured so that they are in direct contact with the guidance channels (MT or MF), longitudinal movement of the guidance channels could theoretically occur. If longitudinal movement of the guidance channels did occur, it could very well be non-uniform. Some filaments or microtubes may slip proximally while others within the same nerve guide would occupy a position more distal in the nerve guide. Although this is theoretically possible, every attempt was made to prevent this from occurring during this study. Since the outer nerve guide becomes translucent when hydrated, it is possible to see the position of the nerve stump within the outer nerve guide; we were thus able to ensure the nerve end contacted the guidance channels prior to securing it with suture. Additionally, the 10 mm

intraluminal nerve gap was confirmed by measurement with a vernier caliper via the translucent outer nerve guide.

The only movement that is poorly controlled is the lateral movement of the solid collagen filaments. The filaments fail to remain uniformly distributed within the lumen of the outer nerve guide. In several specimens, 32 individual filaments could be identified while in many others the filaments aggregated, thus occluding the spaces between the filaments and obliterating the theoretical guidance channels. The microtubes appear to remain in their position with respect to the outer guide tube better than the filaments.

We were unable to calculate correlation coefficients between the myelinated axon counts and electrophysiology results due to insufficient sampling with electrophysiology. Many of the inferential statistical analysis suffered from limited power due to both small sample size, non-equal variance within groups, and lack of normality. It may be that a larger sample size would have solved some of these problems. Although there was a larger than expected variance in the axon counts it is unlikely due to surgical error. Since in the combined AG groups there was only a 5% (1 out of 20) failure rate and in the 12 week CT group all rats had axon counts greater than 1200, it is fair to state that the variability resulted from the inclusion of type 1 collagen filaments or microtubes in the nerve guides.

It cannot be overstated that a detailed understanding of the gross anatomy of the animal that is used for the model is as essential as the microanatomy.

Some shortcomings of this study came about because of a less than perfect understanding of the rat anatomy at the onset of the study. This affected the electrophysiological assessment in particular.

Investigators that studied nerve regeneration in the rodent have often found that findings of electrophysiology, functional measures, and histological assessments are not correlated (Munro, Szalai et al. 1998). These methods evaluate separate aspects of the changes that take place after nerve injury and repair. For this study (phase II), the sciatic nerve distal to the repair was not routinely harvested for evaluation of myelinated axon number. For phase III we have incorporated harvesting sciatic nerve sections from the region distal to the nerve repair to ensure that number of myelinated axons that have entered the distal nerve stump can be evaluated morphologically, and not solely by extrapolation from electrophysiological data.

Axon Diameter

Although the autograft repairs had more myelinated axons than the other repair groups, the percentage of myelinated axons with diameters between 2.0-5.0 μm is almost identical for the AG, CT, and MT groups at the 12-week time point. Chamberlain et al. found axon diameters centered around a mode of 2.5 μm in collagen tubes with a collagen-GAG complex used for repair of 10 mm rat sciatic nerve gap, at both 30 and 60 weeks post repair (Chamberlain, Yannas et al. 1998). These data are similar to our results and the diameters of regenerated

myelinated axons at these time points are significantly less than the normal control (Keeley, Atagi et al. 1993). Mackinnon et al. found that for direct suture repair of transected rat sciatic nerve, axon diameters were 3.1 μm at 1 month and 3.4 μm at 3 months post up with the mean diameter only increasing to 4.7 μm by 24 months (Mackinnon, Dellon et al. 1991). Normal axon diameter averaged 6.5 μm. Axon diameter is one morphological parameter that correlates with an aspect of functional recovery, nerve conduction velocity, but not necessarily with functional gait parameters (Dellon and Mackinnon 1989).

The light microscopy methods employed in this study were designed to provide estimates of axon diameters that could discriminate differences between groups if they were present. It would require electron microscopy to resolve the axonal-myelin borders to a sufficient degree to provide conclusive data regarding the diameter of regenerated or normal myelinated axons. The methods worked well for this part of the study (phase II) and may be a valuable tool for phase III to demonstrate differences in myelinated axon diameter, which may occur when growth factors are included in the nerve guides. Ho et al. demonstrated increased axonal diameter, neurofilament gene expression, and nerve conduction velocity following rat sciatic nerve repair with collagen nerve guides supplemented with the growth factors CTNF, BDNF, or both, as compared to tubes without these molecules (Ho, Coan et al. 1998).

Functional Recovery

After sciatic nerve injury and repair, rats walk by using their hip flexors and quadriceps to lift and advance the affected limb, and although muscles supplied by the sciatic nerve are denervated immediately after nerve transection the rats use the limb for support. In contrast to normal rats, which support their weight on their digits during walking, the bulk of the rat's weight supported by the experimental hindlimb is focused directly on the heel. We believe that when the rat walks with the insensate hindlimb, the disproportionate amount of weight on the heel leads to ulceration, periarticular inflammation, and eventually fibrosis of the ankle joint. It is the probable cause of the limited ankle movement in this study, and is in agreement with Sunderland's work (Sunderland 1991).

During long periods of denervation, fibrosis of myocytes is a cause of limited joint motion that severely impacts functional recovery, however, this does not occur until 12-24 months post denervation and therefore is not a cause for the rat's limited ankle motion in this study (Mackinnon and Dellon 1988; Sunderland 1991). This ankle joint contracture profoundly limits the recovery of function, independent of muscle reinnervation. Therefore, the relevance of the SFI calculated from walking tracks could be questioned because it incorporates a print length measurement, which is directly related to the animal's ability to plantar flex the ankle (Shenaq, Shenaq et al. 1989).

The print length is small when the rat supports weight on the digits with the ankle plantar flexed by the gastrocnemius and soleus muscles. This elevates

the heel so no true heel print is left during normal walking. It is only when the normal rat slows down to inspect its environment or rises up on the hindlimbs that the heel makes full contact with the supporting surface. When the gastrocnemius, soleus, and the rest of the muscles below the knee are denervated, as they are in this study, the rat cannot plantar flex its ankle against the load imposed by the rest of the body. The print length is therefore large in the denervated state and small in the normally innervated state.

When reinnervation takes place muscle atrophy will start to reverse, however, these muscles will be unable to overcome the force of the rat's body weight during stance phase of walking for quite some time. Even after early reinnervation, the degree of ankle joint contracture can continue to increase because the animal is unable to move the limb through normal physiological motion during functional weightbearing activities such as walking. Consequently, even if reinnervation takes place after a successful nerve repair, the contracture that develops during the period of nerve regeneration is irreversible; and this is what influences the SFI. The SFI may be useful for examining recovery of function following crush injury to the sciatic nerve since the period of convalescence is markedly shorter and fewer complications arise (Bervar 2000), but for 10 mm gap repair it does not correlate with myelinated or unmyelinated axon number (Shenaq, Shenaq et al. 1989).

Investigators have reported finding digital contractures following sciatic nerve transection and repair. We noted toe flexion abnormalities, however, they

were eliminated when the animal was put under anesthesia in preparation for electrophysiological assessment. This indicated to us that these flexion abnormalities were from an imbalance of muscle tone between the flexors and extensors and not joint flexion contractures. This can occur due to an imbalance in the reinnervation of digital flexor and extensor muscles. Another possibility is that there is imbalance of muscle tone because of poor modulation by the CNS after axons have innervated muscles antagonistic to their original role. In other words, some of the axons that previously innervated the extensor muscles have sent sprouts to the flexor compartment, and the higher motor centers cannot coordinate the contraction of opposing muscles. In fact, the animals that most often were noted to have these toe flexion abnormalities were the animals with the highest number of regenerated myelinated axons in the mid section of the repair site. They were the autografts.

Shenaq et al. found that the “clinical observations” of improvement, decreased foot dragging and increased weightbearing in some rats that underwent repair of 10 mm sciatic nerve gaps, was not correlated with an improved SFI, and that these particular animals had a SFI that was no different than those with “clinical observations” of complete dysfunction (Shenaq, Shenaq et al. 1989). In addition, the SFI did not appear to correlate with axon counts.

Unlike the toe flexion abnormalities in the present study, the limited ankle motion noted in all rats was because of true joint contracture; it remained when

we attempted passive mobilization of the limb while the animal was under anesthesia (Dellon and Mackinnon 1989).

The successful functional outcomes following nerve transection injury rely on two dependent, but distinct factors: surgical nerve repair and rehabilitation. Optimal functional recovery will not occur without appropriate rehabilitation therapy, even when experienced surgeons use the most advanced nerve repair technologies. Optimal functional recovery will also not occur without a successful surgical nerve repair, no matter how much rehabilitation takes place. Our current model is designed to best address surgical repair strategies for nerve gap injuries. Although these functional measures were chosen as one of the outcome assessments, perhaps they are better suited for studying rehabilitation strategies. It may be useful to draw distinctions, for research purposes, between successful surgical repair and successful functional recovery, following nerve transection injury. This is an academic distinction however, since patients who have suffered a nerve transection injury are only interested in functional improvement.

Electrophysiology

One of several factors that drove the evolution of the electrophysiological methods was the inconsistency of the results during the earlier part of the study. This inconsistency appeared to be due to some factor other than the expected variability of nerve regeneration. It was suspected, then proven through

experimentation, that our early results of recordings from the gastrocnemius muscle with needle electrodes were confounded by the inclusion of muscle action potentials from the normally innervated biceps femoris muscle. In the final protocol, when the nerve to the biceps femoris muscle was severed and removed, the electrophysiology results were more consistent and more easily interpreted.

Below is a critical review of the electrophysiology methods employed during this study. This discussion focuses not on the differences in the entubulation repair groups based on electrophysiology results, but on the advantages and disadvantages of each method used for this model of studying peripheral nerve injury and repair.

Nerve Action Potentials

Initially evaluation of nerve action potentials was believed to be the simplest and most reliable method to determine the degree of functional nerve regeneration across the gap repair. We believed we would obtain data that could be quantified and allow comparison between the entubulation repair groups as well as allow reference to the normal control and AG group. Additionally, we chose this method because the results were not influenced by secondary events, such as synapse formation at neuromuscular junctions, and axon misdirection to inappropriate targets. Both of these events potentially complicate interpretation of electrophysiological recordings from muscle.

One of the parameters recorded was the minimum stimulus intensity at which a visible muscle twitch occurred. We initially thought this may be valuable information as "better regeneration" should require less stimulus intensity to cause a visible muscle contraction. It was later realized that the non-specificity of the muscle twitch was a major problem. When the sciatic nerve was stimulated in the gluteal region, the entire hind limb frequently moved violently in extension. The fact that the entire limb moved was not noteworthy since the muscles performing that function were likely not denervated by sciatic nerve transection in the mid-thigh. Limb extension was presumably caused by contraction of the hamstrings and possibly the gluteal musculature. In addition, the entire limb movement made observation of the ankle plantar or dorsi flexion, which would be relevant movement and indicative of recovery of function, impossible to isolate visually. The gastrocnemius and tibialis anterior muscles, which cause plantar flexion and dorsi flexion respectively, are innervated distal to the repair site and movement here would be the indicative of regenerating axons reestablishing their peripheral synaptic contacts.

Numerous fibrous adhesions and blood vessels made increasing the size of the surgical exposure challenging. On many occasions, our surgical exposure provided insufficient space to place either the recording or stimulating pair of electrode pairs on the actual sciatic nerve (proximal or distal) without placing one of the electrodes on the collagen nerve guide itself. We were not satisfied with this, but at that time we believed we were unable to enlarge the exposure without

either damaging the sciatic nerve or causing increased blood loss to the animal. The problem with contacting the collagen nerve guide instead of pure nerve is that although some resorption and remodeling of the collagen tube took place by 6 or 12 weeks, it is not normal nerve. The electrical impedance of the nerve guide, in all likelihood, is sufficiently different than nerve tissue and may affect the recordings.

Another problem with this setup, was the recording electrodes placed immediately distal to the nerve guide were approximately 14 mm from the stimulation electrode. Over this short distance there is little drop in the size of the stimulus artifact that is recorded simultaneously with the nerve action potentials. Thus, the recorded stimulus artifact was very large relative to the nerve action potential and in most cases obscured a large part of the recorded nerve action potential. This made determinations of latency or amplitude extremely difficult and in most cases impossible. The results derived from this electrophysiology setup could only indicate whether there was nerve conduction across the gap.

Lastly, prolonged elevation of the sciatic nerve on the hook electrodes may have caused a temporary ischemia and dehydration that accounted for changes that we observed during long experiments. Often the action potential would diminish over time during an experiment. On occasion, simply rehydrating the nerve with sterile saline would restore the amplitude. When the nerve was temporarily taken off the hook electrodes and then replaced a moment later, the evoked action potential would return. Knowing this, we could not use amplitude

measurements to discriminate quality of regeneration between groups, even if the CNAP was clearly visible outside the shadow of the stimulus artifact.

Recording of evoked action potential across a nerve lesion is appropriate for a quick screening of whether axons crossed the injury. In fact, this is often how surgeons evaluate whether to perform surgical nerve repair. If an injury leaves the outer connective tissues of the nerve intact and the patient's complaint is loss of function or pain, as can occur for example with a neuroma incontinuity, and nerve action potentials can be recorded across the lesion, the decision is typically made to perform no further surgical intervention.

Compound Muscle Action Potentials

When the electrophysiology protocol was changed from recording of sciatic nerve action potentials to recording CMAPs from the gastrocnemius muscle we were interested in obtaining quantifiable data. Data, such as latency, amplitude, and estimates of nerve conduction velocity, which may discriminate the quality of regeneration between groups, were all of interest. Recording of CMAPs from muscles that are denervated by the sciatic nerve lesion offers information about whether regenerating axons negotiated through the nerve guides and into the distal nerve stump and reestablished synaptic contact with a muscular target.

Compound Muscle Action Potentials and Anatomy

It was essential for the remainder of the project that the cathode-stimulating electrode made direct contact with a region of normal nerve proximal to the repair site. This involved expanding the surgical incision and dissection proximally. We were careful to prevent compression of the sciatic nerve and this procedure became routine. Because of this enlarged exposure we were able confirm that a nerve previously observed, was branching from the sciatic nerve. This nerve was incorrectly identified as the posterior femoral cutaneous nerve of the thigh, due to its similar relationship of this nerve to the sciatic nerve in the human. Later in the project, after a more thorough anatomical study was undertaken and the anatomy was correlated with electrophysiology findings, this nerve was determined to be a muscular branch from the tibial division of the sciatic nerve, which branches proximal to the sciatic nerve injury and repair site. This proximal nerve branch descends deeply and travels distally to innervate the biceps femoris. The rat anatomic text we consulted did not clearly illustrate this anatomy, the Figures were schematic in nature (Greene 1968).

The tibial nerve emerges distal to our repair site and any axons present in it following the nerve repair represent regenerating axons. This anatomical configuration is similar to the human. The tibial nerve gives off branches that innervate the gastrocnemius muscle. A major anatomical difference between the rat hind limb and the human is that in the rat, the gastrocnemius muscle is completely covered on its lateral aspect by the biceps femoris muscle's anterior

and posterior heads. Thus, when a needle electrode is inserted into the lateral gastrocnemius muscle it must pass through the biceps femoris muscle. If recording electrodes are not insulated, such that the entire needle shaft is conductive, the electrodes will record from the biceps femoris muscle as well as the gastrocnemius muscle when the sciatic nerve is stimulated in the gluteal region. The electrodes in this study were solid stainless steel, not insulated, and therefore capable of recording from the biceps femoris muscle as well as the gastrocnemius muscle. Unlike the gastrocnemius, which is a muscle that had been denervated by the sciatic nerve lesion, and may or may not have been reinervated by regenerating axons, the biceps femoris was innervated by normal nerve that was undisturbed during the sciatic nerve lesion repair.

These findings confounded the analysis of the recordings from the gastrocnemius. One could mistakenly assume successful regeneration when there was none, or incorrectly use the latency/amplitude of the normal biceps femoris CMAP instead of a smaller delayed gastrocnemius CMAP. We demonstrated this during experiments where CMAPs where recorded from the gastrocnemius before and after the nerve to the biceps femoris was severed. A thorough study of the rat anatomy is critical prior to initiating a peripheral nerve regeneration study such as this, and that assumptions based upon knowledge of human anatomy are inadequate.

One additional factor that may influence CMAP recordings from the gastrocnemius muscle is that since the biceps femoris muscle is incised during

the surgical nerve repair there exists a local region of denervated biceps femoris muscle. This region would be attractive to regenerating axons of motor neurons, and during several terminal exposures for electrophysiology, axons that may have "escaped" the repair were noted in the vicinity. These may have erroneously reinnervated the incised region of the biceps femoris, and once again contributed unusual CMAPs to the electrodes targeted for the gastrocnemius muscle.

In light of the above discussion, the tibialis anterior muscle is perhaps, a better choice for percutaneous needle electrode recording following a sciatic nerve lesion than the gastrocnemius muscle. After all, there are no muscles superficial to the tibialis anterior muscle in the rat and it is easily palpated. Following a sciatic nerve lesion, CMAP recordings from the tibialis anterior reflect axons regeneration through the common peroneal (fibular) nerve into the deep peroneal nerve, and reflect the reformation of synapses with the tibialis anterior muscle.

Nerve Conduction Velocity

Regarding methods of obtaining estimates of nerve conduction velocity, there is error when attempting to measure the distance between the stimulating electrode and the recording electrode in the gastrocnemius muscle. First, since the nerve crosses posterior to the knee joint axis it is slack when the knee is flexed. Even when the rat's knee is extended prior to the measurement, the nerve does not take a perfectly straight course toward its entry into the

gastrocnemius. Second, since the nerve glides distally under the stimulating electrode during passive limb extension, it can be difficult to identify the exact measurement location. A measurement error of a few millimeters could greatly affect the resultant calculations. The part of the recording needle that is most accessible for measurement is the part of the needle shaft that remains superficial to the skin. The needle however, was often inserted obliquely on route to the gastrocnemius muscle so that the position of the needle tip may differ significantly from that of the needle shaft at the skin interface. Palpating the needle tip through the tissues, where it rested in the gastrocnemius muscle, was performed in this study to facilitate the more accurate measurements.

On the other hand, if one does not measure the distance and only uses latency as the comparison between groups, one must be perfectly consistent with anatomical land marks used for placement of the electrodes to ensure the same inter-electrode distance between animals. This is not easily accomplished with the percutaneous needle-recording electrode, and could have been facilitated by a surgical exposure of the muscle in question.

A problem with using CMAP amplitude measurements to test for differences between groups is that they can be greatly affected by the placement of the G2 (reference) electrode. In early experiments, the G2 electrode was place subcutaneously, but it may have been too close to the muscle of interest. If the G2 recording electrode picked up potentials from the biceps femoris

muscle, it may have increased CMAP amplitudes in the normal controls, or created a second peak in the recordings of the experimental limb.

Although conceptually this principle was understood, we had difficulty in finding an appropriate location for the G2 electrode. One configuration often sited in texts of electrophysiology is that of placing the G2 electrode over the tendon of the tested muscle (Oh 1993). It was difficult to insert the needle in the region of the Achilles tendon, and limb movement upon stimulation often dislodged the needle from this location. The final location of the G2 electrode was subcutaneous over the lateral malleolus. This gave us results that were more consistent.

MUNE

Although the methods employed for MUNE did not preclude more traditional assessments of latency and amplitude, they took longer than previous experiments. This ultimately led to the decision to collect normal control data from the contralateral limb on only some animals in order to keep up with the schedule that had already been set by the nerve repair dates. There is little report of using MUNE for the study nerve regeneration following transection of peripheral nerve. It is typically used to assess motor unit dropout with progressive degenerative diseases such as ALS. Although one of the research collaborators, R. Madison, has used MUNE for the study of peripheral nerve regeneration in the monkey, the method was validated by using histological assessment of neuromuscular junctions. There was no such plan for validating

this method in the rat sciatic nerve lesion model using the gastrocnemius muscle for MUNE. It did not seem appropriate to assume that since MUNE is valid in the monkey thenar group following a median nerve lesion and repair that MUNE would be valid in the rat gastrocnemius following sciatic nerve lesion and repair.

There are great differences in the median nerve lesion model in the monkey and the sciatic nerve lesion model in the rat. Although both peripheral nerves, the median nerve at the wrist innervates muscles a relatively short distance from the lesion site, with no motor branches to muscle groups that antagonize the thenar group. A mid-thigh sciatic transection is a more proximal nerve lesion in the hindlimb relative to the median nerve transection in the wrist. Therefore, regenerating axons that cross the repaired sciatic nerve gap have many more branch points to navigate before reaching target tissues than axons crossing the repaired median nerve gap. This greatly increases the likelihood of axonal misdirection, and can compromise function recovery even when axons successfully regenerate across the repaired site. In addition, since all of the CMAPs recorded during this time period of the study contained the interference pattern of the biceps femoris, CMAPs analysis was extremely difficult if not impossible. The research group, collectively, decided to discontinue MUNE and concentrate on simple recordings of CMAPs from relevant muscle groups.

Final Electrophysiological Protocol for the phase III rat study

The electrophysiological protocol evolved during this study (phase II). In order to ensure that CMAPs were recorded from the gastrocnemius muscle

several final modifications were tested on a normal animal, and were then implemented for the phase III rat study. To eliminate doubt about the location of the recording needle electrode inserted percutaneously and targeted for the gastrocnemius muscle, an open procedure was implemented. We now surgically expose the gastrocnemius during the terminal electrophysiology assessment. An insulated/coated needle electrode with only a small conductive area at the tip is used.

Although these additional procedures theoretically eliminate the possibility of errant recordings from the biceps femoris muscle, we continue to sever and dissect free the nerve to biceps femoris muscle to prevent any biceps femoris potentials from "bleeding" over to the needles inserted into the gastrocnemius muscle. This could theoretically occur if a high intensity stimulus is given and the recording amplifier gain is turned up to pick up small amplitude potentials. We stimulate both proximal and distal to the repair site to obtain latency values that can be used to calculate NCV across the repair site. To improve accuracy of the distance measurement between the stimulating and recording electrodes, a small suture is tied at both the proximal and distal locations of the stimulus electrodes. This also facilitates the electrodes being placed in the same location if the procedure must be repeated during the experiment. Vernier calipers are used to measure from the sutures to the shaft of the needle recording electrode, which remains in the gastrocnemius muscle until measurements are completed. The knee joint is passively extended to end range. This pulls the sciatic nerve taught

and facilitates a measurement that is as close to a linear as is possible *in vivo*. Following the gastrocnemius muscle recordings and measurements, we record CMAPs from the tibialis anterior muscle as well as the intrinsic muscles of the foot. We sample several metatarsal spaces. We are satisfied with this final protocol in moving into the final phase of the rat study.

Chapter 6: Conclusion

When comparing the two designs of nerve guides with guidance channels, the results from the 12-week myelinated axon counts clearly show the superiority of the MT design over the MF design. However, when microtube guidance channels are constructed with type I collagen without the addition of bioactive molecules (as they were in this phase of the study) the additional surface area provided by the microtubes confers no clear benefit to nerve regeneration over that of the empty type I collagen tube for the entubulation repair of a 10 mm peripheral nerve gap in the rat sciatic nerve.

As previously stated, the presence of channels (microtubes or filaments) in the nerve guides increased the variability of the number of myelinated axons growing through the nerve guide. In a peripheral nerve repair model where compression becomes a pivotal factor influencing the success of a nerve graft, microtubes may provide the essential structural support to maintain the patency of the nerve guide lumen and thus prove to be an essential component.

The most consistent results from entubulation repair occurred in the group without longitudinal channels. Although some of the specimens in the MT group exceeded the highest axon numbers of the CT group, there were considerably more poor results. Neither of these two nerve guides could match the success of

the autograft when compared at the same time point. The autograft appears to accelerate regeneration across the nerve gap relative to the nerve guides.

Cross-linked type I collagen may be the optimal material for the outer nerve guide due to its high tensile strength (Berglund, Mohseni et al. 2003). It allows the nerve guide to accept a suture without tearing, and has the benefit that it is resorbable over time. It is not, however, the optimal substrate for cell migration (Hashimoto, Suzuki et al. 2002; Vleggeert-Lankamp, Pego et al. 2004). In contrast to type I collagen, type IV collagen is a major component of the basal lamina that axons grow upon. It is laminin that has binding sites both for collagen and cellular adhesion molecules in the axonal growth cone (Rogers, Letourneau et al. 1983). Incorporating adhesive molecules such as laminin to the surfaces of the collagen guidance channels may dramatically improve their effectiveness in promoting nerve regeneration. (Rogers, Letourneau et al. 1983; Verdu, Labrador et al. 2002)

An improved study design aimed to strictly test the hypothesis that increased surface area improves nerve regeneration across a biomaterial nerve guide, might include nerve guides with laminin on their interior but no guidance channels, verses nerve guides that contain laminin both in their interior but also contain laminin coated microtube guidance channels. This would provide a comparison of two nerve guides, each with a different architecture and surface area, but both coated with a molecule known to promote cell adhesion and migration. Studies underway at this time in our laboratory are designed to

assess the effect of the inclusion of laminin in microtube guidance channels on nerve regeneration.

The cumulative effect of the longitudinal channels, cellular adhesive molecules, and growth factors, may be greater than simply the increase in surface area. It may provide a synergistic benefit that allows greater regeneration than just growth factors and adhesive molecules in combination, since it provides increased surface area for seeding these molecules. These questions remain to be answered by future studies.

Further study into the complete *in vivo* resorption of the collagen tubes with and without guidance channels is necessary as well.

A final note is that despite the variability in the regenerated myelinated axon numbers, based on histological results, CMAPs were recorded at 12 weeks post nerve repair from the feet of rats in each group, demonstrating the extraordinary ability of the PNS to regenerate. In the case when an autograft repair is not possible, biomaterial nerve guides may be used to successfully bridge a gap in a severed peripheral nerve.

References

Ahmed, Z. and R. A. Brown (1999). "Adhesion, alignment, and migration of cultured Schwann cells on ultrathin fibronectin fibres." Cell Motil Cytoskeleton **42**(4): 331-43.

Ahmed, Z., S. Underwood, et al. (2003). "Nerve guide material made from fibronectin: assessment of in vitro properties." Tissue Eng **9**(2): 219-31.

Anselme, K., C. Bacques, et al. (1990). "Tissue reaction to subcutaneous implantation of a collagen sponge. A histological, ultrastructural, and immunological study." J Biomed Mater Res **24**(6): 689-703.

Arai, T., G. Lundborg, et al. (2000). "Bioartificial nerve graft for bridging extended nerve defects in rat sciatic nerve based on resorbable guiding filaments." Scand J Plast Reconstr Surg Hand Surg **34**(2): 101-8.

Archibald, S. J., C. Krarup, et al. (1991). "A collagen-based nerve guide conduit for peripheral nerve repair: an electrophysiological study of nerve regeneration in rodents and nonhuman primates." J Comp Neurol **306**(4): 685-96.

Asato, F., M. Butler, et al. (2000). "Variation in rat sciatic nerve anatomy: implications for a rat model of neuropathic pain." J Peripher Nerv Syst **5**(1): 19-21.

Bain, J. R., S. E. Mackinnon, et al. (1988). "The peripheral nerve allograft: an assessment of regeneration across nerve allografts in rats immunosuppressed with cyclosporin A." Plast Reconstr Surg **82**(6): 1052-66.

Bain, J. R., S. E. Mackinnon, et al. (1989). "Functional evaluation of complete sciatic, peroneal, and posterior tibial nerve lesions in the rat." Plast Reconstr Surg **83**(1): 129-38.

Battiston, B., P. Tos, et al. (2000). "Nerve repair by means of vein filled with muscle grafts I. Clinical results." Microsurgery **20**(1): 32-6.

Beghe, F., C. Menicagli, et al. (1992). "Lyophilized non-denatured type-I collagen (Condress) extracted from bovine Achilles' tendon and suitable for clinical use." Int J Tissue React **14 Suppl**: 11-9.

Berglund, J. D., M. M. Mohseni, et al. (2003). "A biological hybrid model for collagen-based tissue engineered vascular constructs." Biomaterials **24**(7): 1241-54.

Bervar, M. (2000). "Video analysis of standing--an alternative footprint analysis to assess functional loss following injury to the rat sciatic nerve." J Neurosci Methods **102**(2): 109-16.

Boot-Handford, R. P. and D. S. Tuckwell (2003). "Fibrillar collagen: the key to vertebrate evolution? A tale of molecular incest." Bioessays **25**(2): 142-51.

Borkenhagen, M., R. C. Stoll, et al. (1998). "In vivo performance of a new biodegradable polyester urethane system used as a nerve guidance channel." Biomaterials **19**(23): 2155-65.

Brandt, J., L. B. Dahlin, et al. (1999). "Autologous tendons used as grafts for bridging peripheral nerve defects." J Hand Surg [Br] **24**(3): 284-90.

Ceballos, D., X. Navarro, et al. (1999). "Magnetically aligned collagen gel filling a collagen nerve guide improves peripheral nerve regeneration." Exp Neurol **158**(2): 290-300.

Chamberlain, L. J., I. V. Yannas, et al. (1998). "Early peripheral nerve healing in collagen and silicone tube implants: myofibroblasts and the cellular response." Biomaterials **19**(15): 1393-403.

Chamberlain, L. J., I. V. Yannas, et al. (1998). "Collagen-GAG substrate enhances the quality of nerve regeneration through collagen tubes up to level of autograft." Exp Neurol **154**(2): 315-29.

Charulatha, V. and A. Rajaram (2003). "Influence of different crosslinking treatments on the physical properties of collagen membranes." Biomaterials **24**(5): 759-67.

Chernousov, M. A., R. C. Stahl, et al. (2001). "Schwann cell type V collagen inhibits axonal outgrowth and promotes Schwann cell migration via distinct adhesive activities of the collagen and noncollagen domains." J Neurosci **21**(16): 6125-35.

Cloft, H. J., D. F. Kallmes, et al. (2000). "Bovine type I collagen as an endovascular stent-graft material: biocompatibility study in rabbits." Radiology **214**(2): 557-62.

Daamen, W. F., H. T. van Moerkerk, et al. (2003). "Preparation and evaluation of molecularly-defined collagen-elastin-glycosaminoglycan scaffolds for tissue engineering." Biomaterials **24**(22): 4001-9.

Daube, J. R. (1995). "Estimating the number of motor units in a muscle." J Clin Neurophysiol **12**(6): 585-94.

Daube, J. R. (1996). Compound Muscle Action Potentials. Clinical Neurophysiology. J. R. Daube. Philadelphia, F.A. Davis Company. **46:** 199-234.

Daube, J. R. (1996). Estimating The Number of Motor Units In a Muscle. Clinical Neurophysiology. J. R. Daube. Philadelphia, F.A. Davis Company. **46:** 301-311.

Daube, J. R., C. Gooch, et al. (2000). "Motor unit number estimation (MUNE) with nerve conduction studies." Suppl Clin Neurophysiol **53**: 112-5.

de Medinaceli, L., W. J. Freed, et al. (1982). "An index of the functional condition of rat sciatic nerve based on measurements made from walking tracks." Exp Neurol **77**(3): 634-43.

Dellon, A. L. and S. E. Mackinnon (1989). "Sciatic nerve regeneration in the rat. Validity of walking track assessment in the presence of chronic contractures." Microsurgery **10**(3): 220-5.

Dellon, A. L. and S. E. Mackinnon (1989). "Selection of the appropriate parameter to measure neural regeneration." Ann Plast Surg **23**(3): 197-202.

Dohm, S., M. Streppel, et al. (2000). "Local application of extracellular matrix proteins fails to reduce the number of axonal branches after varying reconstructive surgery on rat facial nerve." Restor Neurol Neurosci **16**(2): 117-126.

Esposito, B., A. De Santis, et al. (2002). "Mast cells in Wallerian degeneration: morphologic and ultrastructural changes." J Comp Neurol **445**(3): 199-210.

Evans, G. R. (2000). "Challenges to nerve regeneration." Semin Surg Oncol **19**(3): 312-8.

Evans, G. R. (2001). "Peripheral nerve injury: a review and approach to tissue engineered constructs." Anat Rec **263**(4): 396-404.

Evans, G. R., K. Brandt, et al. (2000). "Clinical long-term in vivo evaluation of poly(L-lactic acid) porous conduits for peripheral nerve regeneration." J Biomater Sci Polym Ed **11**(8): 869-78.

Evans, G. R., K. Brandt, et al. (1999). "In vivo evaluation of poly(L-lactic acid) porous conduits for peripheral nerve regeneration." Biomaterials **20**(12): 1109-15.

Fansa, H., W. Schneider, et al. (2001). "Revascularization of tissue-engineered nerve grafts and invasion of macrophages." Tissue Eng **7**(5): 519-24.

Fansa, H., W. Schneider, et al. (2002). "Influence of insulin-like growth factor-I (IGF-I) on nerve autografts and tissue-engineered nerve grafts." Muscle Nerve **26**(1): 87-93.

Fine, E. G., I. Decosterd, et al. (2002). "GDNF and NGF released by synthetic guidance channels support sciatic nerve regeneration across a long gap." Eur J Neurosci **15**(4): 589-601.

Fornaro, M., P. Tos, et al. (2001). "Confocal imaging of Schwann-cell migration along muscle-vein combined grafts used to bridge nerve defects in the rat." Microsurgery **21**(4): 153-5.

George, E. B., J. D. Glass, et al. (1995). "Axotomy-induced axonal degeneration is mediated by calcium influx through ion-specific channels." J Neurosci **15**(10): 6445-52.

Geuna, S., P. Tos, et al. (2000). "Morphological analysis of peripheral nerve regenerated by means of vein grafts filled with fresh skeletal muscle." Anat Embryol (Berl) **201**(6): 475-82.

Glasby, M. A., S. Gschmeissner, et al. (1986). "Regeneration of the sciatic nerve in rats. The effect of muscle basement membrane." J Bone Joint Surg Br **68**(5): 829-33.

Godard, J., G. Coulon, et al. (1984). "[Nerve regeneration through a venous graft in the rat. Preliminary results]." Neurochirurgie **30**(6): 407-16.

Goldberg, J. L. (2003). "How does an axon grow?" Genes Dev **17**(8): 941-58.

Grados-Munro, E. M. and A. E. Fournier (2003). "Myelin-associated inhibitors of axon regeneration." J Neurosci Res **74**(4): 479-85.

Greene, E. C. (1968). Anatomy of the Rat. New York, Hafner Publishing Company, Inc.

Hadlock, T. A., C. A. Sundback, et al. (2001). "A new artificial nerve graft containing rolled Schwann cell monolayers." Microsurgery **21**(3): 96-101.

Hare, G. M., P. J. Evans, et al. (1992). "Walking track analysis: a long-term assessment of peripheral nerve recovery." Plast Reconstr Surg **89**(2): 251-8.

Hashimoto, T., Y. Suzuki, et al. (2002). "Peripheral nerve regeneration through alginate gel: analysis of early outgrowth and late increase in diameter of regenerating axons." Exp Brain Res **146**(3): 356-68.

Ho, P. R., G. M. Coan, et al. (1998). "Repair with collagen tubules linked with brain-derived neurotrophic factor and ciliary neurotrophic factor in a rat sciatic nerve injury model." Arch Otolaryngol Head Neck Surg **124**(7): 761-6.

Hunter, J. M., L. H. Schneider, et al. (1997). Tendon And Nerve Surgery In The Hand: A Third Decade. St. Louis, Mosby-Year Book, Inc.

Ide, C. (1983). "Nerve regeneration and Schwann cell basal lamina: observations of the long-term regeneration." Arch Histol Jpn **46**(2): 243-57.

Ide, C., K. Tohyama, et al. (1983). "Schwann cell basal lamina and nerve regeneration." Brain Res **288**(1-2): 61-75.

Ishihara, M., P. N. Shaklee, et al. (1994). "Structural features in heparin which modulate specific biological activities mediated by basic fibroblast growth factor." Glycobiology **4**(4): 451-8.

Itoh, S., K. Takakuda, et al. (2002). "Evaluation of cross-linking procedures of collagen tubes used in peripheral nerve repair." Biomaterials **23**(23): 4475-81.

Keeley, R., T. Atagi, et al. (1993). "Peripheral nerve regeneration across 14-mm gaps: a comparison of autograft and entubulation repair methods in the rat." J Reconstr Microsurg **9**(5): 349-58; discussion 359-60.

Keeley, R. D., K. D. Nguyen, et al. (1991). "The artificial nerve graft: a comparison of blended elastomer-hydrogel with polyglycolic acid conduits." J Reconstr Microsurg **7**(2): 93-100.

Krarup, C., S. J. Archibald, et al. (2002). "Factors that influence peripheral nerve regeneration: an electrophysiological study of the monkey median nerve." Ann Neurol **51**(1): 69-81.

Laurie, G. W., C. P. Leblond, et al. (1982). "Localization of type IV collagen, laminin, heparan sulfate proteoglycan, and fibronectin to the basal lamina of basement membranes." J Cell Biol **95**(1): 340-4.

Lee, A. C., V. M. Yu, et al. (2003). "Controlled release of nerve growth factor enhances sciatic nerve regeneration." Exp Neurol **184**(1): 295-303.

Lubinska, L. (1977). "Early course of Wallerian degeneration in myelinated fibres of the rat phrenic nerve." Brain Res **130**(1): 47-63.

Lundborg, G. (2000). "A 25-year perspective of peripheral nerve surgery: evolving neuroscientific concepts and clinical significance." Journal of Hand Surgery **25**(3): 391-414.

Lundborg, G. (2002). "Editorial: Enhancing posttraumatic nerve regeneration." Journal of the Peripheral Nervous System **7**: 139-140.

Mackinnon, S. E. and A. L. Dellon (1988). Surgery Of The Peripheral Nerve. New York, Thieme Medical Publishers, Inc.**:** 3-4.

Mackinnon, S. E., A. L. Dellon, et al. (1991). "Changes in nerve fiber numbers distal to a nerve repair in the rat sciatic nerve model." Muscle Nerve **14**(11): 1116-22.

Madison, R. D. and S. J. Archibald (1994). "Point sources of Schwann cells result in growth into a nerve entubulation repair site in the absence of axons: effects of freeze-thawing." Exp Neurol **128**(2): 266-75.

Madison, R. D., C. da Silva, et al. (1987). "Peripheral nerve regeneration with entubulation repair: comparison of biodegradeable nerve guides versus polyethylene tubes and the effects of a laminin-containing gel." Exp Neurol **95**(2): 378-90.

Madison, R. D., C. F. Da Silva, et al. (1988). "Entubulation repair with protein additives increases the maximum nerve gap distance successfully bridged with tubular prostheses." Brain Res **447**(2): 325-34.

McComas, A. J., P. R. Fawcett, et al. (1971). "Electrophysiological estimation of the number of motor units within a human muscle." J Neurol Neurosurg Psychiatry **34**(2): 121-31.

Misulis, K. M. (1997). Essentials of Clinical Neurophysiology. Boston, Butterworth-Heinemann.

Mosahebi, A., P. Fuller, et al. (2002). "Effect of allogeneic Schwann cell transplantation on peripheral nerve regeneration." Exp Neurol **173**(2): 213-23.

Munro, C. A., J. P. Szalai, et al. (1998). "Lack of association between outcome measures of nerve regeneration." Muscle Nerve **21**(8): 1095-7.

Ngo, T. T., P. J. Waggoner, et al. (2003). "Poly(L-Lactide) microfilaments enhance peripheral nerve regeneration across extended nerve lesions." J Neurosci Res **72**(2): 227-38.

Norrby, K. (2002). "Mast cells and angiogenesis." Apmis **110**(5): 355-71.

Oh, S. J. (1993). Clinical Electromyography: Nerve Conduction Studies. Baltimore, Williams & Wilkins.

Ramon Y Cajal, S. (1928). Cajal's degeneration and regeneration of the nervous system. New York, Oxford University Press.

Rodrigues Ade, C. and M. D. Silva (2001). "Inside-out versus standard artery graft to repair a sensory nerve in rats." Microsurgery **21**(3): 102-7.

Rogers, S. L., P. C. Letourneau, et al. (1983). "Neurite extension by peripheral and central nervous system neurons in response to substratum-bound fibronectin and laminin." Dev Biol **98**(1): 212-20.

Rosenstein, J. M. and J. M. Krum (2004). "New roles for VEGF in nervous tissue--beyond blood vessels." Exp Neurol **187**(2): 246-53.

Ross, M. H., L. J. Romrell, et al. (1995). Histology A Text And Atlas. Baltimore, Williams & Wilkins**:** 256-300.

Sakiyama, S. E., J. C. Schense, et al. (1999). "Incorporation of heparin-binding peptides into fibrin gels enhances neurite extension: an example of designer matrices in tissue engineering." Faseb J **13**(15): 2214-24.

Santos, X., J. Rodrigo, et al. (1998). "Evaluation of peripheral nerve regeneration by nerve growth factor locally administered with a novel system." J Neurosci Methods **85**(1): 119-27.

Schwab, M. E. (2004). "Nogo and axon regeneration." Curr Opin Neurobiol **14**(1): 118-24.

Shefner, J. M. (2001). "Motor unit number estimation in human neurological diseases and animal models." Clin Neurophysiol **112**(6): 955-64.

Shefner, J. M., M. E. Cudkowicz, et al. (2002). "Comparison of incremental with multipoint MUNE methods in transgenic ALS mice." Muscle Nerve **25**(1): 39-42.

Shenaq, J. M., S. M. Shenaq, et al. (1989). "Reliability of sciatic function index in assessing nerve regeneration across a 1 cm gap." Microsurgery **10**(3): 214-9.

Stoll, G., J. W. Griffin, et al. (1989). "Wallerian degeneration in the peripheral nervous system: participation of both Schwann cells and macrophages in myelin degradation." J Neurocytol **18**(5): 671-83.

Stoll, G., B. D. Trapp, et al. (1989). "Macrophage function during Wallerian degeneration of rat optic nerve: clearance of degenerating myelin and Ia expression." J Neurosci **9**(7): 2327-35.

Sunderland, S. S. (1991). Nerve Injuries and their Repair: A Critical Appraisal. New York, Churchill Livingstone.

Terzis, J., B. Faibisoff, et al. (1975). "The nerve gap: suture under tension vs. graft." Plast Reconstr Surg **56**(2): 166-70.

Trumble, T. E. and F. G. Shon (2000). "The physiology of nerve transplantation." Hand Clin **16**(1): 105-22.

Tyrrell, D. J., M. Ishihara, et al. (1993). "Structure and biological activities of a heparin-derived hexasaccharide with high affinity for basic fibroblast growth factor." J Biol Chem **268**(7): 4684-9.

Utley, D. S., S. L. Lewin, et al. (1996). "Brain-derived neurotrophic factor and collagen tubulization enhance functional recovery after peripheral nerve transection and repair." Arch Otolaryngol Head Neck Surg **122**(4): 407-13.

Valero-Cabre, A., K. Tsironis, et al. (2001). "Superior muscle reinnervation after autologous nerve graft or poly-L-lactide-epsilon-caprolactone (PLC) tube implantation in comparison to silicone tube repair." J Neurosci Res **63**(2): 214-23.

Verdu, E., R. O. Labrador, et al. (2002). "Alignment of collagen and laminin-containing gels improve nerve regeneration within silicone tubes." Restor Neurol Neurosci **20**(5): 169-79.

Vleggeert-Lankamp, C. L., A. P. Pego, et al. (2004). "Adhesion and proliferation of human Schwann cells on adhesive coatings." Biomaterials **25**(14): 2741-51.

Waller, A. (1850). "Experiments on the Section of the Glossopharyngeal and Hypoglossal Nerves of the Frog, and Observations of the Alterations Produced Thereby in the Structure of Their Primitive Fibres." Philosophical Transactions of the Royal Society of London **140**: 423-429.

Woodburne, R. T. and W. E. Burkel (1988). Essentials of Human Anatomy. New York, Oxford University Press.

Woolley, A. L., J. P. Hollowell, et al. (1990). "First place--Resident Basic Science Award 1990. Fibronectin-laminin combination enhances peripheral nerve regeneration across long gaps." Otolaryngol Head Neck Surg **103**(4): 509-18.

Xu, X., W. C. Yee, et al. (2003). "Peripheral nerve regeneration with sustained release of poly(phosphoester) microencapsulated nerve growth factor within nerve guide conduits." Biomaterials **24**(13): 2405-12.

Yin, Q., G. J. Kemp, et al. (2001). "Neurotrophin-4 delivered by fibrin glue promotes peripheral nerve regeneration." Muscle Nerve **24**(3): 345-51.

Young, R. C., M. Wiberg, et al. (2002). "Poly-3-hydroxybutyrate (PHB): a resorbable conduit for long-gap repair in peripheral nerves." Br J Plast Surg **55**(3): 235-40.

Zhang, J., T. M. Oswald, et al. (2003). "Enhancement of rat sciatic nerve regeneration by fibronectin and laminin through a silicone chamber." J Reconstr Microsurg **19**(7): 467-72.

Zochodne, D. W. and C. Cheng (2000). "Neurotrophins and other growth factors in the regenerative milieu of proximal nerve stump tips." J Anat **196 (Pt 2)**: 279-83.

About the Author

Oren D. Rosenthal received a Bachelor's Degree in Psychology from the University of Buffalo in 1989 and a Master's Degree in Physical Therapy from Rutgers University/University of Medicine and Dentistry of New Jersey in 1995. After physical therapy school, Oren's postgraduate continuing education focused on orthopedics and rehabilitation of the spine. He practiced physical therapy in a variety of clinical settings prior to reentering graduate school in the fall of 2000. He enrolled in the Ph.D. program in Medical Sciences with a concentration in anatomy, at the University of South Florida, College of Medicine. While in the Ph.D. program, Oren taught human anatomy to first year medical students and presented research at a national Neuroscience meeting.